INSIDE TRACK with
ERAN ESHED,
ALTAIR SEMICONDUCTOR p32

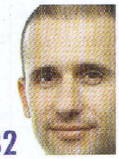

DDS SOURCE DRIVES **FMCW RADAR** p52

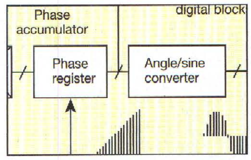

MAKING **NOISE-FIGURE** MEASUREMENTS p68

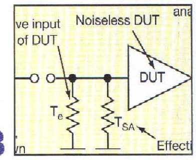

MicroWaves&RF

APRIL 2013 TRUSTED ENGINEERING RESOURCE FOR 50 YEARS www.MWRF.com

WIRELESS INFRASTRUCTURE ISSUE

REAL-TIME ANALYZERS GRAB 50-GHz SIGNALS

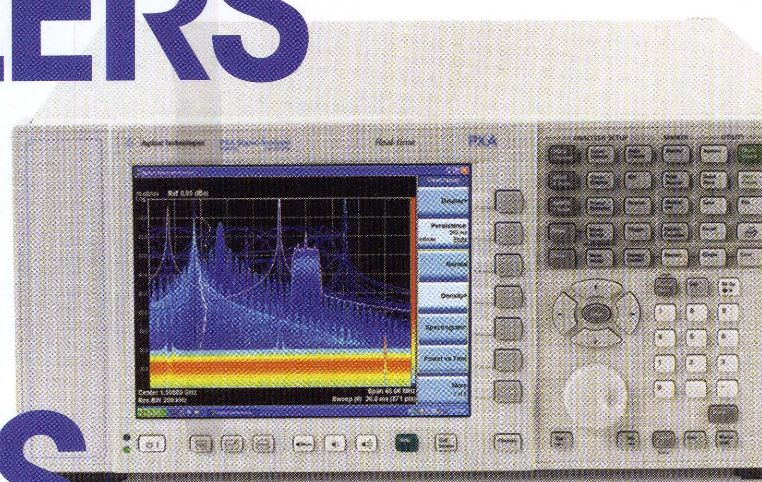

A PENTON PUBLICATION Periodicals Postage Paid • USPS 100 Approved Poly

This is no place for beta testers.

VNA Master™ *Handheld Vector Network Analyzers*

There's a lot riding on the accuracy of your field measurements. Why take a chance on an unproven instrument, when the success of your mission or even national security could be at stake? Count on Anritsu—now in our ninth generation providing handheld Vector Network Analyzers (VNAs) that take the precision of a test lab into the field. Only Anritsu offers you:

- 350 μs sweep speed—over twice as fast as any other handheld VNA.
- Full performance over the specified temperature range to +55° C, even while battery powered.
- Best dynamic range across a wide range of frequencies—over 100 dB at 3 GHz and greater than 85 dB at 20 GHz.
- Best handheld spectrum analyzer dynamic range – greater than 116 dB!

Anritsu's VNA Master™ family is made in the USA, by the company that pioneered the handheld VNA. Why would you choose anything else? Find out more and download our complimentary field guide, ***Advanced VNA Cable Measurements***.

Download it now at **www.anritsu.com/en-us/analyzers**

Call 1-800-ANRITSU to place an order or schedule a demo, or visit **www.anritsu.com.**

Sales Offices: USA and Canada 1-800-ANRITSU, Europe 44 (0) 1552-433433, Japan 81 (45) 223-1111, Asia-Pacific (852) 2301-4980, South America 55 (21) 2527-8922, www.anritsu.com, ©2012 Anritsu Company

Anritsu

Introducing your *one-stop* resource for subminiature passive RF parts and info!

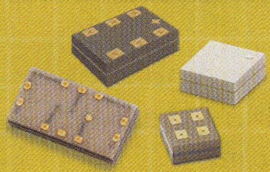

Working on a wireless device where package-size and performance share top priority?

Anaren's Xinger Subminiature passive RF product family is the perfect fit.

And, now, that same family is supported by a single, convenient online information resource: *Submini-Central*.

Here, you'll find a wide and fast-growing selection of tools and information of use when you're working on a footprint-sensitive, performance-driven product development projects — and where Anaren's renowned, Xinger subminiature hybrid couplers, directional couplers, power dividers, balun transformers, and RF crossovers are just the ticket.

Contents currently include:

- **> Applications notes**
- **> De-embed files**
- **> Videos & presentations**
- **> Info on sample kits**

To learn more, visit www.anaren.com/submini-central today.

Xinger Subminiature sample kits now available through Richardson RFPD! Visit Submini-Central to learn more!

Anaren®

What'll we think of next?®

800-411-6596 > www.anaren.com

IMAgine.

Innovative | Multifunction | Adaptable

Integrated Microwave Assemblies

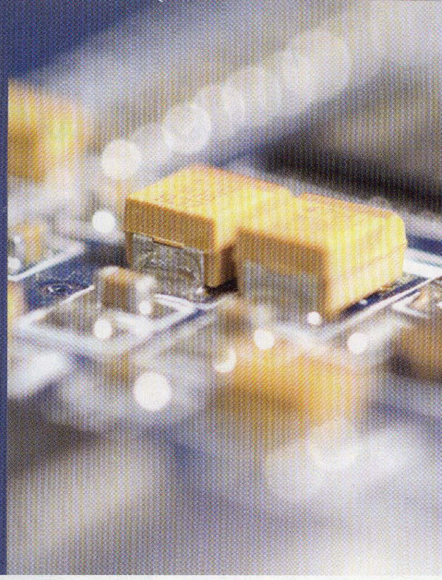

Time to pack it in.

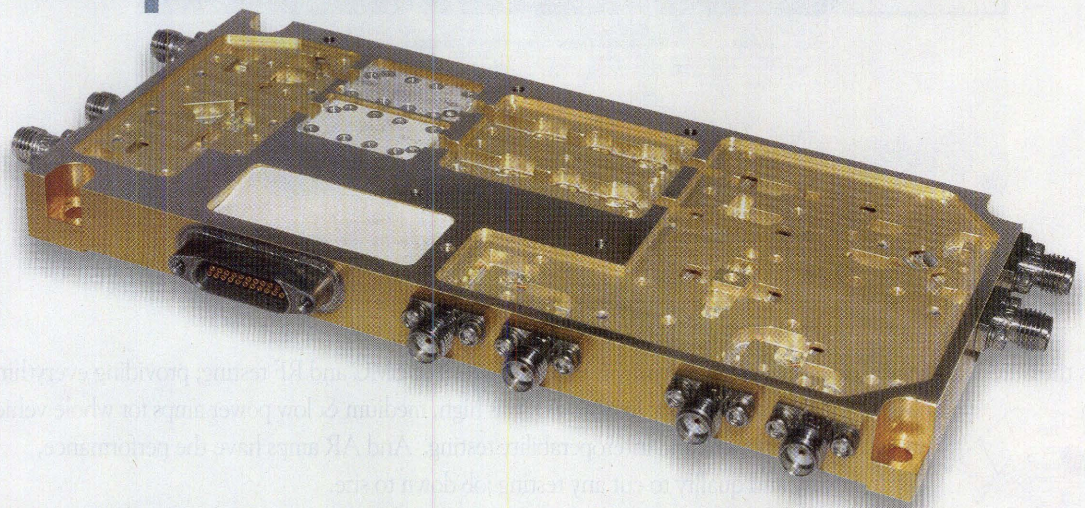

Demand for ever-higher performance probably has you wondering how to get more out of your IMAs. The answer? **Pack more in!** Narda's MMC (Multilayer Microwave Circuitry) Technology offers the most performance in the smallest possible footprints. Traditional approaches can't come close.

The principle behind Narda's MMC is simple enough. Narda MMC uses a single multilayered printed circuit board to interconnect microwave devices (MIC, SMT, or MMIC configurations) with bias, control and digital signal processing components. Typically, these complex IMAs are constructed with the microwave circuitry on the top side, and the control circuitry, conditioning, microprocessor, FPGAs and DSP circuits on the bottom. The Compact Microwave Subsystem measures just 5.75 x 2.66 x 0.515 inches, holding over 60 microwave components including couplers, switches, filters, limiters, amplifiers and more. *It's time to started packing in more performance, with Narda's MMC technology.* ***Contact us today to learn how.***

Scan using your Smart Phone or Tablet to learn more!

narda

an L3 communications company

Engineering, without compromise since 1954.

www.nardamicrowave.com • 631.231.1700

APRIL | 2013
Volume 52, Issue 4

MicroWaves&RF

CONTENTS

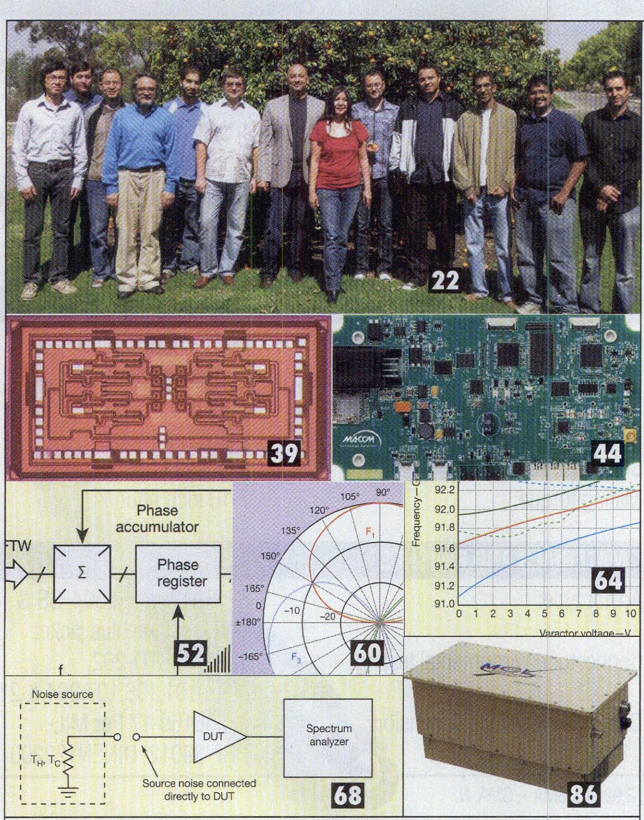

COVER STORY

NEWS & COLUMNS

Penton
Design Engineering & Sourcing Group

INDUSTRY TRENDS AND ANALYSIS

DESIGN FEATURES

PRODUCT TECHNOLOGY

SPECIAL SECTION

Defense Electronics Starts after **p. 88**

Rosenberger® Rmor™ Cables Assembly

PHASE STABLE THROUGH 70GHz

Rosenberger Rmor™ cables are designed for rugged environments for indoor and outdoor applications. Each shielded coaxial cable is protected with flexible, SPIRAL-wound 304 Stainless Steel armor coated with extruded Polyurethane. The connector ends are sealed and encapsulated with a pressure injection-molded polymer strain relief.

This combination of materials and technology provides superior ruggedization, environmental resistance, RF shielding effectiveness and stability under flexure and vibration.

Additional connector interfaces and armor/cable diameters are available on request.

DESCRIPTION

Rosenberger connectors, cable assembly, standard length 915mm or 36 inches

GENERAL ELECTRICAL SPECIFICATIONS

Impedance:	50 +/- 1 Ohms
Operating frequency:	DC to 70 GHz
Return loss:	14 dB minimum up to 70 GHz
Cable insertion loss:	.67 dB/ft @ 10.0 GHz
Velocity of propagation (%):	78 % nominal
Capacitance:	24.7 pf/ft. nominal
Shielding effectiveness:	< -90 dB
Dielectric withstand voltage:	1000 Vrms
Amplitude & phase stable:	+/- .03dB & +/- 1° @10GHz

MECHANICAL SPECIFICATION

Cable jacket & armor outer diameter:	092 inches nominal & .250 inches nominal
Minimum bend radius:	.5 inches
Armor crush strength:	450 lbs/in (min)
Connector retention:	≥25 lbs.
Mating torque:	7-10 inch pounds

MATERIALS AND FINISHES

Armor type:	SPIRAL-wound 304 SS & Polyurethane blue jacket
Connector environmental testing:	Per MIL-STD-202, Meth 101,106,107,204 & 213
Connector interface dimension:	IEC 60169-17 Per MIL-PRF-39012 DINEN122200

Note: Cable assemblies also available with interfaces such as 1.85mm, 2.4mm, 2.92mm, SMA +, SMA, N.

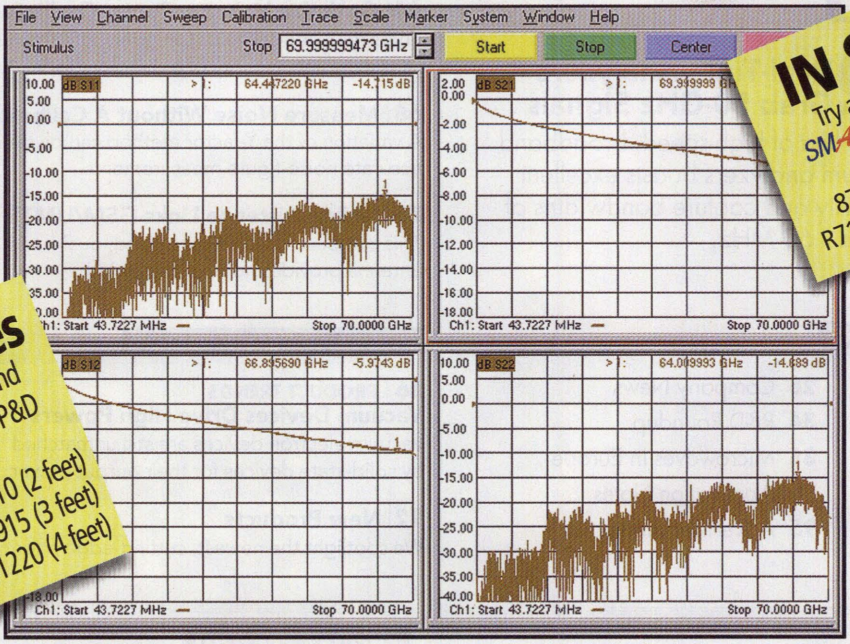

Example of typical 36 inches assembly up to 70 GHz

IN STOCK!
Try an Rmor cable with SMA+™ (operates to 36 GHz)
Call RFMW today
877.367.7369. Ask for p/n
R71-32+S132+S1-00457 (18")

70GHz Cables
1.85mm males each end
Call RFMW today for P&D
877.367.7369
RU5-08S1-08S1-00610 (2 feet)
RU5-08S1-08S1-00915 (3 feet)
RU5-08S1-08S1-01220 (4 feet)

RfMW

RFMW is the exclusive stocking distributor for **Rosenberger**® Connectors and Cable Assemblies
RFMW, 188 Martinvale Lane, San Jose, CA 95119
PH: 408.414.1450 or 877.367.7369 Email: sales@rfmw.com
Website: www.rfmw.com/Rosenberger

RF Amplifiers and Sub-Assemblies for Every Application

Delivery from Stock to 2 Weeks ARO from the catalog or built to your specifications!

- Competitive Pricing & Fast Delivery
- Military Reliability & Qualification
- Various Options: Temperature Compensation, Input Limiter Protection, Detectors/TTL & More
- Unconditionally Stable (100% tested)

ISO 9001:2000 and AS9100B CERTIFIED

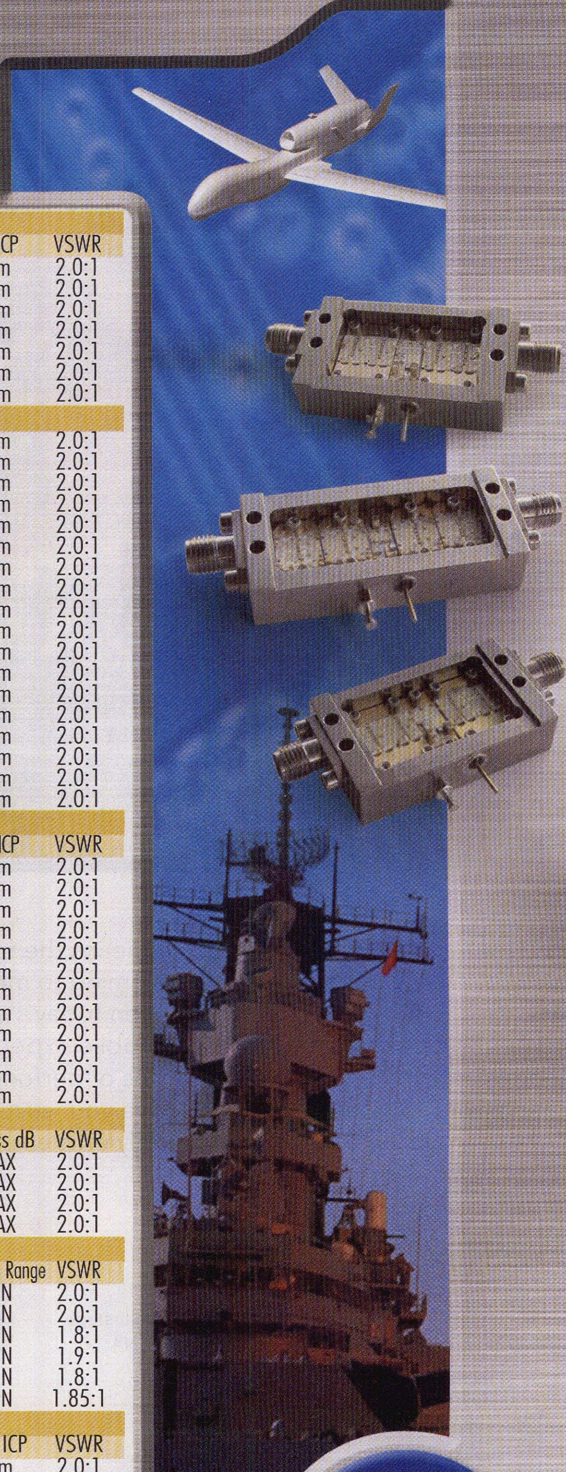

OCTAVE BAND LOW NOISE AMPLIFIERS

Model No.	Freq (GHz)	Gain (dB) MIN	Noise Figure (dB)	Power-out @ P1-dB	3rd Order ICP	VSWR
CA01-2110	0.5-1.0	28	1.0 MAX, 0.7 TYP	+10 MIN	+20 dBm	2.0:1
CA12-2110	1.0-2.0	30	1.0 MAX, 0.7 TYP	+10 MIN	+20 dBm	2.0:1
CA24-2111	2.0-4.0	29	1.1 MAX, 0.95 TYP	+10 MIN	+20 dBm	2.0:1
CA48-2111	4.0-8.0	29	1.3 MAX, 1.0 TYP	+10 MIN	+20 dBm	2.0:1
CA812-3111	8.0-12.0	27	1.6 MAX, 1.4 TYP	+10 MIN	+20 dBm	2.0:1
CA1218-4111	12.0-18.0	25	1.9 MAX, 1.7 TYP	+10 MIN	+20 dBm	2.0:1
CA1826-2110	18.0-26.5	32	3.0 MAX, 2.5 TYP	+10 MIN	+20 dBm	2.0:1

NARROW BAND LOW NOISE AND MEDIUM POWER AMPLIFIERS

Model No.	Freq (GHz)	Gain (dB) MIN	Noise Figure (dB)	Power-out @ P1-dB	3rd Order ICP	VSWR
CA01-2111	0.4 - 0.5	28	0.6 MAX, 0.4 TYP	+10 MIN	+20 dBm	2.0:1
CA01-2113	0.8 - 1.0	28	0.6 MAX, 0.4 TYP	+10 MIN	+20 dBm	2.0:1
CA12-3117	1.2 - 1.6	25	0.6 MAX, 0.4 TYP	+10 MIN	+20 dBm	2.0:1
CA23-3111	2.2 - 2.4	30	0.6 MAX, 0.45 TYP	+10 MIN	+20 dBm	2.0:1
CA23-3116	2.7 - 2.9	29	0.7 MAX, 0.5 TYP	+10 MIN	+20 dBm	2.0:1
CA34-2110	3.7 - 4.2	28	1.0 MAX, 0.5 TYP	+10 MIN	+20 dBm	2.0:1
CA56-3110	5.4 - 5.9	40	1.0 MAX, 0.5 TYP	+10 MIN	+20 dBm	2.0:1
CA78-4110	7.25 - 7.75	32	1.2 MAX, 1.0 TYP	+10 MIN	+20 dBm	2.0:1
CA910-3110	9.0 - 10.6	25	1.4 MAX, 1.2 TYP	+10 MIN	+20 dBm	2.0:1
CA1315-3110	13.75 - 15.4	25	1.6 MAX, 1.4 TYP	+10 MIN	+20 dBm	2.0:1
CA12-3114	1.35 - 1.85	30	4.0 MAX, 3.0 TYP	+33 MIN	+41 dBm	2.0:1
CA34-6116	3.1 - 3.5	40	4.5 MAX, 3.5 TYP	+35 MIN	+43 dBm	2.0:1
CA56-5114	5.9 - 6.4	30	5.0 MAX, 4.0 TYP	+30 MIN	+40 dBm	2.0:1
CA812-6115	8.0 - 12.0	30	4.5 MAX, 3.5 TYP	+30 MIN	+40 dBm	2.0:1
CA812-6116	8.0 - 12.0	30	5.0 MAX, 4.0 TYP	+33 MIN	+41 dBm	2.0:1
CA1213-7110	12.2 - 13.25	28	6.0 MAX, 5.5 TYP	+33 MIN	+42 dBm	2.0:1
CA1415-7110	14.0 - 15.0	30	5.0 MAX, 4.0 TYP	+30 MIN	+40 dBm	2.0:1
CA1722-4110	17.0 - 22.0	25	3.5 MAX, 2.8 TYP	+21 MIN	+31 dBm	2.0:1

ULTRA-BROADBAND & MULTI-OCTAVE BAND AMPLIFIERS

Model No.	Freq (GHz)	Gain (dB) MIN	Noise Figure (dB)	Power-out @ P1-dB	3rd Order ICP	VSWR
CA0102-3111	0.1-2.0	28	1.6 Max, 1.2 TYP	+10 MIN	+20 dBm	2.0:1
CA0106-3111	0.1-6.0	28	1.9 Max, 1.5 TYP	+10 MIN	+20 dBm	2.0:1
CA0108-3110	0.1-8.0	26	2.2 Max, 1.8 TYP	+10 MIN	+20 dBm	2.0:1
CA0108-4112	0.1-8.0	32	3.0 MAX, 1.8 TYP	+22 MIN	+32 dBm	2.0:1
CA02-3112	0.5-2.0	36	4.5 MAX, 2.5 TYP	+30 MIN	+40 dBm	2.0:1
CA26-3110	2.0-6.0	26	2.0 MAX, 1.5 TYP	+10 MIN	+20 dBm	2.0:1
CA26-4114	2.0-6.0	22	5.0 MAX, 3.5 TYP	+30 MIN	+40 dBm	2.0:1
CA618-4112	6.0-18.0	25	5.0 MAX, 3.5 TYP	+23 MIN	+33 dBm	2.0:1
CA618-6114	6.0-18.0	35	5.0 MAX, 3.5 TYP	+30 MIN	+40 dBm	2.0:1
CA218-4116	2.0-18.0	30	3.5 MAX, 2.8 TYP	+10 MIN	+20 dBm	2.0:1
CA218-4110	2.0-18.0	30	5.0 MAX, 3.5 TYP	+20 MIN	+30 dBm	2.0:1
CA218-4112	2.0-18.0	29	5.0 MAX, 3.5 TYP	+24 MIN	+34 dBm	2.0:1

LIMITING AMPLIFIERS

Model No.	Freq (GHz)	Input Dynamic Range	Output Power Range Psat	Power Flatness dB	VSWR
CLA24-4001	2.0 - 4.0	-28 to +10 dBm	+7 to +11 dBm	+/- 1.5 MAX	2.0:1
CLA26-8001	2.0 - 6.0	-50 to +20 dBm	+14 to +18 dBm	+/- 1.5 MAX	2.0:1
CLA712-5001	7.0 - 12.4	-21 to +10 dBm	+14 to +19 dBm	+/- 1.5 MAX	2.0:1
CLA618-1201	6.0 - 18.0	-50 to +20 dBm	+14 to +19 dBm	+/- 1.5 MAX	2.0:1

AMPLIFIERS WITH INTEGRATED GAIN ATTENUATION

Model No.	Freq (GHz)	Gain (dB) MIN	Noise Figure (dB)	Power-out @ P1-dB	Gain Attenuation Range	VSWR
CA001-2511A	0.025-0.150	21	5.0 MAX, 3.5 TYP	+12 MIN	30 dB MIN	2.0:1
CA05-3110A	0.5-5.5	23	2.5 MAX, 1.5 TYP	+18 MIN	20 dB MIN	2.0:1
CA56-3110A	5.85-6.425	28	2.5 MAX, 1.5 TYP	+16 MIN	22 dB MIN	1.8:1
CA612-4110A	6.0-12.0	24	2.5 MAX, 1.5 TYP	+12 MIN	15 dB MIN	1.9:1
CA1315-4110A	13.75-15.4	25	2.2 MAX, 1.6 TYP	+16 MIN	20 dB MIN	1.8:1
CA1518-4110A	15.0-18.0	30	3.0 MAX, 2.0 TYP	+18 MIN	20 dB MIN	1.85:1

LOW FREQUENCY AMPLIFIERS

Model No.	Freq (GHz)	Gain (dB) MIN	Noise Figure dB	Power-out @ P1-dB	3rd Order ICP	VSWR
CA001-2110	0.01-0.10	18	4.0 MAX, 2.2 TYP	+10 MIN	+20 dBm	2.0:1
CA001-2211	0.04-0.15	24	3.5 MAX, 2.2 TYP	+13 MIN	+23 dBm	2.0:1
CA001-2215	0.04-0.15	23	4.0 MAX, 2.2 TYP	+23 MIN	+33 dBm	2.0:1
CA001-3113	0.01-1.0	28	4.0 MAX, 2.8 TYP	+17 MIN	+27 dBm	2.0:1
CA002-3114	0.01-2.0	27	4.0 MAX, 2.8 TYP	+20 MIN	+30 dBm	2.0:1
CA003-3116	0.01-3.0	18	4.0 MAX, 2.8 TYP	+25 MIN	+35 dBm	2.0:1
CA004-3112	0.01-4.0	32	4.0 MAX, 2.8 TYP	+15 MIN	+25 dBm	2.0:1

CIAO Wireless can easily modify any of its standard models to meet your "exact" requirements at the Catalog Pricing.

Visit our web site at **www.ciaowireless.com** for our complete product offering.

Ciao wireless

Ciao Wireless, Inc. 4000 Via Pescador, Camarillo, CA 93012

Tel (805) 389-3224 Fax (805) 389-3629 sales@ciaowireless.com

MWRF.com

MicroWaves&RF ON THE WEB

THE EFFECT OF MOORE'S LAW on RF Instruments

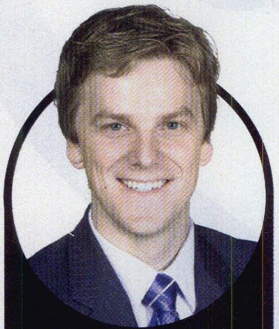

DAVID A. HALL

INTEL CO-FOUNDER GORDON E. MOORE once observed that the maximum number of transistors per square inch of integrated circuit doubles about every two years. In this Web-exclusive article, National Instruments' **David A. Hall** explains how "Moore's Law" has revolutionized the modern RF instrument—enabling new advancements in intermediate-frequency and baseband circuitry, as well as signal processing.

To read the article in its entirety, go to http://mwrf.com/test-amp-measurement/effect-moore-s-law-rf-instruments.

ALSO, BE SURE CHECK OUT THESE OTHER RECENT ARTICLES IN OUR CONTRIBUTED TECHNICAL EXPERT SERIES.

Visit www.mwrf.com/community/contributors.

KANG CHEN

BOB NELSON

MEET THE CHALLENGES OF TESTING EIGHT-ANTENNA LTE

KANG CHEN—
Senior Applications Specialist, Spirent Communications

DEMYSTIFY INTEGRATED-PHASE-DEVIATION RESULTS IN PHASE-NOISE MEASUREMENTS

BOB NELSON—
Product Support Engineer, Agilent Technologies

REVISIT IMS2012

The 2012 installment of the RF/microwave industry's flagship event, the *International Microwave Symposium*, has come and gone. Luckily for you, it needn't live on just in memory. Visit *www.mwrf.com* to check out our show coverage, as well as www.engineering tv.com to view exclusive videos from the show floor.

IMS2012 MONTRÉAL

engineering tv

NEWS UPDATES Sent To Your Desktop

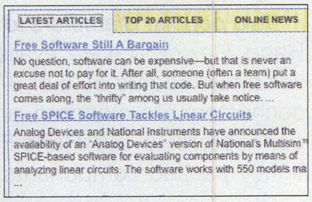

LATEST ARTICLES | TOP 20 ARTICLES | ONLINE NEWS

Free Software Still A Bargain

No question, software can be expensive—but that is never an excuse not to pay for it. After all, someone (often a team) put a great deal of effort into writing that code. But when free software comes along, the "thrifty" among us usually take notice. ...

Free SPICE Software Tackles Linear Circuits

Analog Devices and National Instruments have announced the availability of an "Analog Devices" version of National's Multisim™ SPICE-based software for evaluating components by means of analyzing linear circuits. The software works with 550 models ma ...

Don't believe everything you read, unless it's in the latest issue of *Microwaves & RF UPDATE.* The industry's longest-running weekly e-mail newsletter, it combines insightful commentary with the latest product and industry business news. It is sent directly to your computer desktop each week, and often contains the little things that engineers love, such as links to free white papers and even design software. If you're not already reading it, subscriptions are free, and available from the *Microwaves & RF* website at www.mwrf.com.

MWRF.com has archives of print and online articles dating back to October 2002. Visit mwrf.com today and click the "Back Issues" link. And while you're taking a look around the site, click on "Product Directory" to gain access to our complete directory of products and suppliers.

From the Editor

Drone Debate Continues

IN THIS MONTH'S "News" section, we highlight a portion of the jobs that are expected to be added as a result of the uptick of unmanned-aerial-system (UAS) development and deployment throughout the US. By 2025, the Association for Unmanned Vehicle Systems International (AUVSI) expects more than 100,000 new jobs to be created nationally. Amid the continuing economic slump afflicting the US, new jobs are a sign of recovery and hope. And in many situations, such as forest fires, drones can be critical to containment and even rescue efforts. Yet a storm has erupted over the use of drones, due to concerns over privacy, public safety, political corruption, government abuse, human-rights violations, and more.

Simply put, their small size and stealthy nature make it possible for drones to go places undetected. They do not need a declaration of war to cross a border and take out an enemy. In fact, they make it possible for leaders to commit acts of war without taking any credit for them—which means that such acts may not have to be justified to the public. On the home front, drones are expected to become nearly ubiquitous—eliminating civilian privacy in the process. Individuals worry that we will get used to living in a constant state of surveillance, potentially surrendering our privacy for promises of safety and progress.

No matter what the intended use is for drones, the fear is that the people who have the power to control them are abusing that power and will continue to do so. Given the history of humanity, that is a well-founded fear. It also reflects the feelings—or suspicions—of much of today's inactive voting-eligible population in the US. These individuals largely say that they feel far removed from politicians, who they suspect answer to campaign donors, lobbyists, and big businesses instead of serving the general population.

In the article, "Can Voters Fight Domestic Drones At The Ballot Box?," which was posted on *The Atlantic* on April 1, author Conor Friedersdorf quotes Glenn Greenwald, a columnist for *The Guardian*: Greenwald "argues that opposing a future of ubiquitous drone surveillance by the government 'may be one area where an actual bipartisan/trans-partisan alliance can meaningfully emerge, as most advocates working on these issues with whom I've spoken say that libertarian-minded GOP state legislators have been as responsive as more left-wing Democratic ones in working to impose some limits.'" Friedersdorf adds: "Federal limits on drone surveillance, like the warrant requirement before Congress, ought to be aggressively advocated by everyone who perceives the costs of failure."

It seems that the drone controversy, which became a hot topic over the last couple of years, has continued to gain momentum. Drones will be widely deployed in US airspace in 2015. For the first time since cell towers were met with a "not in my backyard" response, a segment of the microwave industry is mired in controversy. It will be interesting to see how it pans out, as the result will be largely symbolic of how much this country is willing to accept technology's place in citizens' everyday lives. Should some of the current anti-drone legislation efforts prove successful, we also may not get quite the booming job market that we expected. MWRF

Nancy K. Friedrich
Editor-In-Chief

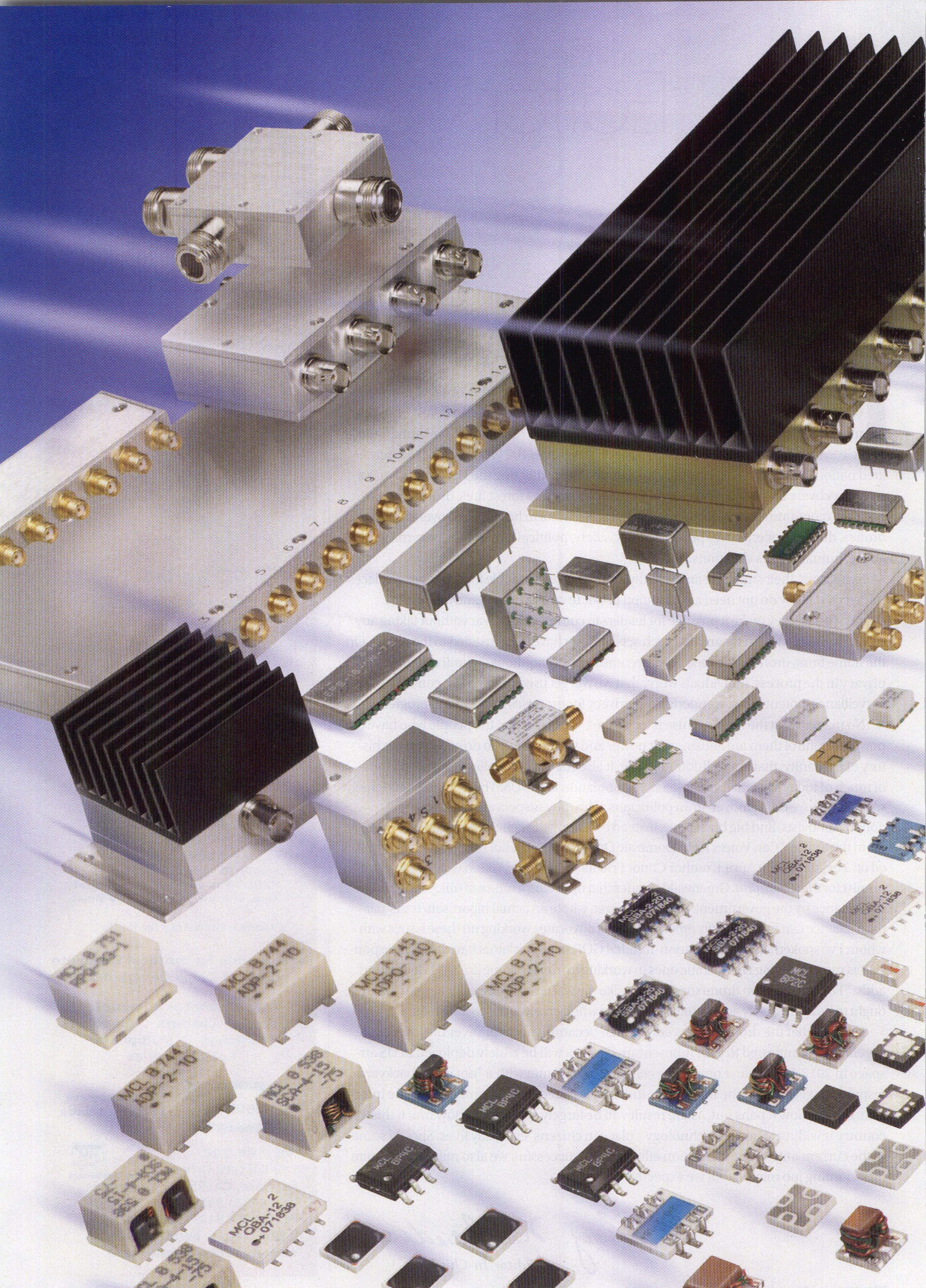
MCL B 744
ADP-2-10
MCL A 745
ADPQ-140-2
MCL B 744
ADP-2-10
MCL B 744
ADP-2-10
MCL
QBA-12
071838
MCL
BPNC

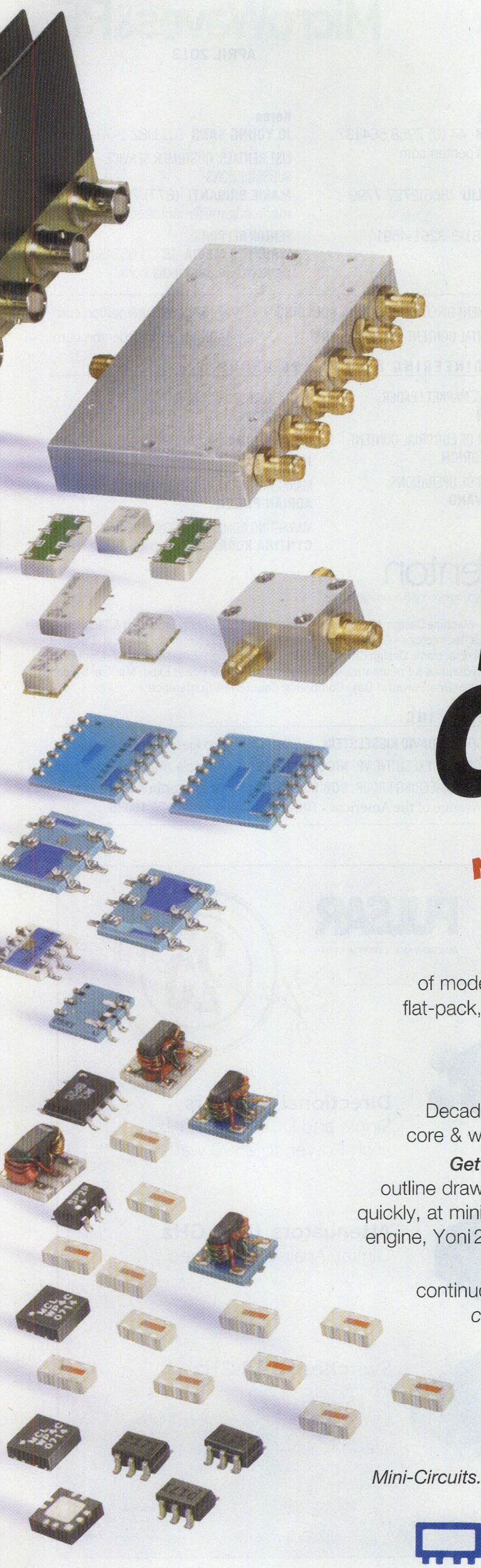

EDITORIAL

EDITOR IN CHIEF: **NANCY K. FRIEDRICH** (212) 204-4373 nancy.friedrich@penton.com

TECHNICAL CONTRIBUTOR: **JACK BROWNE** (212) 204-4377 jack.browne@penton.com

MANAGING EDITOR: **JEREMY COHEN** (212) 204-4243 jeremy.cohen@penton.com

GROUP DESIGN DIRECTOR: **ANTHONY VITOLO** tony.vitolo@penton.com

ART DEPARTMENT

CREATIVE DIRECTOR: **DIMITRIOS BASTAS** dimitrios.bastas@penton.com

SENIOR ARTIST: **JAMES MILLER** james.miller@penton.com

INTERN: **LUISANNY GARCIA**

PRODUCTION

GROUP PRODUCTION DIRECTOR: **JUSTIN MARCINIAK** justin.marciniak@penton.com

AD PRODUCTION COORDINATOR: **KARA WALBY** kara.walby@penton.com

CLASSIFIED PRODUCTION COORDINATOR: **LINDA SARGENT** linda.sargent@penton.com

AUDIENCE MARKETING

AUDIENCE MARKETING MANAGER: **BRENDA ROODE** brenda.roode@penton.com

ONLINE MARKETING SPECIALIST: **RYAN MALEC** ryan.malec@penton.com

Free Subscription • Status of Subscription • Address Change • Missing Back Issues
(866)-505-7173 microwaves&rf@halldata.com

SALES & MARKETING

BRAND DIRECTOR, e/DESIGN:
TRACY SMITH (913) 967-1324
Tracy.Smith@penton.com

REGIONAL SALES REPRESENTATIVES:
Northwest/Northern CA/ Western Canada
JAMIE ALLEN (415) 608-1959
Jamie.Allen@penton.com

South
BILL YARBOROUGH (713) 636-3809
Bill.Yarborough@penton.com

Midwest/Mid-Atlantic
STEPHANIE CAMPANA (312) 840-8437
stephanie.compana@penton.com

BRAND CHAMPION:
DAVID MADONIA (212) 204-4331
Dave.Madonia@penton.com

EUROPEAN SALES:
MARK DURHAM 44 (0) 7958 564137
mark.durham@penton.com

Taiwan, R.O.C
CHARLES C.Y. LIU (866)2727 7799

Japan
HIRO MORITA 81-3-3261-4591

Korea
JO YOUNG SANG (011)82-2-739-7840

LIST RENTALS, CUSTOMER SERVICE-SUBSCRIPTIONS:
MARIE BRIGANTI (877) 796-6947
marie.briganti@meritdirect.com

PENTON REPRINTS:
WRIGHT'S MEDIA (877) 652-5295
penton@wrightsmedia.com

ONLINE

ONLINE DEVELOPMENT DIRECTOR: **VIRGINIA GOULDING** virginia.goulding@penton.com

DIRECTOR OF DIGITAL CONTENT: **PETRA ANDRE** petra.andre@penton.com

DESIGN ENGINEERING & SOURCING GROUP

VICE PRESIDENT & MARKET LEADER: **BILL BAUMANN**

GROUP DIRECTOR OF EDITORIAL CONTENT: **NANCY K. FRIEDRICH**

GROUP DIRECTOR OF OPERATIONS: **CHRISTINA CAVANO**

GROUP DIRECTOR OF MARKETING: **JANE COOPER**

RESEARCH MANAGER: **JULIE RITCHIE**

MARKETING & EVENTS SPECIALIST: **ADRIAN PIAZZA**

MARKETING COMMUNICATIONS SPECIALIST: **CYNTHIA RODRIGUEZ**

Penton
Design Engineering & Sourcing Group

Electronic Design • Machine Design • Microwaves & RF • Source ESB • Energy Efficiency & Technology
Power Electronics Technology • Global Purchasing • Defense Electronics • Medical Design •
Mobile DevDesign • Electronic Design China • Motion System Design • Engineering TV • Electronic
Design Europe • Hydraulics & Pneumatics • Auto Electronics • Fluid Power Expo • Medical Silicon
Medical Prototyping • One Powerful Day • Combating Counterfeit Conference

PENTON MEDIA, INC.

CHIEF EXECUTIVE OFFICER: **DAVID KIESELSTEIN** david.kieselstein@penton.com

CHIEF FINANCIAL OFFICER/EXECUTIVE VP: **NICOLA ALLAIS** nicola.allais@penton.com

SENIOR VP, DESIGN ENGINEERING GROUP: **BOB MacARTHUR** bob.macarthur@penton.com

1166 Avenue of the Americas • 10th Floor • New York, NY 10036

PROBING FOR PORTABILITY

Your March 2013 issue, in particular, the Product Feature on the new pair of real-time spectrum analyzers from Tektronix (www.tek.com), was of great interest to me. The measurement capabilities of these two instruments—model RSA5115A, with a frequency range of 1 Hz to 15 GHz, and model RSA5126A, which operates from 1 Hz to 26.5 GHz—is quite impressive for anyone working in communications and with RF/microwave signals.

Your all-too-brief write-up/review on these analyzers brought back fond memories of the firm's models 492P and 494P portable programmable spectrum analyzers. Although not real-time analyzers, they were ruggedly built and designed for portability, with their large carrying handles and their rechargeable batteries. In their time, the 492P and 494P portable spectrum analyzers could be found at quite a large number of remote test sites, antenna towers, and in communications-industry repair vehicles. It is safe to say that those analyzers were an important part of cellular and other wireless communications systems achieving their reputations for performance and reliability.

But, in spite of your efforts to provide a "Product Feature" on the RSA5115A and RSA5126A analyzers, there was nothing in your review about whether these were portable instruments or not. Many of the applications for me and my associates require that a measuring instrument be brought to a test site and operated under its own power. Although the picture that was included in your report appears to show carrying handles on both sides of the RSA5126A's enclosure, your article never mentions portability, or whether the analyzers can run on a battery pack, or even the carrying weight of each instrument. I would hope when you "feature" a product in the future that you would include more of its vital features for the benefit of your readers.

DR. SIMON MAQUEDA
BLOOMINGBURG, NY

EDITOR'S NOTE

The editors of *Microwaves & RF* certainly appreciate your readership and opinions. Unfortunately, as you noted, it is not possible to cover every detail on a new instrument in a one-page story.

To answer your query, these analyzers are not the portable instruments like their predecessors, the 492P and 494P, since they weigh 64.7 lbs (29 kg). And they are designed for AC power, not battery. But they do include carrying handles to simplify transport and relocation, and they carry impressive measurement capabilities (more information about which can be gleaned from Tektronix's website).

Redefining RF and Microwave Instrumentation

with open software and modular hardware

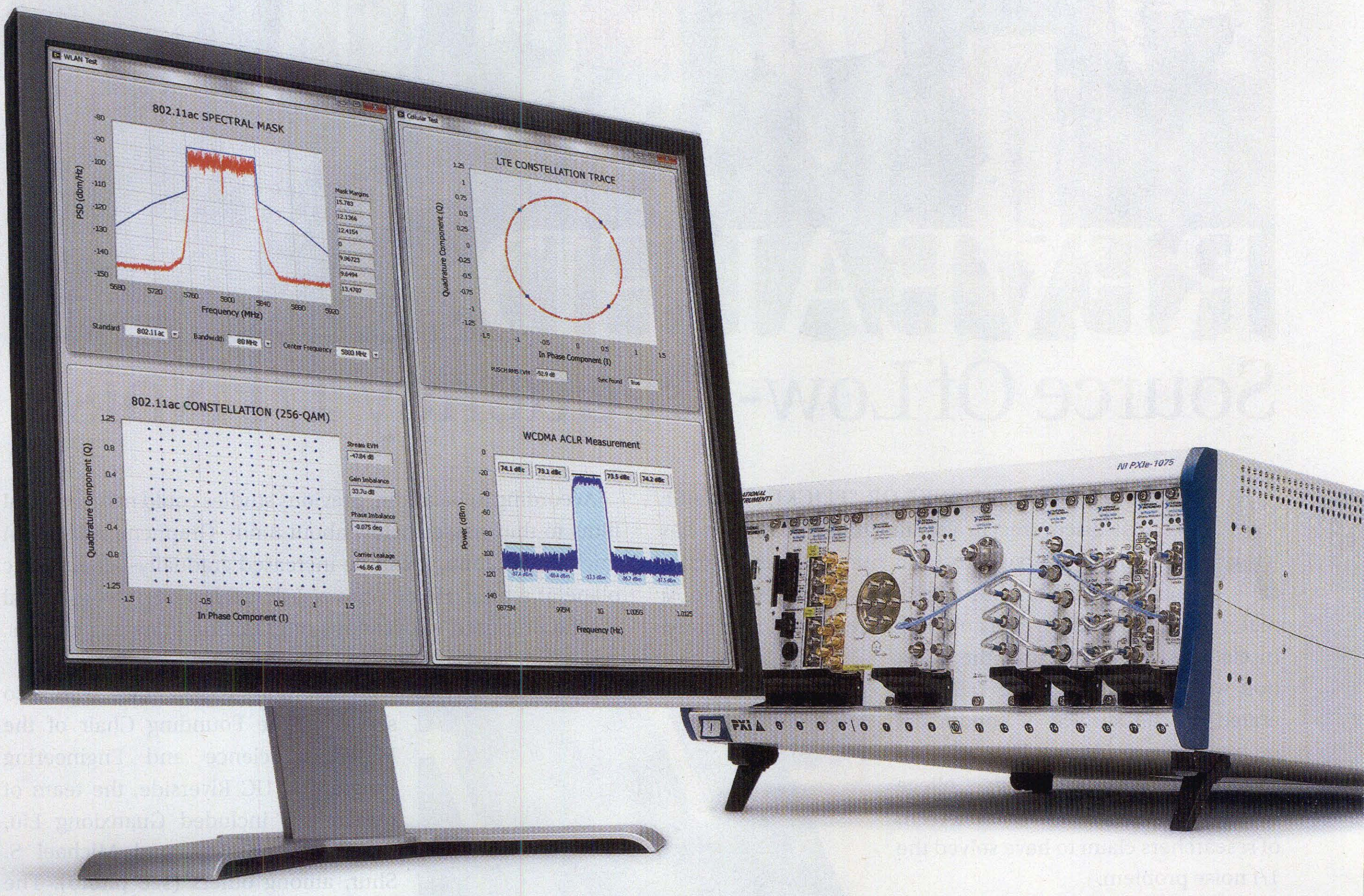

Achieve speed, accuracy, and flexibility in your RF and microwave test applications by combining National Instruments open software and modular hardware. Unlike rigid traditional instruments that quickly become obsolete by advancing technology, the system design software of NI LabVIEW coupled with NI PXI hardware puts the latest advances in PC buses, processors, and FPGAs at your fingertips.

WIRELESS TECHNOLOGIES

National Instruments supports a broad range of wireless standards including:

LTE	GSM/EDGE
802.11a/b/g/n/ac	CDMA2000/EV-DO
WCDMA/HSPA/HSPA+	Bluetooth

>> Learn more at ni.com/redefine

800 813 5078

NATIONAL INSTRUMENTS™

Using multi-layered graphene samples, this team of researchers has figured out what causes low-frequency electronic 1/f noise. They were led by Alexander A. Balandin, who is shown in the center (wearing the blazer). (Photo courtesy of Prof. A.A. Balandin, UC Riverside.)

REVEALED: Source Of Low-Frequency 1/f Noise

ALTHOUGH 1/f (OR "PINK" OR "FLICKER") NOISE was first discovered in vacuum tubes in 1925, it has been found everywhere from human heart rates to electrical currents in materials and devices. In most material systems, however, its origin has remained a mystery. In electronics in particular, the question was whether 1/f noise was generated on the surface of conductors or inside them. At the University of California, Riverside Bourns College of Engineering, a professor and a team of researchers claim to have solved the 1/f noise problem.

This noise is actually a signal or process—one with a power spectral density that is inversely proportional to the frequency. It is a key factor in electronics, impacting electronic device size and more. In a radar or communication device like a smartphone, for example, the signal's phase noise is largely determined by the 1/f noise level in the transistors used.

The team of researchers hailed from UC Riverside, Rensselaer Polytechnic Institute (RPI), and the Ioffe Physical-Technical Institute of the Russian Academy of Sciences. The group was led by Alexander A. Balandin, Professor of Electrical Engineering at UC Riverside. The researchers were able to answer questions on 1/f noise origin using a set of multi-layered graphene samples with thickness that continuously varied from around 15 atomic planes to a single layer of graphene **(see figure)**.

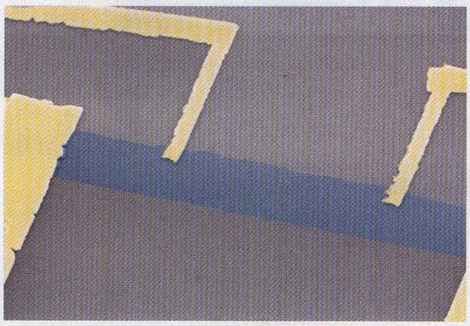

Pictured is a microscopy image of the graphene device used in the 1/f experiments at the University of California, Riverside. (Image courtesy of Prof. A.A. Balandin, UC Riverside.)

According to Balandin, previous studies could not test metal films to thicknesses below about 8 nm. Graphene is 0.35 nm thick. In addition, it can be increased gradually—one atomic plane at a time. He emphasized that this study was essential for the proposed applications of graphene in analog circuits, communications, and sensors.

In addition to Balandin, who also serves as the Founding Chair of the Materials Science and Engineering Program at UC Riverside, the team of researchers included Guanxiong Liu, Sergey Rumyantsev, and Michael S. Shur, among others **(see photo)**. The results of the research have been published in the journal *Applied Physics Letters* under the title: "Origin of 1/f Noise in Graphene Multilayers: Surface vs. Volume."

The research at UC Riverside was supported, in part, by the Semiconductor Research Corp. and Defense Advanced Research Project Agency (DARPA) through the Center for Function Accelerated nanoMaterial Engineering and the National Science Foundation. The work at RPI was supported by the US NSF under the auspices of I/UCRC "CONNECTION ONE" at RPI and by the NSF EAGER program.

Photonics Modulator Reaches 60 Gb/s

TOGETHER WITH Fujikura Ltd. (www.fujikura.co.jp), researchers from Singapore's A*STAR Institute of Microelectronics (IME; www.ime.a-star.edu.sg) have debuted 40- to 60-Gb/s silicon-based optical modulators. The modulators boast advanced multilevel modulation formats for high-speed, long-haul data transmission. In doing so, they bring the industry closer to attaining low-cost, ultra-high-bandwidth and small-footprint optical communications on silicon.

Each modulator consists of a set of silicon phase shifters, which are integrated in a nested Mach-Zehnder configuration. In terms of multilevel modulations, the modulators rely on simple quadrature-phase-shift-keying (QPSK) and differential-QPSK (DQPSK) formats. The result is increased information capacity, which creates more data-communication throughput for a given optical channel.

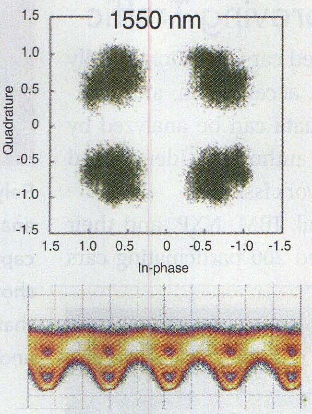

The modulators have demonstrated communication speeds of more than 40 and 60 Gb/s for DQPSK and QPSK, respectively. For channel grid spacing of 50 GHz, for example, 40G DQPSK results in a spectral efficiency that is 2X that of 20G with conventional on-off keying (OOK) format. These new modulators are smaller than conventional lithium-niobate modulators. Being CMOS-compatible, they also are less expensive to fabricate.

MARKET Quote

Top 10 states projected to gain jobs and revenue from unmanned aircraft systems (UASs) from 2015 to 2025:

1.	California	18,161
2.	Washington	9967
3.	Texas	8256
4.	Florida	4803
5.	Arizona	4260
6.	Connecticut	4084
7.	Kansas	3716
8.	Virginia	3517
9.	New York	3363
10.	Pennsylvania	2986

This is according to economic data from the Association for Unmanned Vehicle Systems International (AUVSI), which estimated the jobs that would be created by the unmanned aircraft industry following the integration of unmanned aircraft systems into the US National Airspace System (NAS). Integration is scheduled to take place in 2015. By 2025, AUVSI estimates that more than 100,000 new jobs will be created nationally. To see the full report, go to http://www.auvsi.org/econreport.

STANDARDS UPDATE

- To ensure that its consumers enjoy a uniform wireless power experience, PowerKiss (www.powerkiss.com) is joining the **POWER MATTERS ALLIANCE** (PMA; www.powermatters.org). PowerKiss currently provides over 1000 wireless charging spots at locations across Europe.
- **THE ALLIANCE FOR WIRELESS POWER** (A4WP; www.a4wp.org) has welcomed Samsung Electro-Mechanics, Gill Industries, and Integrated Device Technology (IDT) to its board of directors. These companies join A4WP Co-Founders Qualcomm, Inc. and Samsung Electronics to expand smartphone market-segment representation and impact on the A4WP board. Earlier this year, the group approved the Alliance for Wireless Power Version 1.0 interoperability specification and demonstrated prototype products.
- **THE WI-FI ALLIANCE** (www.wi-fi.org) and **WIRELESS GIGABIT (WIGIG) ALLIANCE** have finalized the agreement defining the consolidation of WiGig technology with certification development in the Wi-Fi Alliance. Essentially, the Wi-Fi Alliance will continue work begun in the WiGig Alliance, which focuses on features that extend WiGig capabilities beyond baseline connectivity. The consolidation of activities in the Wi-Fi Alliance will deliver closely harmonized connectivity and application-layer solutions using WiGig technology. Early 60-GHz implementations based on the WiGig specifications are now entering the market.
- **THE ZIGBEE ALLIANCE** (www.zigbee.org) announced the completion and public availability of its third specification, ZigBee IP. As an open standard for an IPv6-based full wireless-mesh-networking solution, ZigBee IP promises to provide seamless Internet connections to control low-power, low-cost devices. The specification enhances the IEEE 802.15.4 standard by adding network and security layers as well as an application framework.
- **THE PCI-SIG** (www.pcisig.com) and **MIPI ALLIANCE** (www.mipi.org) have begun procedural reviews of the Mobile PCI Express (M-PCIe) specification. The new specification enables the PCI Express (PCIe) architecture to operate over the MIPI M-PHY physical-layer technology. In doing so, it extends the benefits of the PCIe I/O standard to mobile devices.

Eindhoven Is Proving Ground For Improving Traffic

AS AUTOMOBILES ARE designed with more intelligence, they can share what they "know" to improve traffic safety. In a 12-month smarter-traffic trial in Eindhoven, The Netherlands, IBM (www.ibm.com) and NXP Semiconductors (www.nxp.com) demonstrated how the connected car can automatically transmit braking, acceleration, and location data. Such data can be analyzed by the central traffic authority to identify and resolve road network issues.

During the trial, IBM, NXP, and their partners equipped 200 participating cars with a device containing the NXP telematics chip, "ATOP" **(see figure)**. It gathers relevant data from the car's central communication system using the automotive controller-area-network (CAN) bus. Relevant sensor data, such as indicators of potholes or icy roads, was collected in-vehicle and transmitted to the cloud-enabled IBM Smarter Traffic Center.

Using IBM analytics, raw data from the vehicles highlighted 48,000 incidents over a period of six months from 1.8 billion sensor signals. Incidents included heavy rain, black spots, and fog, among others.

Relying on this telematics chip, analytics, and communications capabilities, connected-car technology showed that it can share vehicle data that will help traffic officials identify and resolve road network issues.

RFMD Changes GaAs Strategy

MANUFACTURING WILL SOON be phased out at RF Micro Devices, Inc.'s (RFMD; www.rfmd.com) Newton Aycliffe, UK-based gallium-arsenide (GaAs) pseudomorphic-high-electron-mobility-transistor (pHEMT) facility. Most GaAs manufacturing will be transitioned to the company's GaAs heterojunction-bipolar-transistor (HBT) manufacturing facility in Greensboro, NC. RFMD will partner with leading GaAs HBT foundries for additional capacity.

The transition will occur over the next 9 to 12 months to support existing millimeter-wave customer contracts. Once implemented, RFMD expects annual cost savings of approximately $20 million.

The Newton Aycliffe GaAs pHEMT facility had been RFMD's primary source for cellular switches. In recent years, however, the firm has transitioned to higher-performance, lower-cost silicon-on-insulator (SOI) switches. RFMD is currently seeking a buyer for the Newton Aycliffe facility.

Counterfeit Standard Singles Out Distributors

ACCORDING TO A 2011 Senate Arms Services Committee estimate, counterfeit parts are costing US taxpayers more than $6 billion a year. To address the problem of counterfeit electronic components infiltrating the defense supply chain, the International Electro-technical Commission's Quality Assessment System (IECQ) for electronic components has been proposed. This certification, dubbed AS6081, targets independent distributors.

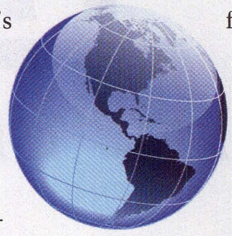

The AS6081 international counterfeit-avoidance standard mandates oversight by third-party auditors. To ensure that testing is performed when required, the certification demands transparency between the distributor and the procurement department purchasing the electronic components.

The SAE AS6081 standard ensures uniform requirements, practices, and methods to mitigate the risk of distributors purchasing and supplying counterfeit electronic parts throughout the defense and aerospace supply chains. This Counterfeit Avoidance Process Certification program is administered by the IEC IECQ based in Geneva, Switzerland. Secure Components LLC (www.securecomponents.com) is the first firm to complete an audit by DNV, which certified that this distributor conforms to the AS6081 Counterfeit Avoidance Standard. The first phase of the Secure Components audit was witnessed by ANAB, the IAF MLA signatory accreditation body of the US.

KUDOS

MARTIN COOPER—The industry legend, who led the engineering team that developed the first mobile phone, has been awarded the Charles Stark Draper Prize by the National Academy of Engineering (NAE). On April 3, 1973, Cooper—at the time, General Manager of Motorola's Communications Systems Division—became the first person to successfully make a handheld cell-phone call in public. The award, the NAE's highest honor, was presented at a ceremony in Washington, DC.

CASCADE MICROTECH—Has been named an Oregon Technology Award finalist in the Technology Company of the Year – Enterprise category. The award will be presented on April 25.

PEREGRINE SEMICONDUCTOR—Chief Financial Officer Jay Biskupski has been named CFO of the Year (Public Company) by the *San Diego Business Journal*. He was one of 45 nominees across four categories.

RF & MICROWAVE FILTERS

RLC has the customized filter solutions you need.

RLC manufactures a complete line of RF and Microwave filters covering nearly every application in the DC to 50 GHz frequency range. We offer different filter types, each covering a specific engineering need.

In addition, our large engineering staff and high volume production facility give RLC the ability to develop and deliver both standard and custom designed filters at competitive costs, within days or a few weeks of order placement.

- **Band Pass, Low Pass, High Pass & Band Reject**
- **Connectorized, Surface Mount, PCB Mount or Cable Filters**
- **Wave Guide Bandpass and Band Reject**
- **4th Order Bessel Filters**
- **Spurious Free, DC to 50 GHz, Low Loss, High Rejection**
- **Custom Designs**

*For more detailed information, or to access **RLC's exclusive Filter Selection Software**, visit our web site.*

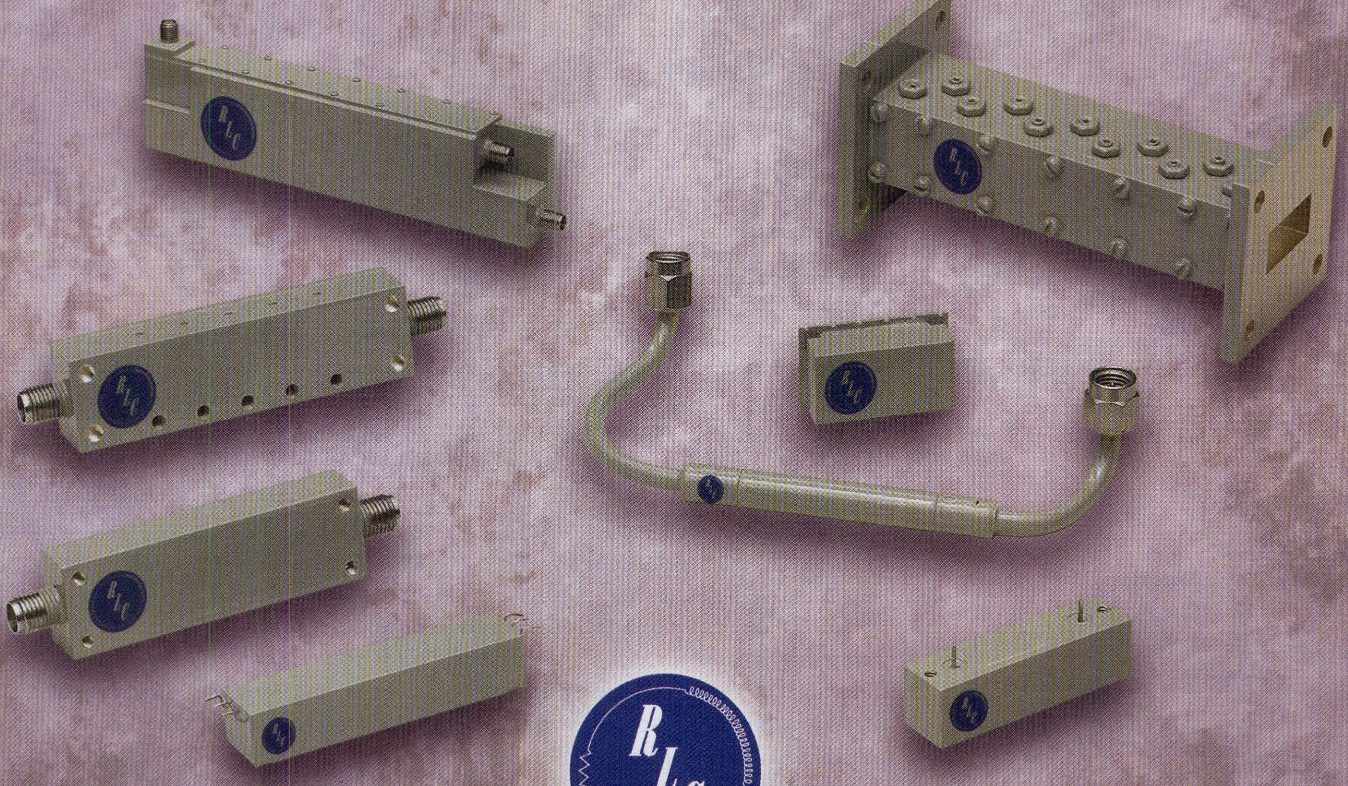

RLC ELECTRONICS, INC.

83 Radio Circle, Mount Kisco, New York 10549 • Tel: 914.241.1334 • Fax: 914.241.1753
E-mail: sales@rlcelectronics.com • www.rlcelectronics.com

ISO 9001:2000 CERTIFIED

VISA MasterCard

RLC is your complete microwave component source...
Switches, Filters, Power Dividers, Terminations, Attenuators, DC Blocks, Bias Tees & Detectors.

Industry Mourns Loss Of Jerry Fishman, ADI CEO

Analog Devices (www.analog.com) has forayed its signal-processing excellence into new capabilities across markets ranging from cellular to medical, entertainment, and automotive. Since 1996, much of these efforts were spearheaded and inspired by Chief Executive Officer (CEO) Jerry Fishman. Fishman was known for inspiring ADI employees with humor, honesty, and an open, direct manner. On March 28, Fishman passed away after an apparent sudden heart attack. He was 67 years old.

Many of today's veteran ADI employees were preceded by Fishman, who joined the firm in 1971 with a role in product marketing. He enjoyed a number of promotions through the years before being named President and Chief Operating Officer (COO) in 1991. In 1996, Fishman was named President and CEO.

In accordance with the company's bylaws, ADI President Vincent Roche has been appointed CEO on an interim basis by ADI's Board of Directors. Relying on the existing leadership team, Roche is hoping to seamlessly manage this dynamic business. The thoughts and prayers of the staff of this magazine—and many in the industry—go out to the Fishman family, as well as to Mr. Fishman's extended family at ADI.

PEOPLE

MAURY MICROWAVE—Zhang Nianmin has been named General Manager of the company's newly opened regional headquarters in Beijing, China. Nianmin previously worked for Agilent Technologies as a Sales Engineer, Marketing Engineer, and Business Development Manager. In addition, Yang Dongliang has joined the company as a Senior Applications Engineer based out of the Beijing office. Dongliang previously worked as an RF Engineer at Ericsson.

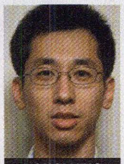
DONGLIANG

RAYTHEON CO.—Dr. Thomas A. Kennedy has been appointed Executive Vice President, Chief Operating Officer by the firm's board of directors. Kennedy previously served as Raytheon's Vice President and President of Integrated Defense Systems.

LEMKO CORP.—Has appointed Norman Fekrat Chief Strategy and Revenue Officer. Prior to joining Lemko, Fekrat served as a Vice President and Partner at IBM Global Services with responsibility for Telecom Networks Solutions.

CTIA–THE WIRELESS ASSOCIATION—Debbie Matties has joined the organization as Vice President of Privacy, a newly created role. Matties was previously Senior Attorney Advisor for Consumer Protection to former Federal Trade Commission (FTC) Chairman Jon Leibowitz. In addition, Heather Blanchard has been named Director of Wireless Internet Development (WID). Blanchard formerly served as a Strategic Communications Consultant for New Cicada.

LADYBUG TECHNOLOGIES—Orwill Hawkins has been named Vice President of Marketing. In addition to this role, Hawkins has served as President for Inter-Pac, Inc. for more than 25 years.


HAWKINS

BOEING—Has appointed Greg Hyslop Vice President and General Manager of Boeing Research & Technology. Hyslop most recently served as Vice President and General Manager of Boeing Strategic Missile & Defense Systems (SM&DS). Replacing him in that role is Jim Chilton, who was previously Vice President and Program Manager for Boeing's Exploration Launch Systems office.

E-CYCLE MOBILE—Co-Founder and Chief Executive Officer Christopher Irion has been recognized as one of 2013's Pros to Know by *Supply & Demand Chain Executive* magazine.

CONTRACTS

RELM Wireless—Has received orders from municipal public-safety agencies totaling approximately $899,000. The agencies are purchasing digital radios, base stations, and related accessories, which are collectively intended for deployment in fire and law-enforcement applications.

NuWaves Engineering—Has been awarded two contracts in support of unmanned-aircraft-system (UAS) data-link range-extension programs. The awards—both from undisclosed US Department of Defense (DoD) prime contractors—include developmental work to customize NuWaves' power-amplifier (PA) modules.

Space Systems/Loral (SSL)—Has been selected by Hughes Network Systems to build a high-capacity, Ka-band broadband satellite. Known as JUPITER 2/EchoStar XIX, the new satellite is expected to increase capacity for Hughes' North American broadband service by 50%.

Mercury Systems—Has received a $2-million follow-on order from an unnamed defense prime contractor. The order is for digital-signal-processing (DSP) modules intended for an airborne synthetic-aperture-radar (SAR) application.

RELM WIRELESS Wins multiple public-safety orders

CAMBIUM NETWORKS Nets Air Force radio deal

Cambium Networks—The company's PTP 45600 radio has been chosen for the US Air Force's Theater Deployable Communications (TDC PMO) program. The radio will be used to provide voice, video, and data functions for both deployable warfighters and first-response missions worldwide.

RFMD—Has been selected by an undisclosed smartphone manufacturer to supply multiple third- and fourth-generation (3G and 4G) Long-Term-Evolution (LTE) components. These components will be utilized in a 4G flagship smartphone platform.

Agilent Technologies—Plextek RF Integration has selected the company's Momentum software to simulate high-frequency circuit and MMIC designs.

Peregrine Semiconductor—The firm's UltraCMOS phase-locked-loop (PLL) frequency synthesizer and prescaler devices were designed into six Globalstar mobile-communication satellites. Built by Thales Alenia Space, the low-Earth orbit satellites were launched on February 6.

FRESH STARTS

AWR Corp.—For a fourth consecutive year, the firm is offering its Graduate Gift Initiative to graduating electrical engineering students worldwide. This program provides qualified graduates with free, fully functional one-year licenses of AWR software.

AR—Has added a subsidiary in Germany, known as AR Deutschland. This distributor joins fellow European subsidiaries AR UK, AR France, and AR Benelux.

Maury Microwave—Has opened a regional headquarters in Beijing, China. This location will offer service and support to Maury's Chinese customer base.

National Technical Systems (NTS)—Has entered into an agreement with RF Exposure Lab, a wireless testing laboratory. RF Exposure will provide specific-absorption-rate (SAR) testing services at NTS' laboratory in Fremont, CA.

Luso Electronics—Has signed a franchised distribution agreement with Rhode Island-based A.T. Wall Co. Luso will distribute A.T. Wall's tubing components in France, Ireland, and the United Kingdom.

Plessey Semiconductors—Atlantik Elektronik GmbH has been named European sales representative for Plessey's full product line. This distribution agreement includes the regions of Central and Eastern Europe, Scandinavia, and Turkey. In addition, Plessey has signed an Asian distribution agreement with Supreme Components, Inc. (SCI) covering the markets in Singapore, Thailand, Malaysia, and Vietnam.

XMA Corp.-Omni Spectra—Has appointed High-tech Sales as its manufacturing representative for the New England region.

Giga-tronics—Has agreed to sell its SCPM product line to Teradyne for approximately $1 million. The closing of the sale was expected to occur on or about April 1.

Vaunix—Has enlisted Amska Amerikanska Teleprodukter as its sales representative for Sweden, Denmark, Norway, and Finland.

GPS Innovation Alliance—Five national organizations have joined the alliance as affiliate members: the American Trucking Association, the Association for Unmanned Vehicle Systems International (AUVSI), Boat US, the National Rural Electric Cooperative Association (NRECA), and the National Society of Professional Surveyors (NSPS).

Digi-Key Corp. and MEMSIC—Have signed a global distribution agreement. MEMSIC's full line of MEMS sensor components, inertial systems, and wireless-sensor networks is now available for purchase through Digi-Key's global websites.

QLP—Has opened a 5600-sq.-ft materials laboratory in Woburn, MA. The facility will focus on developing next-generation materials and processes for electronics and energy-storage applications.

Coaxicom—Has added sales representatives in South America with specific concentrations on Brazil and Argentina. In addition, the firm is developing a network of representatives in Europe, Asia, and other foreign markets.

Emrise Corp.—Has purchased the building and land that house its Pascall Electronics subsidiary in Ryde, England.

Custom MMIC—Has appointed Castle Microwave and SM Electronic Technologies as its technical sales representatives. Castle Microwave will represent Custom MMIC in the United Kingdom while SM Electronic will fulfill that role in India.

Richardson RFPD—Has launched a website resource focused on silicon-carbide (SiC) technology for energy and power applications (www.richardsonrfpd.com/sicpower). In addition to product and supplier information, the section offers links to technical resources.

Analog Devices—Is launching a series of design conferences for analog, mixed-signal, and embedded-systems engineers in collaboration with Xilinx and MathWorks. Two events are currently scheduled: April 25 in Boston, MA, and April 30 in Santa Clara, CA.

WORLD'S WIDEST SELECTION

VCOs

RoHS COMPLIANT

RoHS models available, consult factory.

12 to 6840 MHz from $11.95 ea. (qty. 5)

Want a miniature surface mount, shielded plug-in, or rugged coaxial voltage controlled oscillator with the right stuff for your project? Go to minicircuits.com! You'll find over 800 standard catalog models, ***always in stock***. They're optimized to meet specific requirements, from narrow, broad, or octave bandwidths to linear tuning, low phase noise, dual output, 5V PLL/synthesizer implementation, or size, as small as 0.25 x 0.25 x 0.1". Selection is a snap, even with so many models to choose from! Just enter your requirements, and our patented search engine, Yoni 2, searches *actual test data* to find the models that meet your needs. And if you need a custom design, challenge us with a phone call or email! We constantly design new models to meet new needs—so you'll get a quick response, fast turnaround times, and all at a surprisingly low price. Give your competition *real competition*...specify a Mini-Circuits VCO!

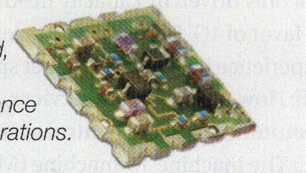

All SMT components are glued, as well as soldered, in place for long-term, reliable performance even after multiple reflow operations.

Mini-Circuits...we're redefining what VALUE is all about!

Mini-Circuits®

ISO 9001 ISO 14001 AS9100

P.O. Box 350166, Brooklyn, New York 11235-0003 (718) 934-4500 Fax (718) 332-4661

Yoni2® U.S. Patents 7739260, 7761442 ***The Design Engineers Search Engine*** *finds the model you need, Instantly* • For detailed performance specs & shopping online see minicircuits.com

IF/RF MICROWAVE COMPONENTS

359 rev U

Inside Track with Eran Eshed,

CO-FOUNDER, ALTAIR SEMICONDUCTOR

Interview by NANCY FRIEDRICH

NF: Long Term Evolution (LTE) is becoming the dominant cellular-communications technology being used by devices in the US. Obviously, the industry has gotten over the initial hurdles. What issues stand in the way of full-scale deployment?

EE: This is primarily a matter of time. The competitive dynamics are such that once one significant carrier starts deploying and achieves meaningful coverage, other carriers respond. The obvious example is the way that AT&T responded to Verizon Wireless' aggressive LTE launch. Deploying cellular infrastructure is a capital-intense process and, even logistically, it takes time. I am very much encouraged by the pace at which leading carriers deploy LTE infrastructure in their respective markets. To note a few, there are Verizon Wireless and AT&T in the US; DoCoMo and Softbank in Japan; SKT and KT in Korea; Yota in Russia; and Reliance Industries soon in India. This represents a potential subscriber base of more than 1 billion before the end of this year.

NF: Having sold your chip to Verizon, you have unique insight into these networks. Beyond meeting the needs of today's data-hungry consumers, what do carriers hope to achieve with their increased capacity?

EE: To clarify, we achieved Verizon Wireless chipset certification. This means that any Altair customer that wishes to develop and deploy a product on the Verizon LTE network has a simpler and lower cost of doing so than before—and in comparison to alternative solutions, which are not yet certified. We will soon start seeing new services, such as HD voice-over-LTE (VoLTE) and video broadcast (using LTE's eMBMS feature), as well as various multimedia services like high-quality video calling. Note that the push toward blanket-covering markets with LTE is not only driven by capacity needs, but also by the desire to re-farm 3G spectrum in favor of 4G. Doing so will lower the cost per bit and substantially enhance user experience by means of higher speeds, lower latency, and better quality.

NF: How do additional services, such as medical applications like remote monitoring and the control of smart homes, factor into these plans?

EE: The machine-to-machine (M2M) segment has high growth potential for LTE. Most M2M services today are delivered over old second-generation (2G) networks (GPRS/EDGE and CDMA). As carriers shut these networks down, they migrate their customers onto LTE. This provides better cost/efficiency while ensuring service longevity. These factors are very important parameters for M2M customers that deploy a network of sensors, for example, and want to avoid the costs associated with truck roles for replacing them when carriers power off their 2G/3G networks.

NF: What do you believe are the biggest issues still facing operators in the US?

EE: A year ago, I would answer spectrum availability. But this doesn't seem to be a problem since AWS spectrum has been auctioned. And LTE's ability to bond narrow bandwidth channels into one logical and higher-bandwidth channel ("carrier aggregation," in LTE terminology) ensures that even non-contiguous and narrowband spectrum can be fully utilized. At the end of the day, this is a CAPEX question—and its answer will help to determine the pace of deployment and coverage.

NF: Looking at other countries and regions rolling out 4G, are they plagued by similar problems or different ones?

EE: LTE has a very fragmented band map. In markets that cannot guarantee an attractive enough return on investment for infrastructure and device vendors, the pace of deployment may be slower. This is not a factor of chipset capability. For a device maker to invest in creating a product variant that supports a certain band combination, a minimum volume is required.

NF: Carriers now want to offer the smartphone to more budget-constrained customers so that they too will start using new data services. How can smartphones be made less expensive?

EE: The key here is to remove 2G/3G support from these phones and make them LTE-only. This will eliminate the very high costs associated with silicon—and maybe more importantly, the royalty cost of 3G technologies. This, of course, requires good enough coverage and the ability to roam between markets. We believe we will start seeing this become a reality in 2015 and beyond.

NF: Does Altair plan to help with this goal?

EE: Absolutely. Our strategy is centered on offering high-performance and very cost-efficient LTE-only semiconductor solutions. A smartphone based on Altair technology and without support for 3G can achieve disruptive price points. We are bringing this concept to bear in markets like India, where cost is paramount.

NF: Altair has a rather storied history. I read that your management and technology executives were among the founding team of Libit Signal Processing. That fabless chip company was acquired by Texas Instruments in 1999 for $365 million. Can you explain how you got from there to Altair Semiconductor?

"I believe you will see devices based on LTE-A chipsets in the market in 2014."

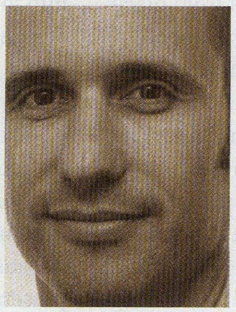

EE: The core team of Altair was always somehow involved in broadband-communications chip development. As a team—and under different companies—we developed more than six broadband-communications technologies from concept to mass production and more than 40 different modem and radio chipsets over the course of the last 15 years. In 2005, we identified the emerging trend of mobile broadband. We decided to start our own company to realize the potential of this market. We then developed a chipset processor, which was software-centric and allowed us to develop three different 4G technologies without having to spin the chip. We started with WiMAX, but quickly realized that the world was going LTE. Since 2006, we have been focusing on this market.

NF: Which key executives have been with the company through all of these iterations?

EE: We are very proud to have almost all senior-level management with us from day one to today. Our management is very enthusiastic and committed to what we are trying to achieve, which has helped us get through some bumps in the road in the past.

NF: Your headquarters is in Israel, correct? I suppose that is more proof that success in the cellular market doesn't depend on an address in Silicon Valley?

EE: Israel is a hub of immense talent in the technology space—and specifically, in the wireless-communications space. We built a team of passionate and professional individuals, who are fully committed to the success of the company and to the vision that we outlined. Over the years, we've established sales offices in the US, China, India, Japan, Europe, and Taiwan.

NF: To succeed in the handset market, a chipmaker has to stay ahead of its competition in price, performance, size, etc.—while its competitors try everything they can to overtake it. What do you consider Altair's strong points, which allow it to stay in the lead?

EE: When it comes to LTE-only chipsets (i.e., without 2G/3G), we believe we have one of the highest-performing modems in the market with unmatched power consumption and—no less important—the smallest silicon die in the market. So we are well positioned to cope with the erosion in LTE-chipset average selling prices (ASPs). We also have a very competitive roadmap. We just announced two baseband processors and a radio chip.

NF: When do you expect LTE-Advanced (LTE-A) chipsets to begin being designed into smartphones and other devices?

EE: We just announced a couple of LTE-A-capable chipsets, which will be in mass production before the end of this year. I believe you will see devices based on these chipsets in the market in 2014.

NF: What challenges must be overcome for the successful adoption of LTE-A?

EE: Power consumption is a major challenge as speeds increase and the amount of processing required from the communications engine grows dramatically. We believe our unique processor architecture will allow us to overcome this challenge and offer 10X higher LTE speeds at comparable power consumption to existing 3G. This is essential for the user experience, which cannot degrade as technology evolves. MWRF

Compact Automotive Antennas Juggle Multiple Bands

AS AUTOMOBILES EVOLVE into individual wireless-communications networks, antenna makers have faced the task of providing ever-smaller antennas that handle more bands. Among the choices serving this market from placement on the roof or trunk are monopole, helix, and printed antennas. Mounted in a rear or side mirror, dashboard, or glove compartment, however, cellular antennas are less at risk to external agents. Unfortunately, such placement also puts them closer to electronic components that may impact antenna performance. At Italy's Politecnico di Torino, two multiband-antenna designs that seek to overcome such issues have been designed by Sergio Arianos, Gianluca Dassano, Francesca Vipiana, and Mario Orefice.

The two antennas cover four frequency bands: GSM, E-GSM, DCS, and PCS. They are specifically designed to be integrated in a printed-circuit board (PCB), placed inside a plastic box, and mounted under the vehicle dashboard. The first version is a planar printed antenna. It is fully integrated into the PCB, minimizing cost. The second design—a three-dimensional antenna—requires no dedicated space on the PCB, as it is an independent part of the whole device.

Though slightly more expensive, this latter antenna does boast better performance. Yet both antennas show satisfactory performance in the required frequency bands. Because they have been created with the presence of other electronic components in mind, the antennas should not be affected by the presence of those components on the PCB. See "Design of Multi-Frequency Compact Antennas for Automotive Communications," *IEEE Transactions On Antennas And Propagation,* Dec. 2012, p. 5604.

Architecture Cracks Terahertz Power Generation And Tuning

TO REALIZE a complete terahertz system, a challenge still remains in the high-power, tunable signal source. When using LC-resonator-based voltage-controlled oscillators (VCOs), performance begins to degrade beyond 100 GHz. While frequency multipliers solve some of these problems, they require a high-power external source—something undesirable in a fully integrated terahertz source. One alternative could lie in a VCO architecture based on coupled oscillators in a loop configuration, which has been created by Yahya M. Tousi and Ehsan Afshari from Cornell University and Omeed Momeni from the University of California at Davis.

To realize a high-power VCO at the sub-millimeter-wave and terahertz band, the signal source should be able to generate high harmonic power above the device f_{max}. The generated power also should be efficiently delivered to the output load. Finally, a frequency-tuning mechanism is needed that will not adversely affect the first two requirements.

In this approach, multiple core oscillators are coupled to generate, combine, and deliver their harmonic power to the output node without using varactor diodes. Leveraging the theory of nonlinear dynamics, the researchers are able to control the coupling between the cores. In doing so, they can set their phase shift and frequency.

Because of the new architecture's approach to frequency control, the tradeoff between frequency tuning and power generation in conventional VCOs is largely resolved. The researchers fabricated two high-power terahertz VCOs in a 65-nm low-power bulk process. According to measurements, the first one provides 0.76 mW output power at 290 GHz with a 4.5% tuning range. The second VCO puts out 0.46 mW at 320 GHz with a 2.6% tuning range. See "A Novel CMOS High-Power Terahertz VCO Based on Coupled Oscillators: Theory and Implementation," *IEEE Journal Of Solid-State Circuits,* Dec. 2012, p. 3032.

Cross-Spectral Phase Noise Is Measured On Terahertz Source

TO ENSURE THE characterization of phase noise for applications that will integrate terahertz components into usable products, many are developing terahertz phase-noise measurement capabilities. The National Institute of Standards and Technology (NIST; www.nist.gov), for example, is working on phase-noise measurement systems that support 670 GHz, 850 GHz, and 1.05 THz. Recently, the first cross-spectral phase-noise measurement of a spectrally clean terahertz source was presented by NIST's J.A. DeSalvo, A. Hati, C. Nelson, and D.A. Howe.

Their approach is to combine even-harmonic mixers with a 2.5-GHz frequency comb. The result is a phase-noise measurement system in waveguide (WR1.5), which is achieved by use of cross-spectral and digital phase-noise measurement techniques. At 670 GHz, an upper bound of this system's noise floor is −20, −40, and −60 dBc/Hz at 1-, 100-, and 10,0000-Hz offsets, respectively.

The team also measured a commercial, low-phase-noise, 670-GHz source at offset frequencies from 0.1 Hz to 1.0 MHz. See "Phase-Noise Measurement System for the Terahertz-Band," *IEEE Transactions on Terahertz Science And Technology,* Nov. 2012, p. 638.


50 MHz to 18 GHz
NOW, JUST TWO AMPLIFIERS COVER IT ALL!
PHA-1+
0.05-6 GHz
$1.99 ea. (qty. 20)
Gain 13.5 dB
Pout 22 dBm
NEW
AVA-183A+
5-18 GHz
$6.95 ea. (qty. 20)
Gain 14.0 dB
Pout 19 dBm
The PHA-1+ is a highly advanced E-PHEMT amplifier poised to be the workhorse for your wireless applications! An ultra-high dynamic range, low noise, and exceptional IP3 performance (42 dBm typical at 2 GHz), make it ideal for LTE or TD-SCDMA (see website for ACLR and EVM data). Good input and output return loss—across almost 7 octaves—extend its use to CATV, wireless LANs, base station infrastructure, and more, with no external matching required for 50 Ω systems!
Our new AVA-183A+ delivers excellent gain flatness (+/-1.0 dB) across its entire frequency range! High isolation (37dB typical) makes it very useful as a buffer amplifier in a wide variety of applications, from satellite to P2P, EWF, & radar—with no external matching required for 50 Ω systems. Just go to minicircuits.com for electrical, mechanical, & environmental specifications, performance curves, and S-parameters—these models are in stock and ready to ship today!
RoHS compliant
Keep a few extras on hand! Order Designer Kit K1-AVA+, and get 10 of each for only $88.95!
Mini-Circuits...we're redefining what VALUE is all about!
Mini-Circuits®
ISO 9001 ISO 14001 AS9100
P.O. Box 350166, Brooklyn, New York 11235-0003 (718) 934-4500 Fax (718) 332-4661
Yoni2® U.S. Patents 7739260, 7761442
The Design Engineers Search Engine finds the model you need, Instantly • For detailed performance specs & shopping online see minicircuits.com
IF/RF MICROWAVE COMPONENTS
478 rev J

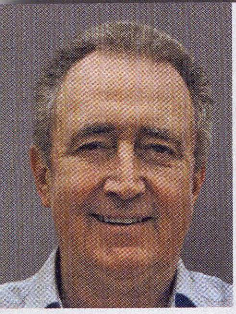

Microwaves in Europe

PAUL WHYTOCK, *European Editor*

Flexible RFID Sensor Tag Could Cut Food Waste

EUROPEAN STUDIES into global food wastage indicate that 40% to 50% of all food being produced for Europe is being wasted. Surprisingly, 10% to 15% of that wastage is happening during supply and delivery operations to consumer retail outlets. In addition, the food industry discards an estimated $25 billion of spoiled goods every year. Within every home, $300 worth of bruised fruit, bad meat, and other perishable goods are thrown away annually. This issue has serious implications for the global supply of adequate food stocks. It also contributes to escalating food costs. In a technological step forward that could combat this wastage, Europe's CATRENE-Pasteur project has developed a flexible tag that can track and monitor the quality of food in the supply chain.

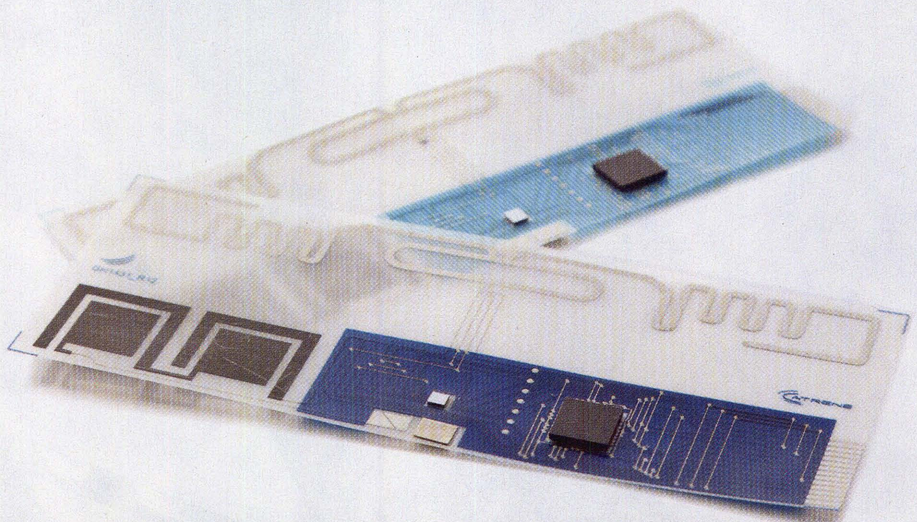

Here is a technology demonstrator of the CATRENE-Pasteur project, which integrates an RFID chip, microcontroller, and sensor IC into a flexible tag.

This monitoring system integrates an RF-identification (RFID) chip, microcontroller, and sensor integrated circuit (IC) into a flexible tag **(see photo).** The sensor IC, which will be made commercially available later this year, incorporates temperature, relative humidity, and light sensors. As a result, it can monitor the quality of a range of foods.

To perform such monitoring, the tag attaches to bulk transportation containers. It then provides continuously updated data on how long the food stored in those containers will stay fresh. This could help food distributors minimize the amount of food that is spoiled before it reaches the retailer.

Researchers from Holst Centre and Imec played a role in integrating the ICs into the flexible tag. This involved the creation of low-temperature encapsulation techniques that would not damage the low-cost plastic substrate used in the tag. To integrate the sensor IC, the team developed a process that protects most of the chip, but leaves the sensing area exposed to make measurements. This process attaches the IC to the encapsulation material using an adhesive conductive film. Using lasers, that film is then machined to the required size and shape. This technique ensures that the sensing area remains uncontaminated.

Holst Centre and Imec also participated in the development of additional gas sensors. Eventually, those sensors may be used to monitor the controlled atmosphere in which many foods are packaged. By creating ultra-thin metal-oxide films, they were able to enhance the sensitivity of oxygen and carbon-dioxide sensors. The sensor can operate at room temperature, which reduces power requirements. For the carbon-dioxide sensor, the team achieved sensitivity in the 300-to-5000-ppm concentration range used in food-packaging applications.

Further models for food-quality prediction are being developed based on available sensor data. They will be translated into algorithms that can be implemented on the smart sensor tag. In addition, technologies are being developed to reduce power requirements and boost read efficiency.

The first-generation (Gen1) demonstrator of the RFID-sensor tag provides a test prototype to validate system feasibility. Although it is a modular test platform, the final, fully integrated version will be a battery-assisted RFID tag with full sensor functionality. In addition to making accurate shelf-life predictions for specific food items, it will be able to sense a number of different parameters, such as temperature, pH, and gas levels.

According to the CATRENE-Pasteur project, a vast variety of applications will result from the successful development of a marketable platform. They include supply-chain uses, such as traceability and quality management. In addition, domestic applications include the detection of hazardous gases like carbon monoxide. Medical monitoring could be performed to ensure therapy compliance. Applications even range to construction—for example, for corrosion monitoring. The CATRENE-Pasteur project was funded by the governments of Austria, Belgium, the Netherlands, and Spain. Participants include major European companies, research institutes, and universities.

JACK BROWNE | Technical Contributor

AMPLIFIERS

Draw Upon A Variety Of Technologies

MANY DIFFERENT DEVICE TECHNOLOGIES ARE EMPLOYED FOR GAIN IN RF, MICROWAVE, AND MILLIMETER-WAVE AMPLIFIERS, BASED ON REQUIRED BANDWIDTHS AND OUTPUT-POWER LEVELS.

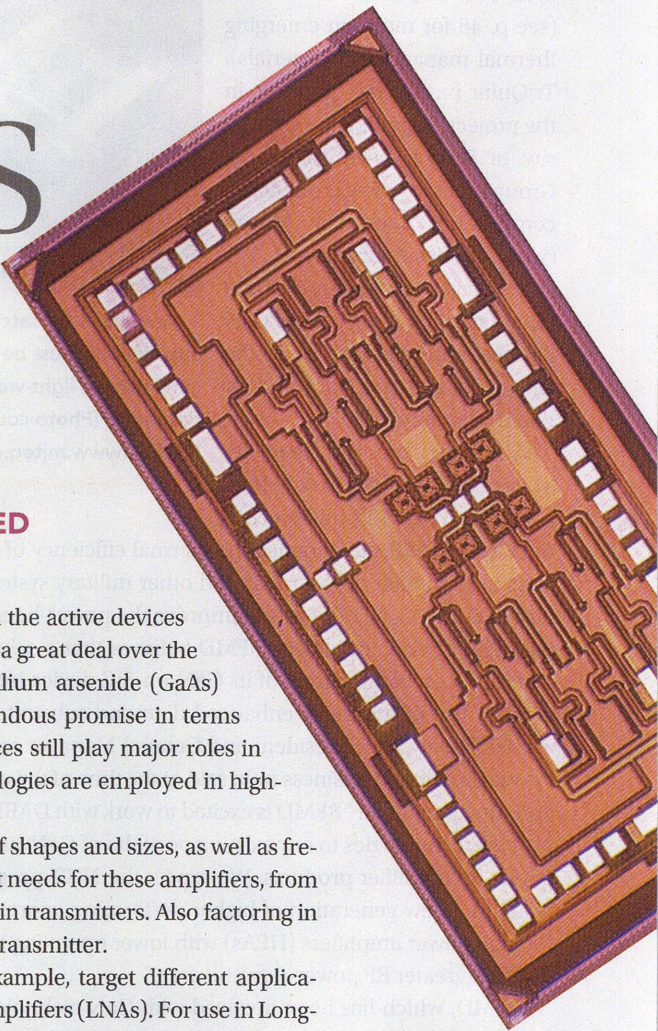

DARPA has not yet abandoned silicon solid-state power in favor of GaN devices, as evidenced by the organization's Efficient Linearized All-Silicon Transmitter ICs (ELASTx) program (see p. 40).

Amplifier technology tends to change over time, depending on the active devices available. Although active-device technologies have advanced a great deal over the past 20 years—with semiconductor technologies such as gallium arsenide (GaAs) maturing, and gallium-nitride (GaN) devices offering tremendous promise in terms of high power levels at high frequencies—vacuum tube devices still play major roles in RF/microwave amplification applications. A variety of technologies are employed in high-frequency amplifiers, each with its own set of benefits and features.

Amplifiers for RF/microwave applications are available in a wide range of shapes and sizes, as well as frequency ranges and power levels. This diversity stems from the many different needs for these amplifiers, from low-noise amplification in receivers to boosting signals to high power levels in transmitters. Also factoring in are the many additional medium-power stages in between the receiver and transmitter.

Companies such as Skyworks Solutions (www.skyworksinc.com), for example, target different applications with different sets of performance levels in their miniature low-noise amplifiers (LNAs). For use in Long-Term-Evolution (LTE) and wideband-CDMA (W-CDMA) cellular communications infrastructure applications, the firm's model SKY65369-11 surface-mount amplifier features a typical noise figure of just 0.9 dB from 832 to 862 MHz with a 35-dB gain control range. To keep things small, it is supplied in a 16-pin MCM housing measuring just 8 × 8 × 1.3 mm. For broader frequency coverage, the same company's model SKY67015-396LF LNA achieves almost the same noise figure (at typically 1 dB) but covers a frequency range from 30 to 3000 MHz. Suitable for ISM-band applications, it is supplied in a similarly small housing as the model SKY65369-11 amplifier and includes 15.5 dB fixed gain across its frequency range.

Certainly, no solid-state technology has shaken up the RF/microwave amplifier design world in recent years quite like gallium nitride (GaN) active devices. The number of companies now producing GaN amplifiers is large and growing, due to the high power density of the technology and the interest on the part of such customers as the Defense Advanced Research Projects Agency (DARPA). One of those GaN producers, TriQuint Semiconductor (www.triquint.com), which has been working on GaN technology since 1999, recently received a $2.7 million contract from DARPA for the nominal purpose of tripling the power-handling capabilities of GaN circuits. This Near Junction Thermal Transit (NJTT) project will build on TriQuint's GaN on silicon carbide (SiC) technology to achieve higher RF/microwave solid-state power levels than currently available.

According to James L. Klein, TriQuint's Vice President and General Manager for Infrastructure and Defense Products, "We are very pleased that DARPA selected TriQuint to develop this critical technology. Like other programs we have supported, NJTT will set the stage for substantial MMIC performance enhancements including reduced size, weight, and power consumption while increasing reliability and output power."

TriQuint hopes to combine its GaN-on-SiC process technology with new thermally conductive materials, thus reducing heat buildup around the active GaN devices and permitting higher output-power levels in their GaN amplifiers and devices (see p. 48 for more on emerging thermal-management materials). TriQuint has several partners in the project, including the University of Bristol (www.bris.ac.uk), Group4Labs (www.group4labs.com), and Lockheed Martin (www.lockheedmartin.com). TriQuint is also heading process and manufacturing projects on GaN devices and amplifiers for the United States Army, Navy, and Air Force laboratories.

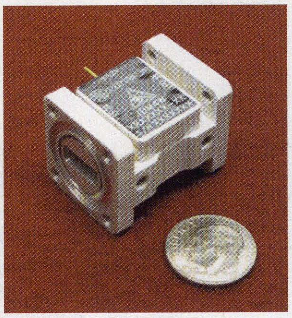

1. Amplifiers for satcom applications must be housed in miniature, light-weight packages. [Photo courtesy of MITEQ (www.miteq.com).]

Similarly, late last year, RF Micro Devices, Inc. (www.rfmd.com) received a $2.1 million contract from DARPA to enhance the thermal efficiency of GaN circuits used in high power radar and other military systems. Also part of DARPA's NJTT efforts to improve the power-handling capabilities of GaN amplifiers, RFMD believes that a solution will be found as a combination of its GaN-on-SiC device technology and the use of thermally enhanced diamond substrate materials. Jeff Shealy, Vice President and General Manager of RFMD's Power Broadband business unit, said at the time of the contract's announcement that "RFMD is excited to work with DARPA to apply new technologies to our existing portfolio of GaN-based high power RF amplifier products. We expect the NJTT program will result in a new generation of higher performing, more compact RF high power amplifiers (HPAs) with lower operating temperature and greater RF power-per-unit area."

RFMD, which has been involved with GaN technology since 2000, is also working with Group4Labs on the contract, along with the Georgia Institute of Technology (www.gatech.edu), Stanford University (www.stanford.edu), and the Boeing Co. (www.boeing.com). The firm has been a strong supplier of GaN-based power amplifiers for cable-television (CATV) applications.

For those seeking an informal education on GaN technology, Advantech Wireless (www.advantechwireless.com) offers an eight-page white paper on GaN amplifiers, "A new generation of Gallium Nitride (GaN) based Solid State Power Amplifiers for Satellite Communication," available for free download from the firm's website. It details how GaN amplifiers fare in satellite-communications (satcom) applications when compared with silicon LDMOS or GaAs-based power amplifiers. The GaN amplifiers are claimed to be about 50% smaller than their technology counterparts, with considerably less power consumption and less generation of heat. Advantech Wireless, which designs and manufactures GaN power amplifiers through Ku-band frequencies for commercial and military use, is currently offering its GaN power amplifiers as replacements for traveling-wave-tube amplifiers (TWTAs) in satcom applications.

In embracing the growing popularity of GaN amplifier technology, EMPower RF (www.empowerrf.com) is selling its lines of GaN power amplifiers as replacements for silicon bipolar, MOSFET, LDMOS, and GaAs FET amplifiers. It is offering the newer GaN amplifiers as smaller, lighter, and more reliable units for a given frequency range than any of the other solid-state amplifier types. The firm offers both GaN amplifier modules and complete amplifier systems with power supplies in a rack-mount housing.

As an example of the former, model BBM3K5KKO is a compact Class AB linear GaN power amplifier design capable of 100 W minimum output power and 125 W typical output power from 500 to 2500 MHz. It provides 50-dB minimum power gain with -20 dBc typical harmonic levels and –70 dBc typical spurious levels. At a package size of 7.4 × 3.6 × 1.06 in., it consumes 10 A from an external +28-VDC supply. It is also available as a rack-mount unit with the power supply inside the housing.

Of course, DARPA wouldn't enjoy its successful track record in research without "hedging its bets" and investing in a number of different technologies for high-frequency amplifiers. The organization still believes that silicon technologies will support high-frequency amplification through millimeter-wave frequencies.DARPA's Efficient Linearized All-Silicon Transmitter ICs (ELASTx) program is seeking novel approaches for increases in power amplifier efficiency, while at the same time achieving improved linearity by way of integrated linearization architectures. One of the goals of the program is a silicon-based transmitter with 65% power-added efficiency (PAE) with low distortion for 64-state quadrature-amplitude-modulation (64QAM) waveforms. The program is looking at bandwidths of 3.5 GHz at 45 GHz, 5 GHz at 94 GHz, and 8 GHz at 138 GHz for these next-generation silicon amplifiers and transmitter ICs.

2. The large heat sink is required to help dissipate heat from the power amplifier's active devices. [Photo courtesy of Mini-Circuits (www.minicircuits.com).]

An important design goal for many applications is sufficient amplifier power for a light-weight package, especially in airborne applications or in satcom systems. Amplifiers for the latter, such as the JDMW-Series amplifiers from MITEQ (www.miteq.com), are low-noise amplifiers (LNAs) designed to operate from 18 to 21 GHz with 30-dB gain in a hermetic package measuring just 1.18 × 0.87 in. and weighing just 23 g (**Fig. 1**). These LNAs feature a noise temperature of 97 K (a noise figure of only 1.25 dB) with current consumption of only 75 mA at +12 VDC. The amplifier has an operating temperature range of –30 to +65°C and yields +8 dBm output power at 1-dB compression. The amplifiers are available with numerous options, including RF input limiters and waveguide flanges.

For any RF/microwave amplifier technology, delivering consistent performance levels with high reliability is an important goal whether the amplifier is for low-noise or power applications. As an example, the model ZHL-100W-13+ power amplifier from Mini-Circuits (www.minicircuits.com) is designed to withstand short-circuit and open-circuit operating conditions even when running at full output-power levels, but depends on a heat sink to dissipate excess heat (**Fig. 2**). The amplifier is also designed to be unconditionally stable under a wide range of operating conditions. The transistor amplifier is rated for 100 W typical saturated output power from 800 to 1000 MHz but is also usable from 750 to 1050 MHz. It provides 50-dB typical gain with gain flatness of typically ±1 dB from 800 to 1000 MHz. Supplied with SMA input connectors and Type-N output connectors, it draws 10 A at a typically supply of +28 VDC. The amplifier, which has a typical noise figure of 7 dB, achieves +49 dBm typical output power at 1-dB compression and +50 dBm typical output power at 3-dB compression.

To achieve the high reliability, users are asked to provide proper heat sinking and heat removal from the amplifier, ensuring that its making base-plate temperature is +60°C to ensure proper performance. Users can establish favorable long-term conditions for the amplifier by supplying a heat sink with thermal resistance of 0.035°C/W or better.

In spite of the excitement about GaN technology, solid-state amplifiers have not yet replaced RF/microwave tubes and amplifiers based on vacuum tubes. As noted in the report beginning on p. 86, such amplifiers may be considerably larger than solid-state amplifiers for the same frequencies, but they are also capable of much higher continuous-wave (CW) and pulsed output-power levels. It is the hope of organizations such as DARPA that vacuum tubes may one day be replaced at high frequencies by solid-state amplifiers with much higher power densities than possible today. But for now, tubes and transistors coexist fruitfully in RF/microwave applications. MWRF


Tight quarters,
crowded conditions, no room for error.
It's all in a day's work.
See how FieldFox measures up—watch the video. Scan the code or visit http://qrs.ly/r520pow
People count on you every day. And you can count on the compact Agilent FieldFox vector network analyzer (VNA). It's a full 2-port VNA delivering the precise measurements you've come to expect from a benchtop unit, but in a kit-friendly 6.6 lb. package. So no space is too small to stop you from achieving big success.
FieldFox Vector Network Analyzers
Four models up to 26.5 GHz
MIL-PRF-28800F Class 2 rugged
Agrees with benchtop measurements
94 dB dynamic range
Agilent and our Distributor Network
Right Instrument.
Right Expertise.
Delivered Right Now.
TESTEQUITY
800-732-3457
www.testequity.com/agilent
Learn about hassle-free calibration and more with our application note series
www.testequity.com/Agilent_FieldFox
© Agilent Technologies, Inc. 2012

JACK BROWNE | Technical Contributor

Automobiles Racing To Higher Frequencies

Wireless technologies are helping to boost the convenience and safety of modern automobiles by taking advantage of ISM bands and unused frequencies.

AUTOMOBILES AND AUTOMOTIVE markets represent a growing area of opportunity for suppliers of high-frequency components and hardware. Just look at wireless safety products: Many newer cars are being designed with short-range sensors operating at 24 GHz and adaptive-cruise-control (ACC) and long-range forward-looking radar systems at 77 GHz. These transmitter and receiver devices rely on dependable high-frequency integrated-circuit (IC) processes that are also competitive enough to support products in a wide range of automotive markets. So far, achieving reliable performance at 77 GHz has not been a hurdle for a growing number of IC manufacturers and high-frequency companies supporting automotive RF/microwave applications.

The frequency band from 76 to 77 GHz has proven to be attractive for a number of automotive radar-based safety applications, including for adaptive cruise control (ACC), blind-spot detection (BSD), emergency braking, forward collision warning (FCW), and rear collision protection (RCP). Freescale Semiconductor (www.freescale.com), for example, has used its silicon-germanium (SiGe) BiCMOS semiconductor process as the basis for its Xtrinsic brand model PRDTX11101 VCO+Tx voltage-controlled oscillator (VCO) and transmitter combination IC for 77-GHz automotive ACC and long-range radar applications—as well as for shorter-range applications, such as BSD and cross traffic alerts.

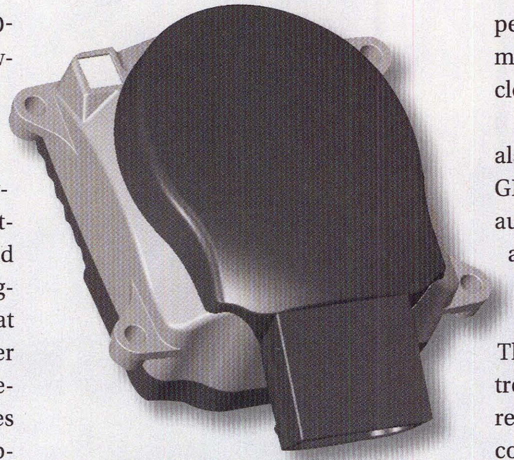

1. Model AC3 is an automotive radar system working at 77 GHz that can detect "targets" as far as 250 m. [Photo courtesy of TRW Automotive (www.trw.com).]

The PRDTX11101 SiGe radar transmitter includes an on-chip frequency divider with output ports for frequency control. It can operate with a single +3.3-VDC supply (with only 1.5-W power consumption) and support short-range (to 20 m) as well as long-range (to 200 m) automotive radar applications at 77 GHz. It features low phase noise of –93 dBc/Hz offset 1 MHz from a 77-GHz carrier, and can produce two outputs at +13 dBm and 77 GHz. The IC incorporates an amplifier circuit that maintains stable current consumption during activation and de-activation of the radar pulses to minimize thermal drift of the oscillator signal. The device has an on-chip temperature sensor to maintain consistent performance by monitoring device temperature and making gain adjustments, and uses a peak power detector for enhanced transmitter efficiency by applying open- and closed-loop output power control.

Infineon (www.infineon.com) has also developed a high-frequency (200-GHz) SiGe semiconductor process for automotive applications, which it uses as the basis for its Radar System IC (RASIC™) series of components for applications in the 76 to 77 GHz range. The product line includes voltage-controlled oscillators (VCOs) and dielectric resonator oscillators (DROs) as well as complete automotive radar transceiver functions for ACC and collision-warning applications. The devices are available as unpackaged bare die. For example, the model RXN740 single-chip transceiver includes all of the core functions of a radar front end, such as a VCO, transmit power amplifier, and as many as four frequency mixers, as well as on-chip test functions. With the device, a radar sensor manufacturer can produce a four-channel monostatic radar system for long-range (such as ACC) automotive radar applications at 76 to 77 GHz, taking advantage of the chip's self-test and diagnosis functions to monitor temperatures and output levels. The radar IC is usable across the full temperature range from –40 to +125°C; it has full automotive qualification according to Automotive Electronic Congress (AEC) AEC-Q100 requirements.

TriQuint Semiconductor (www.triquint.com) supports automotive radar sensor designers with a variety of 77-GHz GaAs monolithic-microwave-integrated-

circuit (MMIC) products for ACC and FCW applications. The function-specific devices allow system designers to develop customized transmit and receive configurations at 77 GHz. As an example, model TGA4705-FC is a flip-chip low-noise amplifier (LNA) that is usable from 72 to 80 GHz. Based on 0.13-µm GaAs pseudomorphic-high-electron-mobility-transistor (pHEMT) technology, the amplifier has nominal noise figure of 6 dB from 76 to 77 GHz and nominal gain of 23 dB from 76 to 77 GHz. The LNA chip measures just 2.24 × 1.27 × 0.38 mm and operates on typical drain voltage of +2.5 VDC, typical drain current of 60 mA, and typical gate voltage of +0.18 VDC.

For larger signals, the company's model TGA4706-FC flip-chip medium-power amplifier is designed for applications from 76 to 83 GHz. It offers 15-dB gain at 77 GHz with saturated output power of +14 dBm at that frequency. Also based on 0.13-µm GaAs pHEMT technology, the chip measures 1.86 × 1.37 × 0.38 mm and runs on typical drain voltage of +3.5 VDC, gate voltage of +0.2 VDC, and quiescent drain current of 125 mA.

TriQuint also offers the model TGC4702-FC, a flip-chip downconverting in-phase/quadrature (I/Q) mixer for automotive radar applications. It covers RF and local oscillator (LO) ranges of 75 to 82 GHz and an intermediate-frequency (IF) range of DC to 100 MHz. The mixer achieves RF-LO isolation of 18 dB at 77 GHz with 12-dB conversion loss at 77 GHz. The mixer chip, which measures 2.46 × 1.89 × 0.38 mm, is based on GaAs heterojunction-bipolar-transistor (HBT) technology. It is rated for maximum bias current of 15 mA at +2 VDC bias voltage.

TRW Automotive (www.trw.com), a company with a long history of semiconductor development, offers automotive radar solutions at both 77 and 24 GHz. For example, the model AC3 77-GHz long-range radar **(Fig. 1)** provides outstanding speed resolution at distances as far as 250 m. The firm's cost-effective model AC100 midrange radar system operates at 24 GHz and provides ACC and FCW functionality. The high-end model AC1000 is a scalable 77-GHz platform that provides a full 360-deg. sensing capability. All three of the automotive radar systems are capable of operating under all weather conditions.

Of course, not all opportunities for electronic devices in automotive applications require such high frequencies. For some time, Toshiba (www.toshiba.co.jp) has produced ICs for automotive remote-keyless-entry (RKE) applications, including the model TB31372FNG receiver IC for the 315-MHz band and the model TC32306FTG receiver IC for the 434-MHz band. Both chips work with an IF of 220 kHz and feature on-chip IF filters with 300-kHz bandwidth, detector circuits, and on-chip VCO with phase-locked-loop (PLL) circuitry. The RKE ICs are supplied in 24-pin SSOP housings.

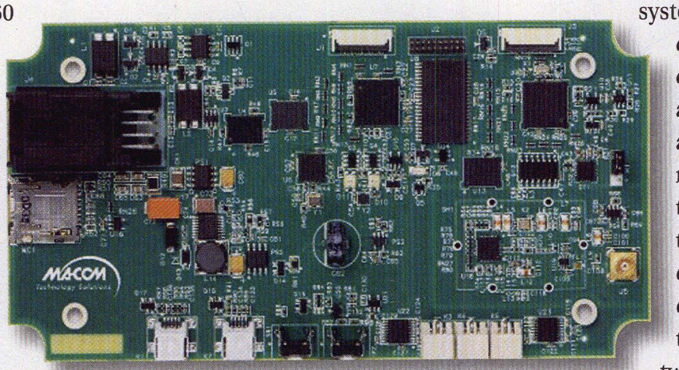

2. The eHorizon module combines a processor, GPS receiver, and electronic map to provide a "look ahead" on a road. [Photo courtesy of M/A-COM Technology Solutions (www.macomtech.com).]

The model PQJ7910 variable intelligent polling receiver (ViPER) from NXP Semiconductors (www.nxp.com) operates within Industrial-Scientific-Medical (ISM) band frequencies to support car access and tire-pressure monitoring system (TPMS) applications. The device features a programmable state machine and a polling timer, so it can operate autonomously while waiting for access signals from car keys and TPMS transmitters. The device's programmable channel filter enables optimum performance for all possible protocols and applications. Model PQJ7910, which is designed for operating temperatures from –40 to +105°C, is available in versions for use from 315 to 915 MHz or 434 to 915 MHz.

The models ATA5830 and ATA5780 are transceiver and receiver ICs designed for multiband use at ISM frequencies of 310 to 318 MHz, 418 to 477 MHz, and 836 to 928 MHz for a variety of wireless automotive applications. These include RKE, remote start, passive entry go (PEG), and tire-pressure-monitoring-system (TPMS) applications. The devices combine receiver or transceiver circuitry with a microcontroller core, enabling each device to poll multiple application channels to create a cost-effective automotive electronics remote control. The two ICs are pin-compatible devices to simplify their reuse in one-way and two-way automotive access systems. They are each supplied in a 5 × 5 mm QFN32 package and draw very little current in their power-down states, thereby conserving battery life.

Lastly, the Advanced Driver Assist System (ADAS) eHorizon module from M/A-COM Technology Solutions (www.macomtech.com) is a board-level automotive electronic product that functions more like an "assistant driver" than an electronic aid. The module **(Fig. 2)**, which integrates a Global Positioning System (GPS) receiver and microprocessor along with a NAVTEQ map, attempts to plot upcoming road features to improve the quality and safety of a driver's ride.

Using the map and GPS information, the processor works with an automobile's systems to save fuel, reduce carbon-dioxide emissions, and boost the efficiency of an automobile for a given travel route. Although high-frequency electronics cannot yet tell the future, this is one module that certainly prepares an automobile for what roads lie ahead. MWRF

JACK BROWNE | Technical Contributor

Handling The Heat In RF/MW Circuits

Thermal management of RF/microwave circuits is growing more challenging as the power densities of newer high-frequency transistors continue to so dramatically increase.

THERMAL MANAGEMENT OF AN RF/MICROWAVE COMPONENT, circuit, or system is simply a matter of removing heat from sensitive areas of a design that can suffer damage or performance degradation from the heat. Of course, providing the right mix of thermally conductive materials to extract heat from an active source (such as a power transistor) or a thermal pathway (like a transmission line or circuit trace) may not always be so simple. For some designs, the addition of a component that may improve thermal management—e.g., a heat sink to an amplifier—may also thwart efforts at making the design as small as possible. But any attempt to understand the flow of heat through an electronic design can help improve the performance and reliability of that design. For most electronic components, circuits, and systems, maintaining a design at a lower operating temperature usually translates into improved performance and reliability.

The flow of heat through a high-frequency circuit can involve various input and output connectors and/or waveguide components. Most microwave components and systems, however, are built upon printed-circuit-board (PCB) materials and rely heavily on them for thermal management. Heat that is applied to or generated within a PCB material must flow away from the PCB materials and its active devices, then be dispersed in the equipment packaging, heat sinks, and ambient air. The choice of PCB material is therefore key in the thermal management of a high-power circuit or system.

Ideally, a PCB material can handle energy with a minimum amount of loss, with energy from on-circuit devices (such as transistors) or an external source (such as an amplifier from another circuit) transferred without generating undue heat. A circuit with a high amount of energy loss will transform some of the energy into heat, and that heat must be effectively dissipated to ensure the reliability of the circuit. An RF/microwave PCB is formed with dielectric materials and conductive metals, such as copper, to transfer high-frequency signals with minimal loss and distortion.

Because a PCB material will expand and contract with changing temperatures (caused by the heating effects of lost energy), the material components of a PCB are usually carefully selected. They usually have closely matched coefficient of thermal expansion (CTE) so that, for example, a PCB's dielectric material and copper conductors will expand at the same rate (usually about 17 ppm/°C) when power is applied or generated within a circuit on the PCB. Ideally, a PCB material has been engineered with dielectric and conductor that are closely matched in the three dimensions (x, y, and z or width, length, and thickness) of the material to minimize possible stress that can occur at joints between the conductors and the dielectric materials as they expand and contract.

The way a circuit is designed can also contribute to its thermal management. One example is through practical application of plated through holes (PTHs) to dissipate heat from an active device. Multiple PTHs can provide thermal paths from an active heat source—such as a power transistor—through a circuit's dielectric layer or layers to a metal ground plane, dissipating the heat produced by the active device.

Manufacturers of RF/microwave integrated circuits (ICs) in

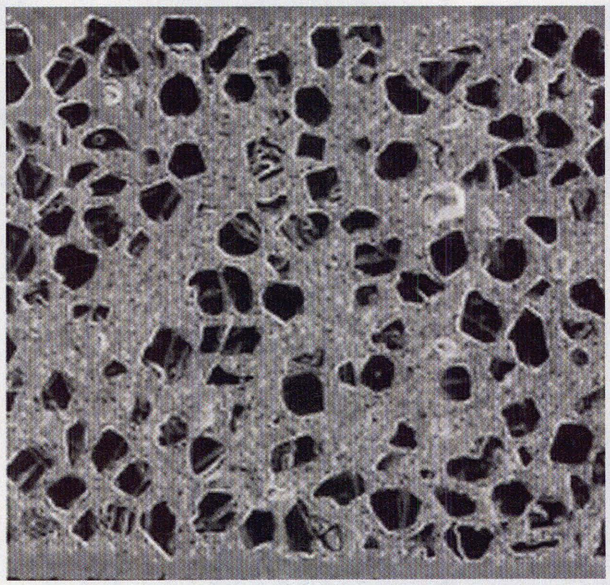

This photograph shows the microstructure of the high-thermal-conductivity aluminum diamond material used for heat sinks and in packages for high-power RF/microwave devices, such as GaN transistors. [Photo courtesy of Nano Materials International Corp. (www.nanomaterials-intl.com).]

surface-mount housings typically provide mounting instructions for their devices in terms of proper heat flow away from the component and through the PCB. The number of solder-filled PTHs, their diameters, and their density on the PCB are often specified for a particular active device to ensure that sufficient thermal flow is achieved through the PCB and to the ground plane, without also rendering a circuit board that is unfit for manufacturing. Some surface-mount IC manufacturers will go as far as providing measurements of the thermal resistance from the package junction to the PCB's heat sink—of benefit for circuit designers desiring to incorporate the thermal models in their computer-aided-engineering (CAE) high-frequency simulation software.

A PCB material's thermal conductivity, which is presented in watts of power per meter of material per degree Kelvin (W/mK), provides some indication of its effectiveness in dissipating heat, since it is a measure of the material's capability to conduct heat. It can be used to compare the different rates of energy loss as heat through different materials. Quite simply, a PCB material with high value of thermal conductivity enables a circuit to operate at higher power levels with better heat flow away from active devices than a PCB material with lower value of thermal conductivity. In a PCB material, a conductor, such as copper, has very high value of thermal conductivity (about 400 W/mK) while the PCB's dielectric material has very low value of thermal conductivity. In fact, the dielectric material serves as a thermal insulator.

However, the use of PTHs can help the flow and dissipation of heat from the top circuit layer through the dielectric layer to the bottom ground layer. In addition, different PCB material products can be compared by their composite thermal conductivity values, when comparing different materials for high-power applications in which a goal is to minimize operating temperature.

Controlling the temperature of a high-frequency circuit can have a direct impact on circuit performance since the relative dielectric constant of a PCB varies as a function of temperature. This quality is defined by a material parameter known as the thermal coefficient of dielectric constant, usually defined in units of ppm/°C. Because changes in a PCB material's dielectric constant result in changes in an RF/microwave circuit's impedance (which is typically maintained at 50 Ω), it is critical to minimize temperature effects at high frequencies (and high signal power levels) to minimize signal reflections at mismatched impedances that can lead to amplitude losses and phase distortions. Tightly controlled thermal coefficient of dielectric constant and CTE characteristics are signs that a PCB material will deliver high levels of performance (with minimal swings in temperature) when handling high power levels.

> **Attempts to understand the flow of heat through an electronic design can ultimately help to improve the performance and reliability of that design.**

Of course, in some extremely high-power applications, such as radar and electronic-warfare (EW) systems, designers may be facing the integration and thermal management of a high-power vacuum electron device such as a traveling-wave tube (TWT) or magnetron (see p. 86 for more on vacuum-tube devices). As described in an application note from Communications & Power Industries (www.cpii.com), "Recommendations for Cooling High-Power Microwave Devices," (publication AEB-31) multiple water baths are often necessary to safely transfer the heat produced by these devices away from the devices themselves and critical components within their systems.

Thermal management should be a high-level priority for any high-frequency design intended for high long-term reliability, especially if that design must operate at higher power levels and/or in an operating environment at elevated temperatures. A wide range of PCB material products are currently available, with a wide range of performance parameters including low loss and high thermal conductivity. A PCB material's MOT, while not the ultimate guideline for selecting a circuit material for high-power applications, can be used as a parameter for comparison among different PCB products for a potential application.

In some cases, newer RF power semiconductor devices, such as gallium-nitride-on-silicon-carbide (GaN-on-SiC) power transistors, are challenging the best designers of "thermally responsible" circuits with their extremely high power densities. In many cases, materials with higher thermal conductivities are being sought in place of or in addition to traditional PCB materials as a means of channeling heat away from these high-power-density semiconductor devices. The two-pronged challenge is in finding a heat spreader material that has a CTE close in value to the high-power semiconductor material, such as GaN or SiC, but also with high thermal conductivity.

After considerable research, work is currently being done on aluminum diamond metal-matrix-composite (MMC) materials **(see figure)** with extremely high thermal conductivity (500 W/mK or more) for efficient withdrawal of heat from GaN and other high-power semiconductors in high-frequency circuits. The MMC materials are typically based on a primary metal such as aluminum, copper, or silicon, and a secondary material, such as diamond or silicon carbide. Aluminum diamond MMC materials have shown a great deal of promise in their capabilities of meeting this two-pronged challenge for reliable thermal management of high-power RF/microwave devices—either when used as heat sinks or as base materials in semiconductor packages. So far, commercial adoption of these materials has been limited by high costs, but numerous suppliers are working to improve their production methods. MWRF

KENNETH V. PUGLIA
Principal
E x H Consulting Services,
146 Westview Dr., Westford, MA 01886;
(978) 692-4850, e-mail: kvpuglia@verizon.net.

Source Serves FMCW RADAR

DIRECT-DIGITAL-SYNTHESIZER (DDS) TECHNOLOGY CAN PROVIDE THE AGILITY AND FREQUENCY AND PHASE CONTROL NEEDED TO DRIVE HIGH-PERFORMANCE FREQUENCY-MODULATED-CONTINUOUS-WAVE RADAR SYSTEMS.

RADAR SENSORS based on frequency-modulated-continuous-wave (FMCW) methods benefit from high-quality signal sources. To complement them, a frequency-agile linear-FM source with excellent spectral purity was developed using a commercial direct-digital synthesizer (DDS) as a reference source for a wide-bandwidth phase-locked-loop (PLL) frequency synthesizer. By employing a simple FMCW radar architecture, it was possible to evaluate a linear-frequency-modulated (LFM) source under closed-loop operational conditions.

Due to their architectural simplicity, FM-based radar systems are among the most elementary types of radar equipment.[1] Radar sets based on FM require a minimum number of components compared to other radar systems and offer ease of signal processing, owing to the narrow signal bandwidth of the received information following frequency translation to baseband.

The capability of FMCW radar systems to achieve high receiver sensitivity and range resolution is directly related to the phase noise and linearity of the transmit and receive signal sources or oscillators.[2] In many cases, these sources are unitary. Numerous techniques have been applied in source design to achieve good spectral purity, such as low spurious content and low phase noise, particularly for sophisticated radar and signal generation applications. DDS integrated-circuit (IC) devices have matured in recent years and have shown a great deal of promise for radar applications.

Unfortunately, DDS devices still suffer fundamental limitations with respect to clock frequency, the linearity available from digital-to-analog converters (DACs), spurious-free-dynamic-range (SFDR) performance, and tuning word memory capacity.[3] To overcome these, a number of frequency synthesizer architectures have been developed. Specifically, a DDS device in combination with PLL techniques offers a simplified architecture to achieve good frequency agility and low phase noise.

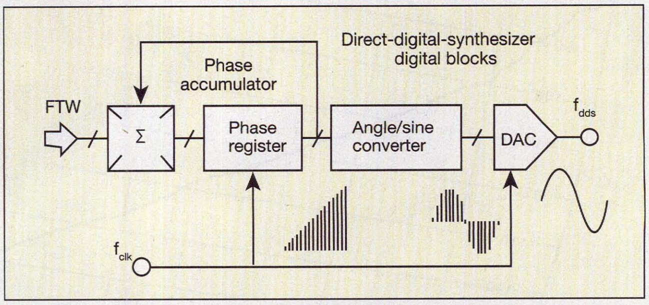

1. This simplified diagram shows the basic function blocks in the radar system's DDS signal source.

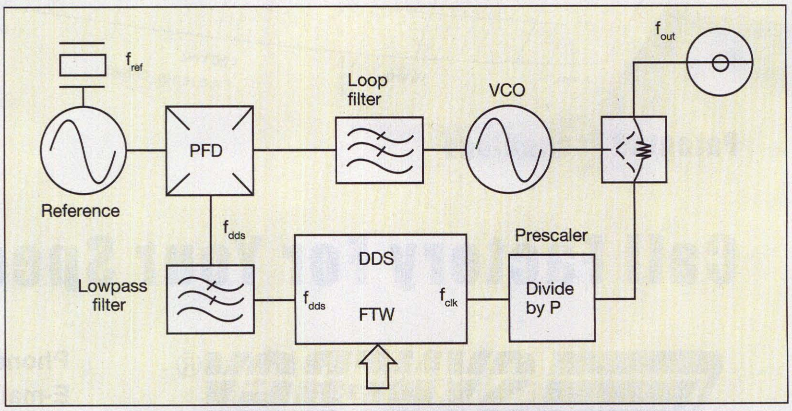

2. In this block diagram, a DDS device is installed with a PLL feedback path.

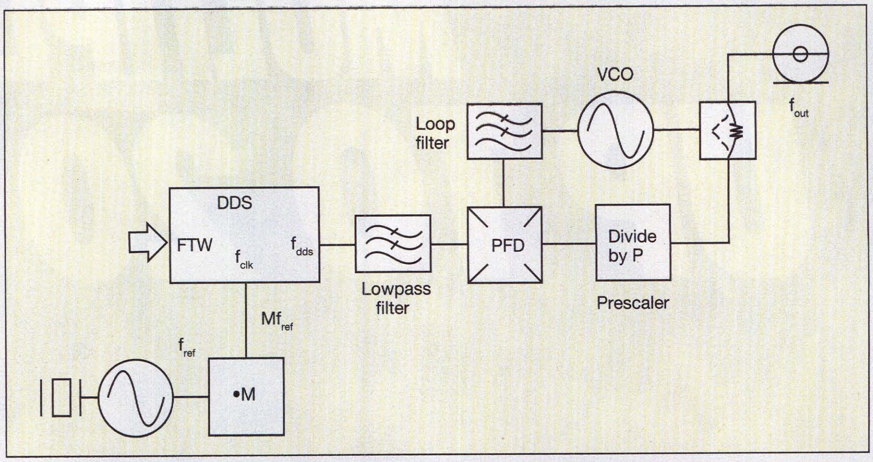

3. This block diagram shows a DDS reference for a PLL frequency synthesizer.

Figure 1 displays a very basic structure for a DDS, with a phase accumulator, angle-to-sine-wave converter, and digital-to-analog converter (DAC) graphically represented. A frequency tuning word (FTW) establishes the phase increment to be added to the phase register upon each cycle of the reference clock. The output of the phase accumulator provides the address for the angle-to-sine-wave converter—basically, a lookup table—where the address is converted to the respective point of a sinusoid and subsequently transformed from the digital domain to the analyzer domain by means of the digital-to-analog converter.

Because the data points of the output waveform are represented by digitally stored values, the DDS defines a sampled data system with the attendant constraints—e.g., Nyquist sampling, output amplitude rolloff, DAC quantization noise and spurious, and image and harmonic signals. In spite of these limitations, many of a DDS' spectral limitations can be mitigated through the use of output filters and judicious selections of reference clock parameters and output frequency plan.[3]

Table 1: Summarizing the performance of a commercial DDS source.

Parameter	Symbol	Requirement
Frequency range	f_0	530 to 630 MHz
Frequency resolution	f	1 Hz
Phase noise	ℓ(fm)	-130 dBc/Hz (at 10 kHz)
Spurious (max.)	---	-75 dBc
Switching speed	---	200 µs
Reference frequency	f_{re}	10 MHz
Prescaler modulus	P	1
Loop modulus (max.)	M	63
Loop bandwidth (approx.)	BW	150 kHz

The output frequency of a DDS can be found from Eq. 1:

$$f_{dds} = (FTW/2^n)f_{clk} \quad (1)$$

where:
f_{dds} = the DDS output frequency;
FTW = the binary frequency tuning word;
n = the number of digital bits in the frequency tuning word (typically 24 to 48 b); and
f_{clk} = the clock frequency (in Hz).

The DDS output frequency is a fraction of the clock frequency, with resolution that can be found by means of Eq. 2:

$$\Delta f_{dds} = f_{clk}/ 2^n \quad (2)$$

By way of example: For a FTW of 32 b and 1-GHz clock frequency, the DDS output frequency resolution is 0.23 Hz. While such fine frequency resolution is rarely needed, this capability is quite useful in reducing the spurious distortion of the output signal.

In addition to using them as stand-alone designs, some DDS circuits can be enhanced via integration with PLLs. The following block diagrams illustrate two DDS/PLL configurations which may be useful in various synthesizer applications. **Figure 2** shows a DDS within the feedback loop of a PLL. A prescaler divides the VCO output frequency to the clock input frequency range of the DDS. Meanwhile, the DDS output signal phase

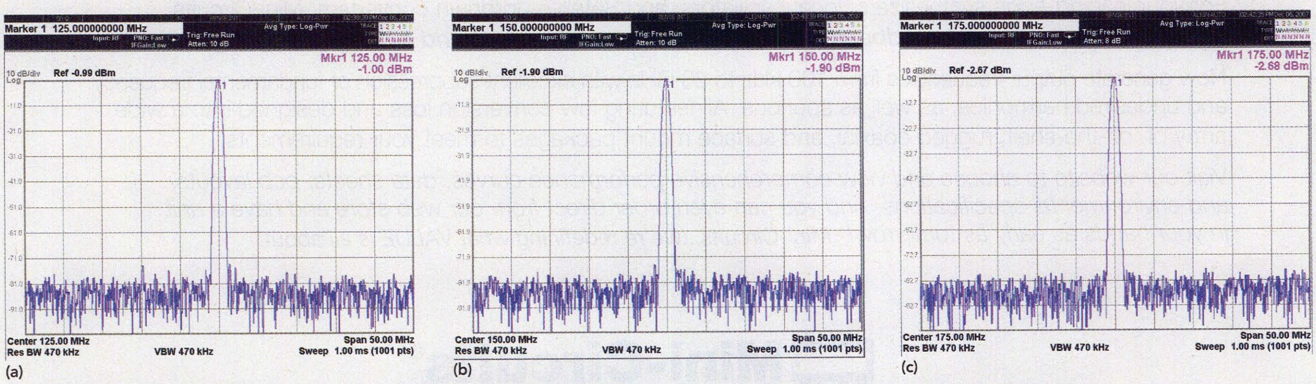

4. The spectral purity of the commercial AD9910 DDS device is shown here at (a) 125, (b) 150, and (c) 175 MHz.

is compared to a high-spectral-quality reference within the phase detector. A phase error signal is thereby created, which subsequently tunes the VCO to the phase-locked condition.

The output frequency based on the frequency reference and other DDS parameters can be found from Eq. 3:

$$f_{out} = (2^n/FTW)P(f_{ref}) \qquad (3)$$

where:

P = the division ratio of the prescaler and

f_{ref} = the frequency of the reference source.

In essence, the DDS operates as a high resolution fractional frequency divider allowing the use of a high reference frequency and reduction of the feedback loop modulus.

Reference 2 provides an excellent example of the performance of this synthesizer architecture, with DDS performance summarized in **Table 1**.

Figure 3 shows a DDS used as a high-resolution reference source for a PLL. This architecture takes advantage of the fine frequency resolution of a DDS along with its wide loop bandwidth for fast frequency switching. A modest prescaler modulus—i.e., P < 100—may be used for frequency synthesis to 10 GHz. An offset or sum loop synthesizer architecture essentially ensures low phase noise beyond 10 GHz (**Fig. 4**).

The equation for the output frequency may be written by inspection (as Eq. 4):

$$f_{out} = (FTW/2^n)MP(f_{ref}) \qquad (4)$$

where:

M = the multiplier ratio.

Before proceeding to the LFM synthesizer architecture, it is instructive to examine the DDS as the unique and performance determinant of the synthesizer. A model AD9910 DDS from Analog Devices (www.analog.com) was specifically selected as the PLL reference due to several features and properties intrinsic to the device, as summarized in **Table 2**.

Principal sources of spurious signals at the DDS output are DAC resolution and tuning word bit truncation.[4] Elimination of spurious signals due to tuning word bit truncation may be accomplished with the attendant consequence of reduced frequency resolution.[1] Using this technique, the LFM architecture may be appropriate for several other high-spectral-quality applications.

Figure 5 shows a block diagram of the linear FM frequency synthesizer, where the constituent components and interconnections have been identified. The AD9910[6] DDS integrated circuit (IC) provides the agile frequency capability as well as the low phase noise reference for the offset PLL. The AD9910 features are uniquely applicable to linear FM due to a user defined, digitally controlled, digital

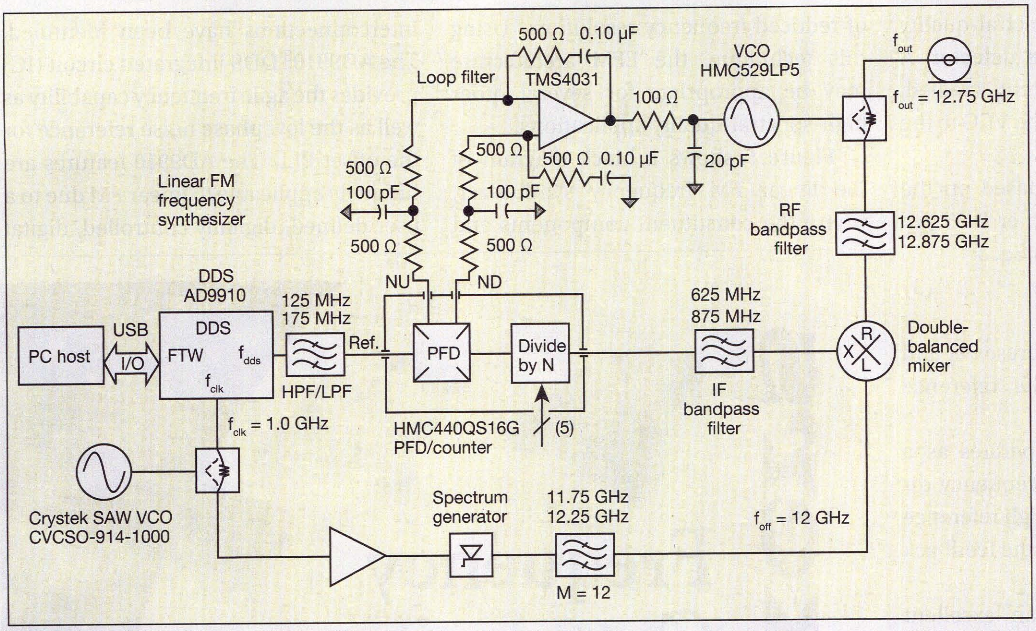

5. This block diagram represents a linear FM frequency synthesizer operating at a clock frequency of 1 GHz. The clock source is a commercial SAW oscillator.

ramp mode of operation. In this mode, the frequency, phase, or amplitude can be varied linearly over time. The AD9910 also features a 14-b, 1.0-GHz sample DAC and clock capability which provides a maximum output frequency of 400 MHz and greater than –80 dBc spurious-free dynamic range. A wide loop bandwidth (3 MHz) is required to accurately track the reference signal frequency agility and assures phase continuous frequency agility for modest frequency steps.

A low-noise, commercial 1.0-GHz surface-acoustic-wave (SAW) oscillator was used to provide the DDS clock as well as the reference for the offset loop local oscillator via frequency multiplication using a step recovery diode. Under linear sweep operation, the AD9910 is dynamically tuned from 125 to 175 MHz using the digital ramp generator feature. In accordance with the output frequency equation, the offset loop and feedback modulus produce an output signal frequency from 12.625 to 12.875 GHz:

$$f_{out} = [(FTW/2^n)N + M]f_{ref}$$

where:
FTW = the frequency tuning word (binary);
n = the FTW resolution (32 b);
N = the feedback loop modulus (N = 5);
M = the offset loop frequency multiplier factor (M = 12); and
f_{clk} = the clock frequency (f_{clk} = 1.00 GHz).

The feedback loop modulus is fixed at five but could be altered to extended synthesizer bandwidth, although this feature may require use of a switched filter bank to reduce spurious content. The offset loop effectively reduces the feedback loop modulus from 85 to 5, thereby lowering the phase noise by 24.5 dB within the loop bandwidth.

The component elements of the loop filter are specifically delineated to emphasize that accurate tracking and fre-

Table 2: Features and properties of the AD9910 DDS.

Feature/ property	Data	LFM synthesizer impact
Sample clock	1 GHz	higher output frequency reference
Internal memory	1024 x 32 RAM	internal frequency, phase,and/or amplitude modulation
Output DAC	14 b	reduced output spurious, increased SFDR
Phase accumulator	32 b	fine frequency resolution
Linear ramp generator mode	32 b	linear in time AM, FM, PM capability which allows users to control both rising and falling slopes of ramp, upper and lower boundaries of ramp, step size, and step dwell time
Residual phase noise	–150 dBc/Hz offset 10 kHz from a 100-MHz output	not a limit to output phase noise
I/O control	serial and parallel	variable control options

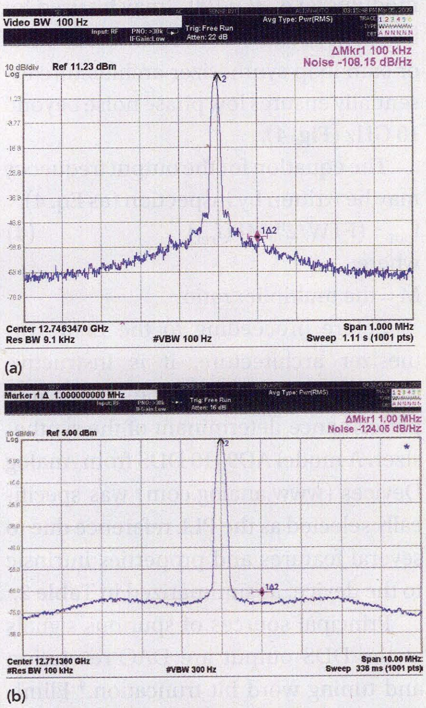

6. These plots show (a) the narrowband and (b) the wideband spectra for the LMF synthesizer.

quency agility of the AD9910 can only be assured with a wideband loop; in addition, and more specifically, the loop damping must be greater than critical—i.e., > 0.707—to prevent transient overshoot and assure asymptotic settling.

Figure 6 represents the center frequency (12.75 GHz) spectral quality of the LFM synthesizer under narrow and wideband conditions. The phase noise of the narrow band spectrum (–108 dBc/Hz offset 100 kHz from the carrier) is near the phase noise floor of the spectrum analyzer. An estimate of the phase noise from the wideband spectrum indicates phase noise measurement (–124 dBc/Hz offset 1.0 MHz offset frequency)—which correlates well with the phase noise estimate (–128 dBc/Hz) in accordance with refs. 2 and 5.

The dynamic closed-loop response of the LFM synthesizer is indicated in **Fig. 7** for two ramp generator configurations: (a) a total sweep of 250 MHz using 50,000 steps of 5.0 kHz and 4-ns dwell time; (b) 10-MHz frequency deviation using two-steps and 5.0-μs dwell time at each step-note frequency settling less than 1 μs. The time waveforms of **Fig. 7** represent the VCO control voltage under the indicated frequency agile conditions. For the conditions specified in **Fig. 7(a)**, the maximum deviation from linear frequency versus time may be calculated using the formula of Eq. 5:[1]

$$\text{frequencysweeplinear}(\%) = (\Delta f/\Delta F)100 = (5.0 \times 10^3)/(250 \times 10^6)100 = 0.002\% \quad (5)$$

This is extraordinary linearity performance and ensures that the radar range measurement resolution is not degrad-

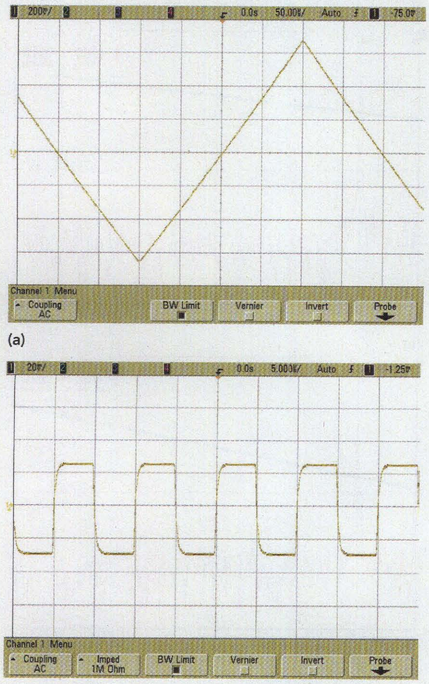

7. The dynamic response of the LFM synthesizer is shown for (a) a 250-MHz sweep in 50-kHz steps at a 4-ns dwell time and for (b) 10-MHz steps with 5-μs dwell time.

ed due to spectral spread following signal processing.[1]

The effectiveness of the DDS based LFM synthesizer as a transmitter and receiver local oscillator source for FMCW radar may be determined with the closed-loop equipment configuration of **Fig. 8**, where the LFM synthesizer output provides the local oscillator drive signal for a double-balanced mixer as well as a received signal. The received signal is delayed via 100 ft. of RG-141 semirigid cable.[7]

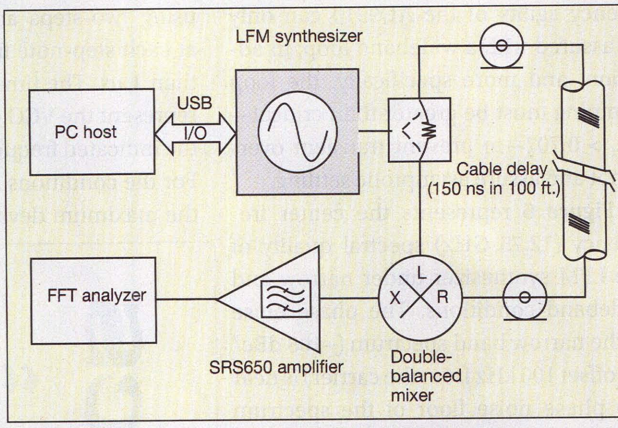

8. The test system for closed-loop evaluation of the LFM synthesizer employed a Fast Fourier Transform (FFT) analyzer.

The IF at the mixer output can be calculated by Eq. 6:

$$f_{if} = (\Delta F/\Delta T)\tau_d = 3.625 \text{ kHz} \quad (6)$$

The equipment produces an IF signal proportional to the ramp rate and the time delay associated with the cable. The output signal is spectrally resolved to qualitatively determine the linearity and, possibly, the phase noise. The results of the closed-loop test are shown in **Fig. 8.** Test parameters, collected from a Hamming window analysis, include frequency deviation of 250 MHz, scan time of 0.010 s, sample rate of 1 MSamples/s, FFT length of 10,000 points, frequency resolution of 100 Hz, range resolution of 83 Hz/m, and cable delay of 145 ns.

Figure 8(a) represents the IF spectrum of the LFM source and **Fig. 8(b)** is the IF spectrum following substitution of the model E8257D8 signal generator as the source for the closed-loop test. Close examination of **Fig. 8** reveals higher signal-to-noise ratio and narrower spectral width of the LFM synthesizer IF spectrum. The closed-loop equipment functions as an FM discriminator. Therefore, the broader spectral width of the IF signal using the E8257D signal generator is indicative of higher residual FM noise and/or degraded linearity, since both conditions will extend the width of the IF signal spectrum. The lower signal level in the IF spectrum of the E8257D indicates that signal energy is distributed to adjacent frequency bins of the spectrum.

Although the test methodology is somewhat subjective, the results provide credible evidence of the quality and suitability of the LFM synthesizer to function effectively as a source for FMCW radar, as well as other frequency agile applica-

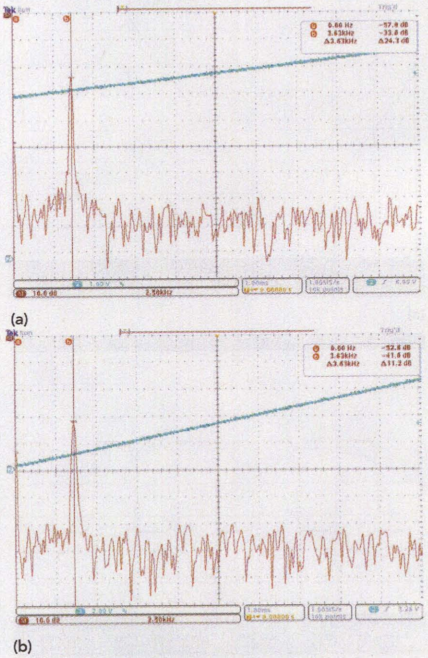

9. The LFM synthesizer performance is plotted here for a Δf of 25 MHz and a ΔT of 10 ms for (a) the LFM source and (b) a commercial signal generator, a model E8257D from Agilent Technologies (www.agilent.com).

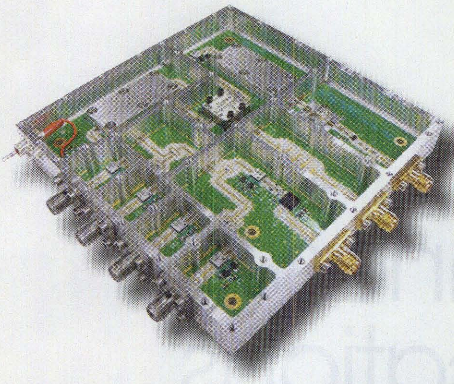

10. The RF section of the LFM synthesizer occupies only 4 x 4 in. in this assembly.

tions.[7] **Figure 9** offers a view of the RF section of the LFM synthesizer, revealing the use of discrete and surface-mount components. Support electronics, power supply conditioning, and control interface/functions are integrated on the lower surface (not shown). Isolation walls and energetic grounding techniques are clearly illustrated and required to reduce spurious signals. The source features low-loss microstrip line fabricated on RO4350 circuit substrate material from Rogers Corp. (www.rogerscorp.com). The RF section of the synthesizer is approximately 4.0 × 4.0 × 0.5 in. **(Fig. 10)**. To ensure adequate coupling and isolation, attempts were not made to reduce the size of the synthesizer. MWRF

ACKNOWLEDGMENTS

The work reported within the article was conducted by the author while employed at M/A-COM in 2008. The author acknowledges the diligence of Scott Crawford and Chris Monroy in assembly, breadboard, and measurement tasks, as well as Bert Henderson (from M/A-COM in San Jose, CA and formerly of Watkins-Johnson Co.) for analysis, design, and prototypes of the X-band filters. The author acknowledges and appreciates the generous and timely support of Hittite Microwave Corp. (Chelmsform, MA; www.hittite.com); rapid acquisition of MMIC devices and evaluation boards was significant in validation of the LFM synthesizer architecture and management of an aggressive program schedule.

REFERENCES

1. Kenneth V. Puglia, "Technical Memorandum: FMCW Radar Primer," M/A-COM GmbH, Schweinfurt, Germany; August 1995.
2. Keneth V. Puglia, "Technical Memorandum: Transmitter FM Noise and Frequency Sweep Nonlinearity in FMCW Radar," M/A-COM, GmbH, Schweinfurt, Germany, July, 1995.
3. "Technical Tutorial on Digital Signal Synthesis," Analog Devices, Inc., 1999, www.analog.com.
4. Ulrich L. Rohde and Ajay Kumar Poddar, "VCSO Technology Silences Synthesizers," Microwaves & RF, Vol. 50, No. 2, February, 2011.
5. Kenneth V. Puglia, "Oscillator Phase Noise: Theory and Prediction," Microwave Journal, Vol. 50, No. 9, September, 2007, pp. 178-194.
6. Analog Devices, AD9910 data sheet, www.analog.com.
7. D. Scherer, "Design Principles and Test Methods for Low Noise RF and Microwave Sources," Hewlett-Packard RF and Microwave Measurement Symposium, October, 1978.

FOR ADDITIONAL READING

H.D. Griffiths, "New Ideas in FM Radar," Electronics and Communication Engineering Journal, October 1990, pp. 185-194.
A.G. Stove, "Linear FMCW Radar Techniques," IEEE Proceeding-F, Vol. 139, No. 5, October 1992, pp. 343-350.
J. Figueras Ventura and H. Russchenberg, "Improvement of the Performance of FM-CW Radar Systems by using Direct Digital Synthesizers: Comparison with Voltage Controlled Oscillators," available for download via IEEE Explore (www.ieeexplore.ieee.org).
D. Morgan, P.D.L. Beasley, K.E. Ball, and W.P. Jones, "Exploitation of direct digital synthesis for sweep generation in FMCW radar," ARMMS Conference, November, 7-8, 2005, Newport Pagnell, England.

DR. JOHN HOWARD
President and Chief Executive Officer
Electromagnetic Technologies Industries, Inc.,
50 Intervale Rd., Boonton, NJ 07005; (973) 394-1719, FAX: (973) 394-1710,
www.etiworld.com.

Phased-Array Antennas Aid Wireless Communications

The use of hardware-based NIMO techniques can improve the performance and increase the coverage area of a wireless communications system, especially in densely populated areas.

WIRELESS SYSTEMS overcome a number of different limitations to provide reliable coverage, including limited available frequency bandwidth and efficient use of the available bandwidth. This efficiency can be boosted by using higher modulation rates, more sensitive receivers, and more accurate bit error detection/correction methods. Nevertheless, wireless telecommunication systems must still comply with the bandwidth or spectrum limitations established by governing authorities. And once bandwidth is used in one area, the bandwidth is not available for other systems.

Because of this, current wireless communications technologies an be limited in terms of data and user capacities. For example, a typical GSM cell site divides 360 deg. of coverage into three sectors with three frequency channels **(Fig. 1)**. Within a sparsely populated area this may be acceptable; however, networks covering dense urban areas often require hundreds of such cell sites. Such a large number of sites incur high costs associated with the cell equipment, site management, and site rental. In addition, with every new site, RF planning becomes more complex. These same difficulties and high costs impact all wireless communications systems, including third-generation (3G) cellular, Long Term Evolution (LTE), and WiMAX systems. In a 3G system, if each of three or six sectors employs the same band **(Fig. 2)**, the system will suffer a reduction of codes per sector.

Fortunately, wireless non-interfering multiple-output (NIMO) systems can overcome the bandwidth and capacity limitations in densely populated areas, and even multipath problems. These systems, as designed and manufactured by ETI, combine beamforming techniques with multiple-input, multiple-output (MIMO) architectures to provide higher quality of service (QoS) than systems based on conventional beamforming methods. NIMO strategies can provide multiple narrow beams from a single antenna, enabling improved efficiency, user capacity, and throughput.

The two types of MIMO currently employed in wireless systems are MIMO Matrix A and MIMO Matrix B. Both use more than one antenna to minimize signal fading. The antennas can be placed within a single mechanical structure or exist as separate mechanical structures. Radios that transmit and receive signals in these wireless systems can typically select between MIMO Matrix A and MIMO Matrix B. MIMO Matrix A uses two or more distinct paths with the same information transmitted to a subscriber and back **(Fig. 3)**. If fading or multipath affects one path, at least one other path is available as a backup. A receiver will be designed to distinguish or combine two (or more) signal paths as needed to overcome the fading or mul-

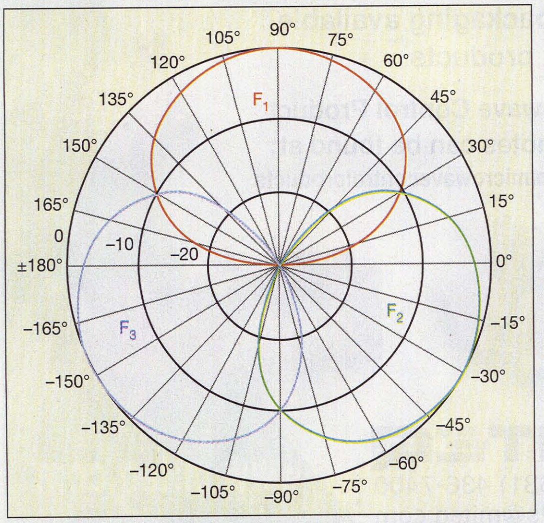

1. A typical cellular communications site used three different frequency channels.

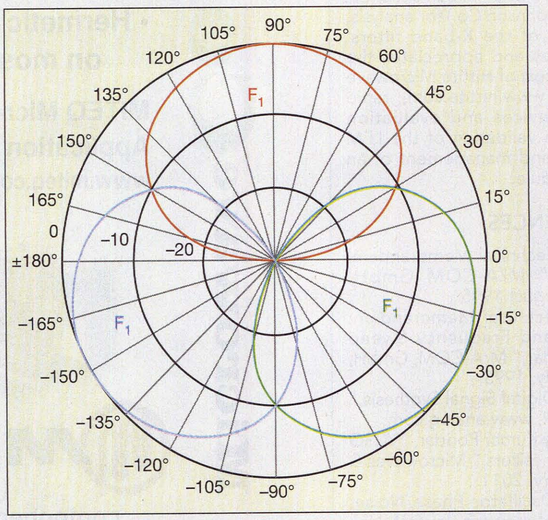

2. A typical 3G cell site repeats the same frequency in three channels

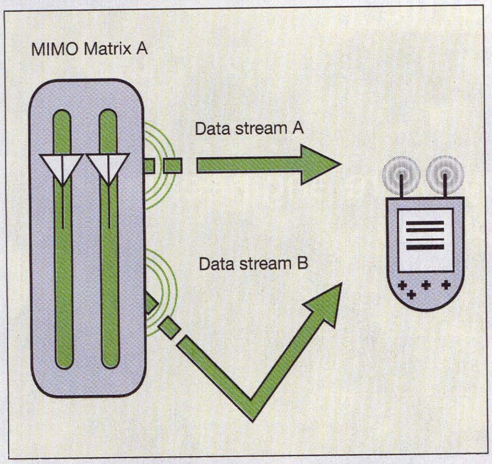

3. In the MIMO Matrix A approach, both data streams A and B carry the same signals.

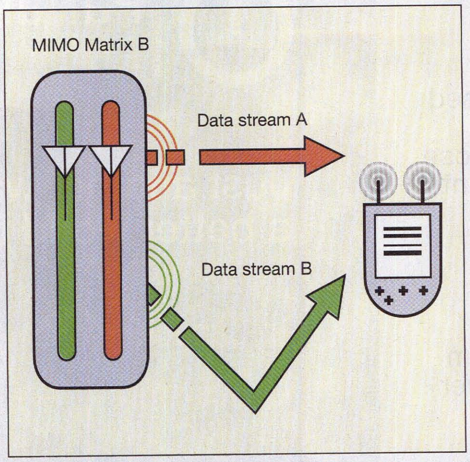

4. In the MIMO Matrix B approach, data stream A carries different data than data stream B.

tipath effects. In a MIMO Matrix B approach, two (or more) distinct signal paths carry different signals over the same frequency band **(Fig. 4)**. In this method, twice as much data can be transmitted, increasing the efficiency of the link. The signals are received at different times or with sufficiently different directions of arrival to differentiate them.

Beamforming techniques create a narrow beam from a high-gain, phased-array antenna to link a subscriber and base station. Of the two types of beamformers, one uses software to mathematically construct the beam and the second, NIMO, employs hardware for the same effects.

Beamforming can generally increase the power of a signal in the direction in which it is transmitted. For reception, it can increase receiver sensitivity in the direction of desired signals and decrease sensitivity in the direction of interference and noise. In these ways, beamforming can provide longer communications distances and wider coverage areas. With NIMO, a greater number of subscribers can be reached with higher data rates.

The processing requirements for software-based beamforming can be sophisticated and resource-intensive, depending on the complexity of the channel (environment) and the number of subscribers connected on the system. Implementation of software-based beamforming approaches can result in delays of 5 to 10 ms. Such delays are not an issue with NIMO systems.

NIMO provides multiple simultaneous narrow beams **(Fig. 5)** using a single phased array antenna and provides improved characteristics compared to conventional beamforming techniques. As many as 48 beams may be employed in a 360-deg. angle; for mobile systems as many as 12 beams is recommended.

Compared to traditional MIMO systems, NIMO methods offer numerous advantages, including high antenna gain, long communication distances, and reduction in implementation costs compared to other approaches. The main disadvantage of NIMO is the lack of an adaptive phased-array antenna scheme. **(Fig. 6)**

To overcome the limitations of modern wireless communication systems, equipment manufacturers have devised various equipment improvements. Phased-array antenna subsystems are employed for some of these techniques. While increasing the modulation rate can increase data speeds per customer, there are limits to the distances over which higher modulation rates can be used.[5] Fortunately, hardware-based NIMO techniques can provide significant advantages compared to software-based beamforming approaches. MWRF

REFERENCES

1. Electromagnetic Technologies Industries, Inc., white paper, "Simply Years Ahead," 2009, www.etiworld.com.
2. Motorola, white paper, "A Practical Guide to WiMAX Antennas: MIMO and Beamforming Technical Overview," Motorola, Libertyville, IL, www.motorola.com.
3. Electromagnetic Technologies Industries, Inc., white paper, "ETI Multibeam/Bandwidth for Free," 2010, www.etiworld.com.
4. Constantine A. Balanis, Antenna Theory, 3rd Ed., Wiley, New York, 2005.
5. Terry Norman, "WiMAX vendor consolidation continues as Cisco withdraws from the market, Analysis Mason, March 2010, www.analysysmason.com.

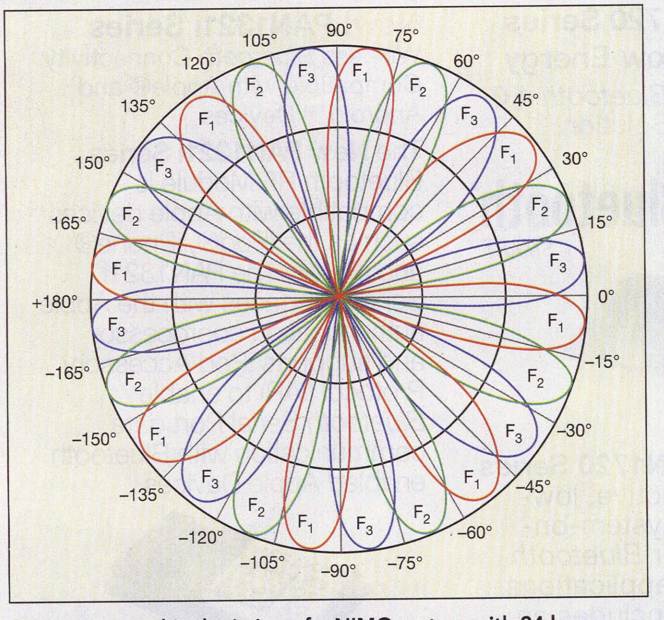

5. This is a graphic depiction of a NIMO system with 24 beams and 3 frequency channels: F1, F2, and F3.

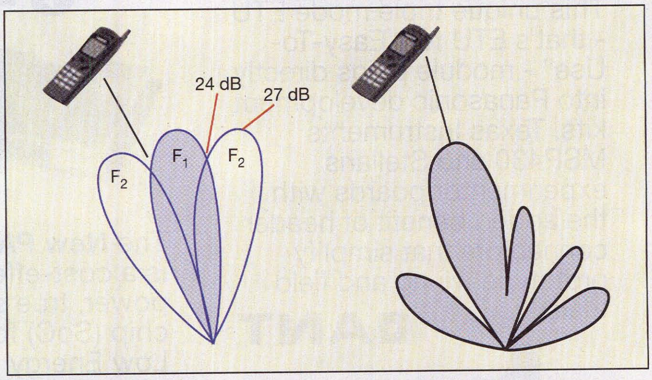

6. This is a graphical representation of a NIMO system with two channels: F1 and F2.

Introducing our new line of Phase Locked Signal Sources with *Ultra* Low Phase Noise

Model	Frequency (MHz)	Phase Noise (dBc/Hz) [Typ.] @10 kHz	Phase Noise (dBc/Hz) [Typ.] @100 kHz	Package
FCTS800-10	800	-148	-168	
KFCTS800-10	800	-146	-168	
KFSA1000-100	1000	-145	-160	
FXLNS-1000	1000	-149	-154	
FCTS1000-10	1000	-147	-160	
KFCTS1000-10	1000	-147	-160	

Features

- Cost Effective
- Eliminates Noisy Multipliers
- Patented Technology

Applications

Test & Measurement Equipment
High Frequency Network Clocking
Scanning & Radar Systems
High Performance Frequency Converters
Base Station Applications
Agile LO Frequency Synthesis

Up to 3.0 GHz

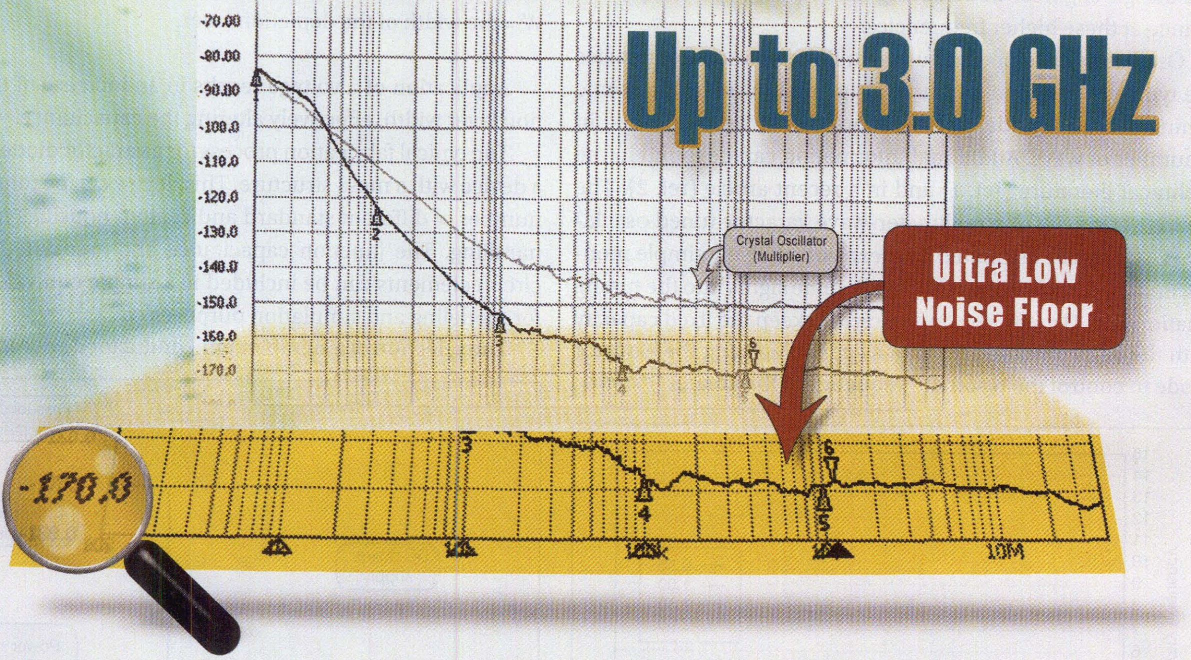

Call Factory For Your Specific Requirement

SYNERGY® MICROWAVE CORPORATION

Phone: (973) 881-8800 | Fax: (973) 881-8361
E-mail: sales@synergymwave.com | Web: www.synergymwave.com
Mail: 201 McLean Boulevard, Paterson, NJ 07504

SAABRA DEEN
Design Engineer
Osctek Ltd., Harrow, Middlesex, United Kingdom;
+44 (0) 2084207043, e-mail: saabradeen@yahoo.com, www.osctek.com.

Optimize Varactor-Tuned Oscillators

This simple model helps to understand the tuning sensitivity and linearity of a varactor diode for more predictable and precise tuning of oscillators at millimeter-wave frequencies.

MILLIMETER-WAVE FREQUENCY bands are attractive for their wide available bandwidths. There are a number of ways to generate these signals but, for each type of oscillator, it is desirable to be able to tune the source electronically, as well as in a defined, controlled, and consistent manner. By using a suitable reactive device (such as a varactor diode) for tuning these millimeter-wave oscillators, the relationship between an applied voltage and the resulting frequency can be precisely defined. This can aid the design engineer in achieving the required spectral performance at these higher frequencies.

Oscillators developed for use at millimeter-wave frequencies are typically designed around waveguide housings. Electronic tuning of a waveguide-type oscillator can be accomplished in a number of ways. Additional information can be found in the technical literature (ref. 1) and in a recent article (ref. 2). The tuning sensitivity of a millimeter-wave varactor-tuned oscillator (VTO) can be estimated by means of relatively simple models, and this article hopes to provide some sights into the tuning relationship. Usually, the approach is to keep the fixed capacity with the varactor diode as large as possible, using the varactor diode to control the resonant frequency to the greatest extent.

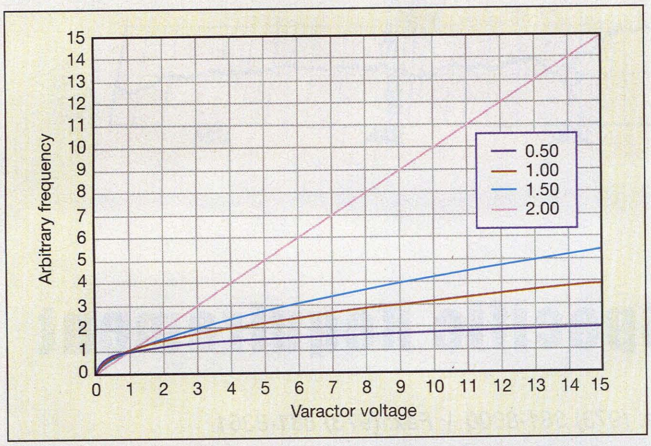

1. Frequency variations can occur due to variations in varactor diode voltage.

A varactor diode is essentially an active device with positive-negative (PN) junction which has reverse bias applied. This results in a movement of charge carried away from the junction, so that this region is referred to as the depletion layer. The depletion layer has charge on either side of the junction and acts like a parallel-plate capacitor. The capacitance relationship for a parallel-plate capacitor is $C = \varepsilon A/W$, where:

A = the effective cross-sectional area of the device,
ε = the relative dielectric constant of the depletion layer, and
W = the width of the depletion layer.

Application of a voltage results in an increase of the depletion layer width, effectively altering the capacitance.

The typical fabrication process for a varactor diode results in a device with a mesa structure. This device can be mounted in a number of different standard and custom housings to simplify handling. The junction capacitance and associated parasitic circuit elements can be included in a simple equivalent circuit for modeling and simulation purposes.

The selection of a suitable semiconductor device for a varac-

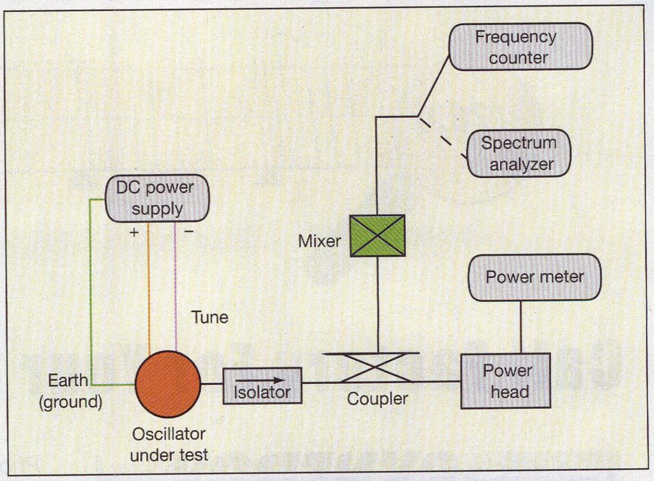

2. This block diagram shows the instruments needed for the VCO test system.

tor diode can make an impact on the performance of the diode, although this receives little coverage in the literature. Varactors are true diodes with a clearly defined junction, which can be characterized by means of a particular doping profile; this is effectively captured in the gamma parameter for each varactor diode. The gamma parameter can be placed in two categories: abrupt and hyperabrupt. Quite simply, a varactor diode is effectively a variable reactance which is a function of some applied DC tuning voltage. More detailed models of varactor diodes are available in the literature, which are useful for a specific package or unpackaged devices. To obtain a general understanding of a varactor diode's behavior, it would be reasonable to ignore packaging and parasitic affects in the first instance, as this allows the designer to appreciate the merits of such devices.

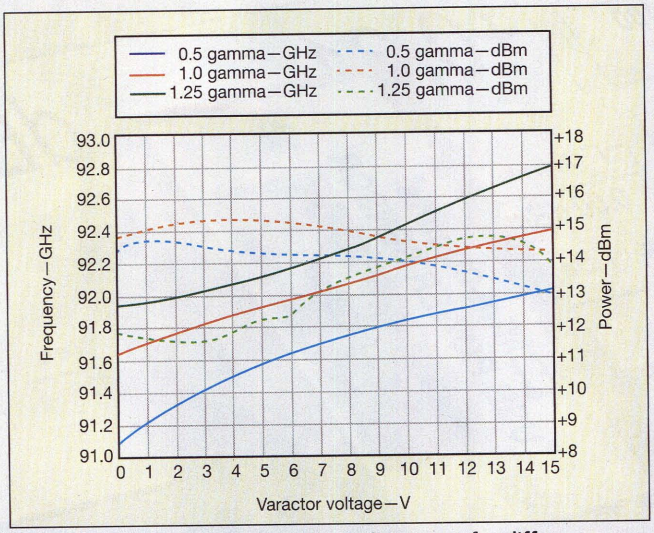

3. These curves show the changes in frequency for different applied varactor voltages.

This basic approach leads to the following expression:

$$C_v + kV^{-\Gamma} \quad (1)$$

where:

V = control voltage;
k = a constant;
C_v = varactor capacitance; and
Γ = the gamma or doping profile.

For the case where the circuit capacitance is much greater than the varactor capacitance, or if $C_d << C_v$:

$$F \approx (L/C_v)^{0.5} \rightarrow F = K/(C_v)^{0.5} \quad (2)$$

where:

F = the resonant frequency;
L = the circuit inductance; and
K= a constant.

Combining Eqs. 1 and 2 yields an expression that represents a relatonship between frequency and voltage:

$$F = K/[k(V)]^{\Gamma} \rightarrow \approx V^{\Gamma/2}$$

in which the importance of the varactor material's doping profile can be clearly seen on both sides of the equation.

This very simplistic approach provides a basic relationship between frequency and the applied voltage, with Γ representing a doping constant, equal to 0.5 for an abrupt diode and 1.0 or 1.25 for a hyperabrupt diode:

$$\Gamma = 0.5 \rightarrow F \approx V^{0.25}$$
$$\Gamma = 1.0 \rightarrow F \approx V^{0.50}$$
$$\Gamma = 2.0 \rightarrow F \approx V$$

In reality, it is difficult to achieve a practical diode capable of Γ = 2.0, although devices with values equal to 1.0 and 1.25 are commercially available.

A more detailed analysis[3] of a varactor's influence on frequency tuning can be complicated. This is due to the issues of the varactor construction and device to device variation, as can be seen in **Fig. 1**. Package assembly and parasitic circuit elements can have profound effects at high frequencies in particular the type and shape of the internal bond wires. For this analysis, a number of commercially available packaged varactor diodes were procured and installed into a W-band Gunn oscillator to compare performance levels.

Each varactor/oscillator combination was evaluated with a test system that included a DC power supply for tuning the varactors (**Fig. 2**). The output of the Gunn oscillator in each case was monitored with the aid of high-frequency test instruments that included a frequency counter, spectrum analyzer, and power meter. A frequency mixer was used to translate the Gunn oscillator's outputs to frequencies within range of the test equipment.

Although the varactor package type was the same in each case, each device package had its own subtle differences in dimensions as well as in internal construction, with ramifications at the higher frequencies. Difference between sources can occur because of variations in reactance and skin effect due to fringing fields, the lengths of current paths, and various parasitic effects. No serious efforts were made to optimize the circuit, particularly for power. Measured performance is shown in **Fig. 3**.

The crude model and measured data demonstrate that the tuning sensitivity (and thus, linearity) can be influenced significantly by the selection of a suitable varactor diode. This also opens the possibility of tailoring the doping profile of the varactor diode to achieve a specific tuning sensitivity; this could be achieved during the semiconductor fabrication process. However, in practice, linear tuning must take into account circuit and oscillator characteristics as well as the varactor diode. MWRF

REFERENCES

1. Jack Holzman and D. Robertson, Solid-State Microwave Power Oscillator Design, Artech House, Norwood, 1992, www.artechhouse.com.
2. S. Deen, "Designing Compact V/W-Band Gunn Sources, MicroWaves & RF, April, 2011, p. 82.
3. Joseph F. White, Semiconductor Control, Artech House, Norwood, 1978, www.artechhouse.com.
4. David M. Pozar, Microwave Engineering, 2nd ed., Wiley, New York, 1998.
5. G.S. Hobson, The Gunn Effect, Clarendon Press, Oxford, England, 1974.
6. J.S. Panesar, private communication.

ROY MONZELLO
RF/Microwave Design Engineer
E-mail: roy.monzello@gmail.com

Measure Noise Without A Calibrated Source

This new technique is based on a variation of the Y-factor method to achieve accurate noise-figure measurements without the need for a calibrated noise source.

MANUAL NOISE-FIGURE measurements are often necessary when automated measurement systems are not available. One of the more popular techniques for making noise-figure measurements is the Y-factor method, which is accomplished with the aid of a hot/cold noise source to provide two different noise power levels (for this article, cold will be assumed at 290K). The difference between the two noise power levels is the excess noise ratio (ENR), which is given numerically by $(T_H - T_C)/T_C$, where T_H represents the hot temperature and T_C is the cold temperature. Under true impedance-matched conditions, the actual available noise power would be equal to kTB, where k is Boltzmann's constant ($1.3806503 \times 10^{-23}$ m^2kg/s^2K), T is the temperature (in degrees Kelvin) or S/B (in Kelvin), and B is the bandwidth of the circuit under test.

The Y-factor is the ratio of output noise power from a device under test (DUT) with the noise source set to hot, divided by the output noise power with the noise source set to cold. Using the Y-factor approach, the noise figure of a DUT can be calculated by using Eq. 1:

$$\text{Noise figure of DUT} = 10\log_{10}[ENR/(Y - 1)] \quad (1)$$

where ENR is the numerical ratio of the ENR in dB, or ENR = $10^{(ENR/10)}$. The ENR is defined as $(T_H - 290)/290$. **Figure 1** shows a typical setup for measuring the Y-factor. The resistor in the noise source is a fictitious component with a body temperature that can be changed to produce different levels of output noise power.

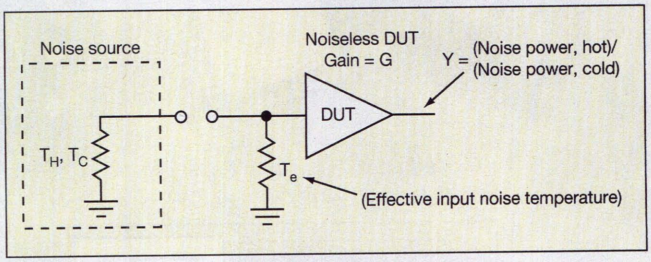

1. This basic circuit is used to evaluate the Y-factor of a DUT when using a calibrated noise source.

The resistor at the input of the DUT, T_E, represents a fictitious resistor at a temperature of T_E K that, when multiplied by the gain of the DUT, would produce the proper amount of noise at its output corresponding to its internally generated noise. The input noise temperature is related to the noise figure by Eq. 2:

$$T_E = 290(NFac - 1) \quad (2)$$

where NFac, the noise factor, is the numerical value of the noise figure—e.g., NFac = $10^{[(\text{Noise Figure})/10]}$.

As shown in **Fig. 1**, the standard circuit for a noise figure measurement is simple and can provide an accurate measurement of the DUT's noise figure if one were able to accurately measure the output noise power of the DUT. Since an instrument must be used to make the noise power measurement at the output of the DUT, the noise power measurement is a composite of the noise power coming out of the DUT, along with the internal noise generated by the measuring device (for manual measurements, the

Table 1: Noise figures measured for the spectrum analyzer, using standard and variation Y-factor methods.

ENR (dB)	Noise temp.	Measured P_0 (dBm)	Ti	dTi	dENR	Y-factor	dY	dY/dENR	Nfac	Nfig	Standard Y-factor method Nfig
---	290 K	-131	6017.6								
15.30	10116.5 K	-126.9	15467.7	9450.1	32.59	2.57	---	---	---	---	13.34
20.15	30309.1 K	-123.3	35434.5	19966.8	68.85	5.89	3.32	0.048	20.75	13.17	13.26

measuring instrument is usually a spectrum analyzer).

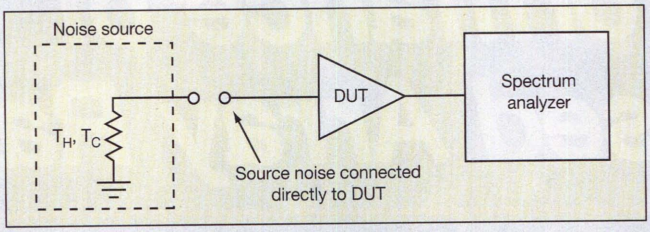

2. A spectrum analyzer can also be used for measuring the noise figure of a DUT.

Spectrum analyzers usually have a large noise figure in the 20-to-30 dB range or, for more sophisticated instruments with an internal preamplifier, the noise figure may be reduced to the 10-to-15 dB range. The typical procedure for making a noise-figure measurement is to first measure the noise figure of the spectrum analyzer by placing the noise source directly on the analyzer's input port. A measurement is then made with the DUT placed between the noise source and the input to the spectrum analyzer, as shown in **Fig. 2**. Once the two measurements have been made, the noise figure of the device is calculated from the following equations:

Noise factor of spectrum analyzer = $ENR/(Y_{SA} - 1) = NFac_{SA}$ (3)

Total noise factor of the DUT plus the spectrum analyzer:

$NFac_{TOTAL} = ENR/(Y_{TOTAL} - 1)$ (4)

Noise factor of the DUT = $NFac_{TOTAL} - (NFac_{SA} - 1)/G_{DUT}$ (5)

where G_{DUT} is the gain of the DUT.

The novel noise-measurement approach about to be described follows the procedure for first characterizing the noise figure of a spectrum analyzer, and then evaluating the noise of a DUT in cascade with the analyzer. One important difference is that results with the new method are obtained by means of the derivative of the Y-factor. Measurements are independent of the absolute value of the input excess noise level to the DUT and eliminate the need for a calibrated noise source.

The new method begins with the standard equation for the noise factor of a DUT, given the ENR of the noise source and a Y-factor measurement as detailed in Eq. 6:

$NFac = ENR/(Y - 1)$ (6)

Rearranging terms results in Eq. 7:

$Y = ENR/NFac + 1$ (7)

Taking the derivative of each side with respect to the ENR yields Eq. 8:

$dY/dENR = 1/NFac$ (8)

which leads to Eq. 9:

$NFac = 1/(dY/dENR)$ (9)

What this shows is that the noise factor of a DUT can be determined without knowing the absolute ENR; only the difference in ENR, which results in a difference of the Y-factor measurement, is needed. This new noise factor approach consists of making two Y-factor measurements at two different noise power levels at the input of the DUT. These two Y-factor values, along with the corresponding source noise power values, provide the information needed to construct the ΔY and ΔENR values. These will produce the slope or dY/dENR, producing the noise factor result according to Eq. 9.

The method used to vary the ENR involved using an arbitrary source of noise power (e.g., a high-gain amplifier) with its noise output level controlled by a step attenuator. This produces a range of ENR values based on the setting of the step attenuator. This method does not

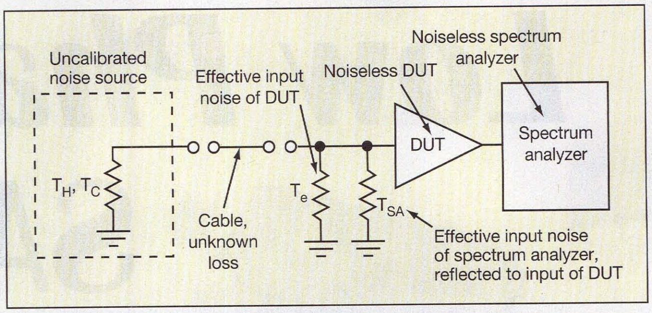

3. A spectrum analyzer can also be used when measuring the change in ENR of an uncalibrated noise source to check the noise figure of a DUT.

require knowledge of how much noise power is being generated, nor details about the attenuation characteristics of the step attenuator. The only purpose of the noise source/attenuator is to provide two different levels of noise power. This also means that a cable with unknown loss characteristics can be used to connect the noise source/attenuator to the DUT without impacting the noise-figure calculations.

The key to this new noise measurement approach is to determine the change in ENR at a DUT's input, using power readings from the spectrum analyzer translated to the input plane of the DUT. For example, if the spectrum analyzer reads –121 dBm, and the gain between the input to the DUT and the input to the spectrum analyzer is 15 dB, then the translated noise power at the input reference plane of the DUT would be –136 dBm. The noise temperature model of **Fig. 3** shows how the internal noise power generated by the analyzer can be translated to the input reference plane of the DUT as an effective input noise temperature. The effective input noise power at the input to the DUT is a composite of three sources:

1. The input noise power (generated by the noise source);

2. The effective input noise power of the DUT (related to the noise figure of the DUT); and

3. The effective input noise power of the spectrum analyzer translated to the input of the DUT (related to the noise figure of the spectrum analyzer).

This can be written as:

$$P_{n1} = KB(T_{H1} + T_{DUT} + T_{SA}) \quad (A)$$

and

$$P_{n2} = KB(T_{H2} + T_{DUT} + T_{SA}) \quad (B)$$

where $P(p)_{ni}$ is defined as the effective input noise power into the DUT for different values of hot input temperature, T_{Hi}, and is determined from the measurements by:

$$P(p)_{ni} = 10[(P_{dB\ MEASURED} - Gain_{dB})/10]$$

and where parameter $Gain_{dB}$ represents the small-signal gain (in dB) from the input of the DUT to the input of the spectrum analyzer.

Taking the difference of the two noise powers, $P(p)_{n2} - P(p)_{n1}$, yields Eq. 10:

$$\Delta P_n = KB(T_{H2} - T_{H1}) \rightarrow (T_{H2} - T_{H1} = \Delta P_n/KB \quad (10)$$

Table 2: Noise figure of the spectrum analyzer determined by using the difference in ENR directly from calibrated noise source data.

ENR linear	Noise temp.	Measured P_0 (dBm)	dENR	Y-factor	dY	dY/dENR	Nfac	Nfig
---	290 K	-131						
15.30	10116.5 K	-126.9	---	2.57	---	---	---	---
20.15	30309.1 K	-123.3	69.63	5.89	3.32	0.05	20.99	13.22

At this point, it is necessary to solve for ΔENR by means of Eq. 11:

$$ENR_1 = (T_{H1} - 290)/290$$

and

$$ENR_2 = (T_{H2} - 290)/290 \rightarrow \Delta ENR = ENR_2 - ENR_1 = (T_{H2} - T_{H1})/290$$

and from Eq. 10,

$$\rightarrow \Delta ENR = \Delta P_n/(290KB) \quad (11)$$

Parameter dY can be calculated from Eq. 12:

$$Y_1 = 10^{(Pn1 - Pn0)/10)}$$

and

$$Y_2 = 10^{(Pn1 - Pn0)/10)} \quad (12)$$

where P_n is in dBm and P_{n0} is the noise power measured on the spectrum analyzer with an input noise power to the DUT of 290 K (the input of DUT terminated with a matched load at 290 K):

$$\rightarrow \Delta Y = Y_2 - Y_1 \quad (13)$$

To evaluate the new noise figure test method, measurements were made of a spectrum analyzer's noise figure (with the preamplifier turned on) using two calibrated noise sources. Using the standard Y-factor method for the two different ENR noise heads, a noise figure of 13.34 dB was measured for the ENR head with 15.30 dB value. For the second calibrated noise source, with an ENR value of 20.15 dB, the standard Y-factor method yielded a spectrum analyzer noise figure of 13.26 dB. Using the new method detailed in this article yielded a noise figure of 13.17 dB for the two different ENR noise heads (**Table 1**).

The noise figure of the spectrum analyzer was also evaluated by means of a method in which the difference of the two ENR noise heads is used with the calibrated noise source data. This is the new method detailed in this report, in which the difference in ENR is determined by taking the difference in the ENR values of the calibrated noise sources (**Table 2**). The value of the spectrum analyzer's noise figure from this approach, at 13.22 dB, was roughly between the values of the first measurement approach and the result from this new approach. Additional measurements were made [results available in the online version of this article (www.mwrf.com) as **Tables 3, 4, and 5**] to show the effectiveness of the new method using a model HP 8970A noise figure test set from Hewlett-Packard/Agilent Technologies (www.agilent.com), with results available for both the measurement equipment and the amplifiers under test.

In summary, a manual noise figure test method has been presented which eliminates the need for a calibrated noise source. The method is as accurate as the previous Y-factor method, while eliminating the expense and calibration routine associated with a calibrated noise source. The method allows the use of a lossy test cable to connect the noise source to the DUT without any need to account for the cable's loss in the noise figure calculations. The accuracy of this method will also depend upon such parameters as measured gain accuracy and ambient room temperature. MWRF

MOHAMMAD BOD
Ph.D. Candidate
mbod@aut.ac.ir

ALI FOUDAZI
Research Engineer
foudazi@shahed.ac.ir

ALI ARAGHI
Research Engineer
a.araghi@shahed.ac.ir

ALI MOHAMMAD MONTAZERI
Research Engineer
montazeri@itrc.ac.ir

MAHMOUD RAMEZANI
Research Engineer
ma.ramezani@shahed.ac.ir

Helical Antenna Links GSM/UMTS

This compact, circularly polarized, dual-band antenna provides sufficient bandwidth making it ideal for GSM and UMTS base-station applications.

ANTENNAS ARE vital to modern communications systems. But as the number of wireless services grows, the number of antennas across the landscape grows, encouraging the design of more compact antenna structures and multiple-antenna solutions. To meet these needs, the authors have developed a compact, dual-band circularly polarized antenna for cellular Global System for Mobile Communications (GSM) systems. It consists of a pair of helical antennas with the same axial coordinate. The outer helical antenna covers the GSM 900-MHz band while the inner antenna is for GSM-1800 MHz and Universal Mobile Telecommunications System (UMTS) 1900-MHz use. Each antenna employs a different rotation to minimize mutual coupling effects and provide high isolation.

Demands for mobile cellular communications services, including voice, short message service (SMS), and high-speed data, continue to increase with the growing number of cellular communications users. For high-capacity mobile stations (MS), optimum dimensioning or cell planning is needed, requiring placement of microcells within macrocells for maximum coverage.[1] Yet, multipath fading is one of the major problems to be overcome in wireless cellular communications networks, and it can be alleviated through space or polarization diversity.[2]

In space diversity, two receiving antennas at the base transceiver station (BTS) are separated by a distance of minimally 10 times the operating wavelength. In polarization diversity, a pair of dipole or slot antennas with ±45-deg. slant polarization is used. Since these conventional schemes require a large area for installation, the design of a compact, dual-band antenna is more applicable for use in a microcell.

To reduce multipath fading effects for BTS antennas, the use of single circularly polarized antennas is often preferred instead of conventional space or polarization diversity antennas. There is no need to align a circularly polarized antenna due to the flexible reciprocal orientation between the transmitter and receiver antennas. Therefore, a circularly polarized antenna can be used instead of two separate antennas using space or polarization diversity.

Although a number of dual-band GSM handset antennas have been reported in the literature,[3,4] some research was performed on designing GSM antennas for BTS applications with high-gain performance. In ref. 5, for example, the feed network of a conventional BTS antenna was modified to achieve a broader impedance bandwidth to cover the UMTS 1900-MHz and GSM 1800-MHz bands simultaneously. However, their final antenna structure was not able to cover the lower-frequency GSM 900-MHz band. In ref. 6, a compact printed dipole antenna was proposed for dual-band GSM applications with a ±45-deg. slant polarization. However, the dipole antenna exhibited low gain, making it inappropriate for use in outdoor GSM applications.

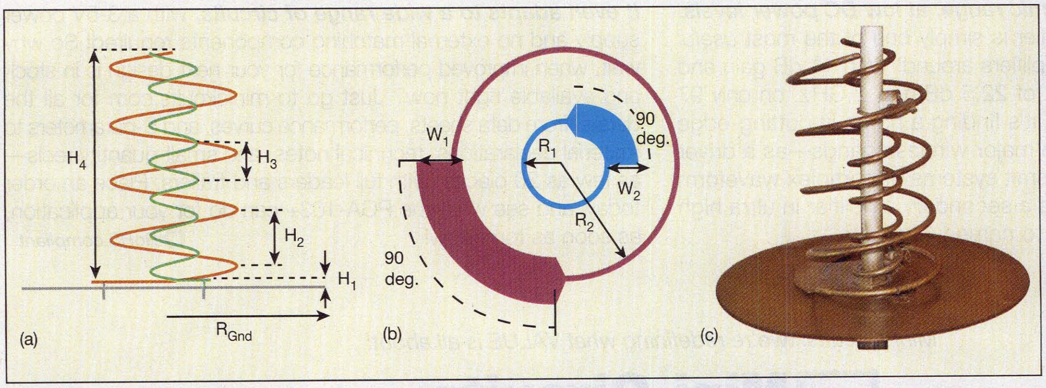

1. These different views show a (a) side view of the proposed dual-band antenna, (b) a top vide of the antenna, and (c) a photograph of the fabricated prototype used in testing.

In the current report, a compact circular polarized antenna was developed for both GSM and UMTS frequency bands. It consists of two axial-mode helix antennas, closely mounted, with inner and outer antenna sections resonating at 1770 to 1870 MHz and at 890 to 990 MHz, respectively. This configuration reduces the dimen-

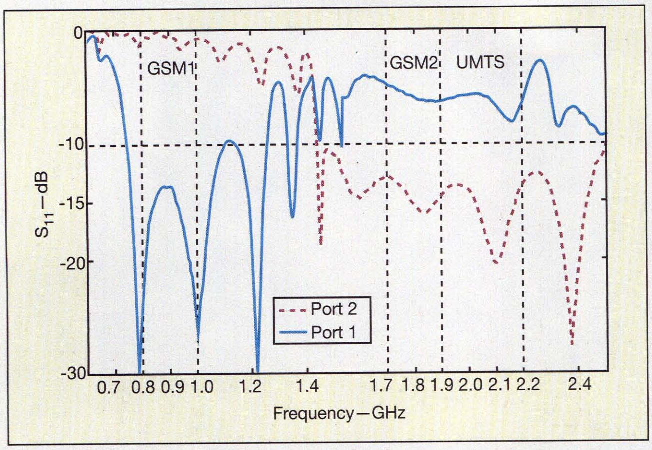

2. These are measured S_{11} results for the proposed dual-band helical antenna.

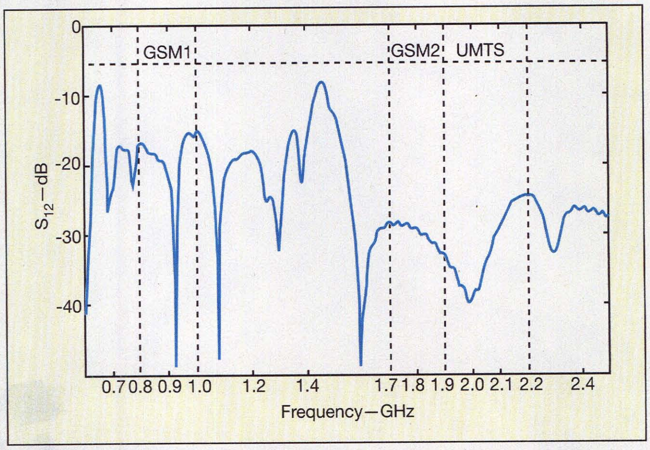

3. These are measured S_{12} results for the proposed dual-band helical antenna.

sions of the antenna without affecting its performance. The compact antenna was designed to produce stable radiation patterns, making it a viable candidate for microcellular GSM base stations as well as for portable BTS use. In addition to covering both GSM bands, itcan also cover UMTS band frequencies.

Figure 1 shows the proposed dual-band helical antenna, with a side view in **Fig. 1(a)**, a top view in **Fig. 1(b)**, and a look at the engineering prototype in **Fig. 1(c)**. Simulation of the antenna was performed with the commercial computer-aided-engineering (CAE) software Ansoft HFSS from Ansys (www.ansys.com). It is a three-dimensional modeling package based on electromagnetic (EM) simulation.

The antenna consists of a pair of helical antennas with the same axial coordinate and different rotation orientation, nested in each other. The inner helical antenna is responsible for GSM 1800 MHz and UMTS 1900 MHz using left-handed circular polarization (LHCP) while the outer antenna is responsible for GSM 900 MHz using right-handed circular polarization (RHCP). By designing two helical antennas with the same axial coordinate, it was possible to achieve the performance of two separate antennas in the physical space of only one. As part of the design of an axial-mode dual-band helical antenna, the circumference of each of the helical antennas was chosen as approximately one wavelength.

The antenna parameters of each helix should be designed to operate at its desired frequency bands with good impedance matching ($S_{11} < -15$ dB). It is desired that each helical antenna has negligible effects on the other antenna. For that reason, each of the helical antennas is employed with different circular polarization, which should result in the mutual coupling effects between the antennas to be diminished.

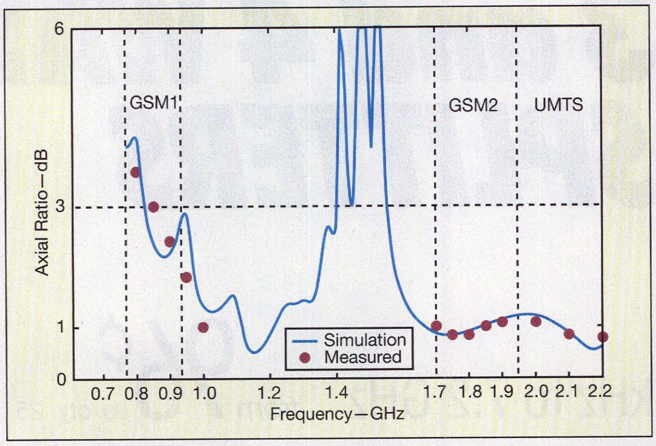

4. These plots compare the simulated and measured axial ratio values at boresight for the dual-band helical antenna.helical antenna.

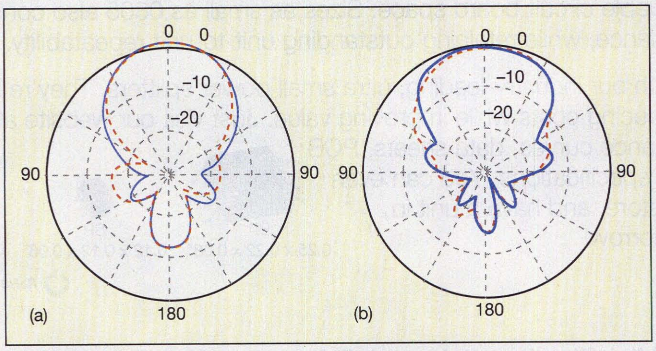

5. These plots show the measured radiation patterns for the dual-band antenna at (a) 950 MHz and (b) 1800 MHz. The blue solid lines and red dashed lines represent $\phi = 0$ and 90 deg., respectively.

For good impedance matching between the impedance of the helical antenna (140 Ω) and a conventional 50-Ω 7/16 coaxial connector, a 90-deg. impedance transformer was used. The optimized parameters of the compact, dual-band circularly polarized helical antenna were as follows: $H_1 = 6$; $H_2 = 52$; $H_3 = 34$; $H_4 = 4*52$; $R_{gnd} = 145$; $R_1 = 23$; $R_2 = 50$; and $W_1 = W_2 = 18$. The inner helical antenna has 6.2 turns while the outer helical antenna has 4 turns. The helical antenna wire diameter is fixed at 3 mm. The fabricated prototype of the proposed antenna is shown in **Fig. 1(d)**.

Figures 3 and 4 show the measured S-parameters for the proposed dual-band helical antenna. As it can be seen, the antenna's impedance matching for port 1 (the inner helical antenna) is well below −10 dB in the 1700-to-2200-MHz frequency band allocat-

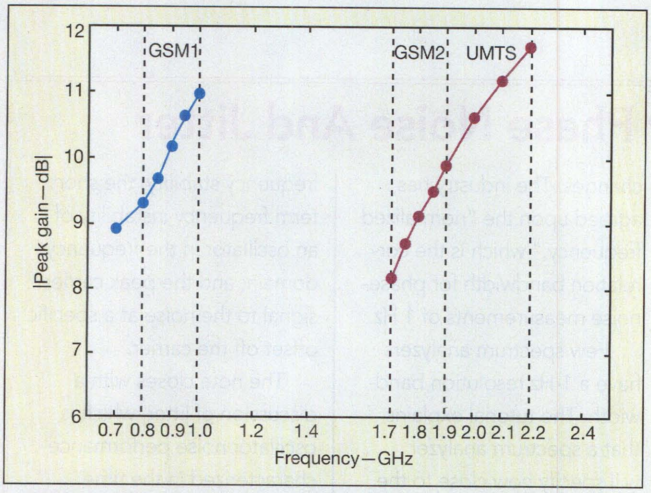

6. These plots show the measured peak gains for the dual-band helical antenna in the two frequency bands of interest.

ed to GSM and UMTS use. In addition, the impedance matching of port 2 (the outer helical antenna) is well below −10 dB in the 800-to-1000-MHz frequency band.

Figure 4 shows the simulated and measured results of the antenna's axial-ratio (AR) performance. The antenna yields good results, with AR of less than 3 dB in the frequency bands of 800 to 1000 MHz and 1700 to 2200 MHz. **Figure 5** shows the measured radiation patterns for the proposed dual-band antenna at 950 and 1850 MHz. As can be seen, the antenna delivers stable radiation patterns in both the principle plane of $\phi = 0$ and 90 deg. at both frequencies. **Figure 6** shows the peak gain results for the proposed dual-band antenna. The peak gain varies slightly between 9 to 11 dB in the two separate frequency bands.

To calculate the coverage area for the proposed dual-band antenna the Okumura-Hata-COST231[7] model was used as a channel model. For the sake of calculating the link budget using this antenna, a height of 40 m above the ground was assumed, with a 12-deg. tilt angle with respect to horizontal. These values of tilt and height are common in terrestrial BTS antennas to provide maximum achievable coverage.

The link budget parameters were considered as follows. The receiver antenna gain and transmitted power for the mobile station were set at 0 dB and +29 dBm, respectively. The average building height of the modeled operating environment, the mobile station height, the street width, and miscellaneous loss (including cable losses and losses within the BTS equipment) were assumed to be 15 m, 1.8 m, 10 m, and 13 dB, respectively. **Figure 7** shows the expected coverage area (in km) for the proposed antenna at 950 and 1850 MHz.

In summary, a new compact dual-band dual-port helical antenna for GSM 900, GSM 1800, and UMTS 1900 MHz was presented. The antenna consists of a pair of helical nested in each other with the same axial coordinate and different rotational orientation. A prototype of the antenna was fabricated and the measured results show that the antenna has good S-parameters, stable radiation patterns, and appropriate peak gain for true dual-band operation. The coverage area of the proposed dual-band circularly polarized antenna, as determined by the Okumura-Hata-COST231 channel model, when the antenna is mounted on a conventional base station, indicates that this design is suitable for use in portable and microcellular BTS applications. MWRF

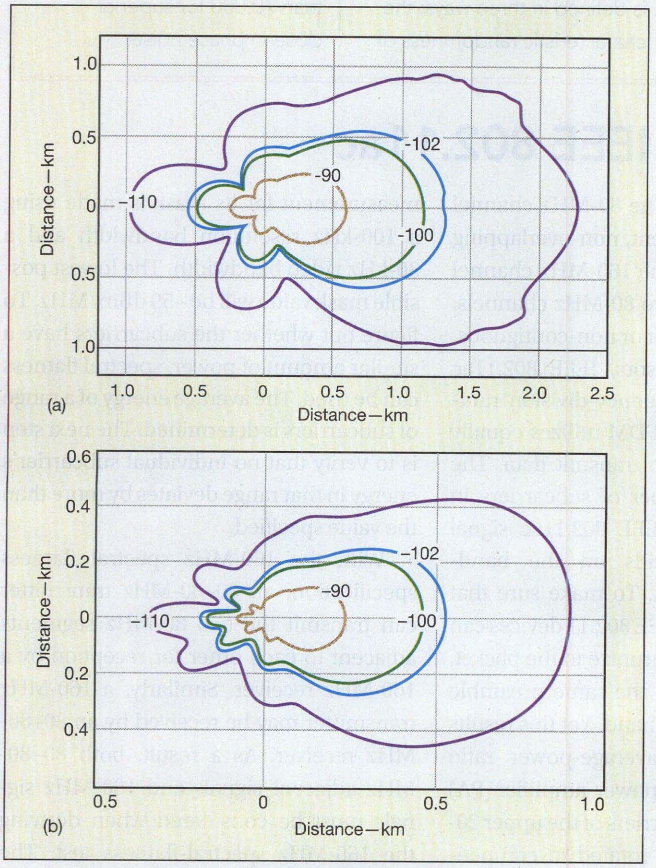

7. This plot shows the coverage area of the proposed dual-band antenna assuming a 40-m elevation and tilt angle of 12 deg. from horizontal at (a) 950 MHz and (b) 1850 MHz.

ACKNOWLEDGMENTS

This work was sponsored by the Satellite Communications Group at the Iran Telecommunication Research Center. The authors would like to express their great gratitude to Dr. M. Shahabadi, Associated Professor of University of Tehran (Tehran, Iran) for his constructive advice.

REFERENCES

1. G. Eason, B. Noble, and I.N. Sneddon, "On certain integrals of Lipschitz-Hankel type involving products of Bessel functions," Phil. Transactions of the Royal Society London, Vol. A247, April 1955, pp. 529-551.
2. J.J.A. Lempiainen and J.K. Laiho-Steffens, "The performance of polarization diversity schemes at a base station in small/micro cells at 1800 MHz," IEEE Transactions on Vehicular Technology, Vol. 47, No. 3, August 1998, pp. 1087-1092.
3. J. Guterman, A.A. Moreira, and C. Peixerio,"Dual-band miniaturized microstrip fractal antenna for a small GSM 1800 + UMTS mobile handset," Proceedings of the 12th IEEE Mediterranean Electrotechnical Conference (MELECON 2004), Vol. 2, May 12-15, 2004, pp. 499-501.
4. G. Zhou, "A non-uniform pitch dual band helix antenna," IEEE Antennas and Propagation Society International Symposium, Vol. 1, 2000, pp. 274-277.
5. S.K. Ibrakee and J.M. Rigelsford, "A broadband antenna for GSM1800 and UMTS BTS applications," Proceedings of the 5th European Conference on Antennas and Propagation (EUCAP), April 11-15, 2011, pp. 511-513.
6. K. Mohammadpour-Aghdam, S. Radiom, G. Vandenbosch, and G. Gielen, "A dual-band printed dipole antenna for indoor GSM-BTS applications," European Microwave Conference digest, Sept. 29-Oct. 1 2009, pp. 634-637.
7. M. Hata and T. Nagatsu, "Mobile location using signal strength measurements in cellular systems," IEEE Transactions on Vehicular Technology, Vol. 29, 1980, pp. 245-251.

GET A HANDLE On Oscillator Phase Noise And Jitter

PHASE NOISE GREATLY differs between commodity and high-performance crystal oscillators. Yet its impact can be significant, as the oscillator's phase-noise characteristic dominates system performance. An application note from Crystek Corp.'s Ramón Cerda, titled "Impact of ultralow phase noise oscillators on system performance," offers a useful tutorial on both phase noise and jitter.

The document starts with a basic definition of phase noise—the rapid, random fluctuations in the phase component of a signal source's output signal. It moves on to explain the noise floor, emphasizing that the goal is to maximize the signal and minimize the noise for a high signal-to-noise ratio (SNR). Noise on a carrier is either random or deterministic. While random noise spreads the carrier, deterministic noise generates sidebands on the carrier.

When specifying spectral purity of an oscillator or signal source, one standard measurement bandwidth should be used to make any comparisons of different oscillators meaningful. After all, when the resolution bandwidth on a spectrum analyzer is changed, the noise magnitude also changes. The industry has agreed upon the "normalized frequency," which is the correlation bandwidth for phase-noise measurements of 1 Hz.

Few spectrum analyzers have a 1-Hz resolution bandwidth. The tutorial explains that a spectrum analyzer will specify how close to the carrier it can measure. For measurements closer than this minimum resolution bandwidth, it is possible to normalize the reading to 1 Hz.

Because a signal's noise spectrum is symmetrical around the carrier frequency, it is only necessary to specify one side. The section closes by noting that phase noise is defined in three ways: the characteristic randomness of frequency stability; the short-term frequency instability of an oscillator in the frequency domain; and the peak carrier signal to the noise at a specific offset off the carrier.

The note closes with a discussion of jitter, which is oscillator noise performance characterized in the time domain. It is a variation in the zero-crossing times of a signal or a variation in the signal period. As phase noise increases in the oscillator, so does jitter. The note closes by explaining that a true ultra-low-phase-noise oscillator uses a discrete, high-performance topology with a precision packaged crystal that has a Q greater than 70,000 for superior close-in phase noise.

Crystek Corp., 12730 Commonwealth Dr., Fort Myers, FL 33913; (239) 561-3311, www.crystek.com.

TAKE AN IN-DEPTH LOOK At IEEE 802.11ac

GIVEN THE SUCCESS of the IEEE 802.11-2007 standard, the industry was inspired to make wireless networks perform as well as their wired brethren. One result of these efforts is the 802.11ac amendment, which offers mechanisms to increase throughput and enhance the wireless-local-area-networking (WLAN) experience. Elaborating on this standard is a new white paper, "802.11ac Technology Introduction."

Beginning with sections on IEEE 802.11ac core documents and key requirements, the 28-page document seeks to truly provide a primer on this technology. The main requirements for IEEE 802.11ac are backwards compatibility and co-existence with IEEE 802.11a and 802.11n devices, as well as certain performance goals for single-station and multi-station throughput. IEEE 802.11ac devices must support 20-, 40-, and 80-MHz channels together with one spatial stream. The 80-MHz channel comprises two adjacent, non-overlapping 40-MHz channels. The 160-MHz channel may be formed by two 80-MHz channels, which can be adjacent or non-contiguous.

Like its predecessors, IEEE 802.11ac uses orthogonal-frequency-division multiplexing (OFDM). OFDM utilizes equally spaced subcarriers to transmit data. The number of subcarriers in the IEEE 802.11ac signal depends on the bandwidth. To make sure that all IEEE 802.11 devices can synchronize to the packet, IEEE 802.11ac sends the same preamble in each 20-MHz sub-band. Yet this results in a high peak-to-average-power ratio (PAPR), which limits power-amplifier (PA) efficiency. The subcarriers of the upper 20-MHz sub-bands are rotated to compensate for this effect.

Rohde & Schwarz, Muehldorfstrasse 15, 81671 Munich, Germany, www.rohde-schwarz.com.

The white paper touches on the IEEE 802.11ac transmitter specification. The measurement for its mask is made using a 100-kHz resolution bandwidth and a 30-kHz video bandwidth. The lowest possible mask value will be –59 dBm/MHz. To figure out whether the subcarriers have a similar amount of power, spectral flatness can be used. The average energy of a range of subcarriers is determined. The next step is to verify that no individual subcarrier's energy in that range deviates by more than the value specified.

With the 160-MHz spectral flatness specification, an 80+80-MHz transmitter can transmit the two 80-MHz segments adjacent to each other for reception by a 160-MHz receiver. Similarly, a 160-MHz transmitter may be received by an 80+80-MHz receiver. As a result, both 80+80-MHz adjacent signals and 160-MHz signals must be considered when deriving the 160-MHz spectral-flatness test. The paper offers many details and tips like this to provide an excellent resource on IEEE 802.11ac.

JACK BROWNE | Technical Contributor

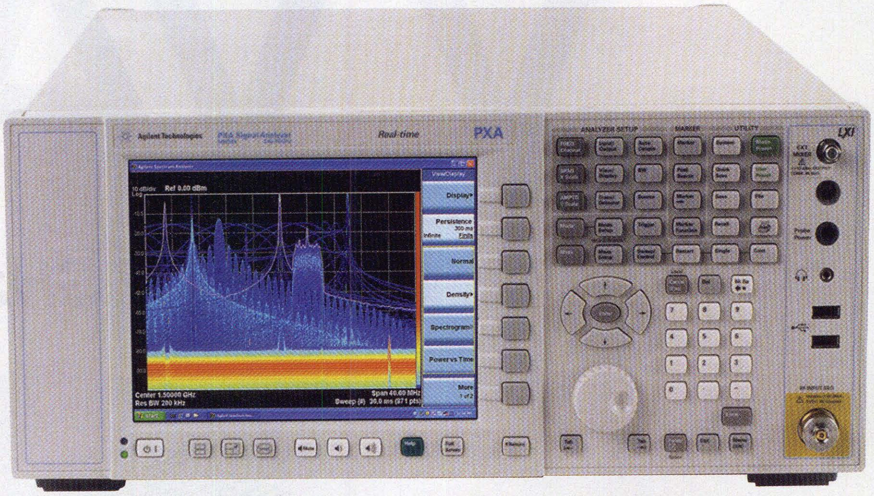

1. The PXA X-Series signal analyzers are available with real-time analysis bandwidths of 85 or 160 MHz for center frequencies from 3.6 to 50 GHz.

REAL-TIME ANALYZERS Grab 50-GHz Signals

A new line of high-speed spectrum analyzers boasts excellent sensitivity and capture bandwidths of 85 and 160 MHz.

HIGH-FREQUENCY SIGNALS grow more elusive with time, making the task of a spectrum or signal analyzer to capture them more challenging with each new generation of commercial and military electronic systems. In response to the increasing agility of modern signals, the PXA X-Series signal analyzers with real-time spectrum analysis (RTSA) from Agilent Technologies (www.agilent.com) provide a measurement range of 50 GHz. These analyzers can record and study a wide range of signals, from extremely short and intermittent signals to traditional sine waves, with a high probability of intercept (POI).

PXA X-Series models are available with real-time spectrum analysis bandwidths as high as 85 and 160 MHz. In addition, they can capture low-level signals with sensitivity of –157 dBm at 10 GHz, without the assistance of an additional preamplifier. These RTSAs are equipped to record and play back the most short-term and complex modulated signals found in modern commercial, industrial, and military electronics systems and their components—even when those signals are designed to be difficult to detect.

Of course, the term "real time" can have a variety of meanings. It is probably best associated with a digital sampling oscilloscope but, as seen with the PXA instruments, can also be applied to spectrum analysis. Agilent offers a thorough education on what "real time" means in terms of the company's instruments (at http://www.agilent.com/about/newsroom/tmnews/background/real-timePXA/). In essence, a real-time analyzer is capable of providing calculation and acquisition speeds that are fast enough to deliver gap-free analysis of measured data that has been sampled or captured with a data converter. In the case of the real-time PXA X-Series analyzers, the gap-free analysis is extended across impressive bandwidths of 85 and 160 MHz.

These RTSA capabilities are available with a new purchase of N9030A PXA signal analyzer (**Fig. 1**), or can be added as upgrade options to existing PXA signal analyzers, with the N9030AK-RT1 upgrade supporting real-time spectrum analysis at bandwidths to 85 MHz and the N9030AK-RT2 upgrade enabling real-time spectrum analysis at bandwidths to 160 MHz. Analyzer models are available for frequency ranges spanning 3 Hz to 3.6, 8.4, 13.6, 26.5, 43, 44, and 50 GHz, and can be extended to 325 GHz and beyond by external mixing. This is the first time that real-time analysis capability has been available as an upgradeable option to a "conventional" signal analyzer, such as one of the PXA instruments. This offers facilities the flexibility to add the real-time measurement capability as needed.

The real-time PXA analyzers deliver outstanding measurement performance by leveraging both hardware and software within each instrument. They promise a 100% POI for signals as brief as 3.57 μs with full amplitude accuracy. Coupled with their wide analysis bandwidths and low noise characteristics, these analyzers can detect and isolate even short-term, low-level signals from relatively noisy signal environments; this includes signals surrounded by higher-level jammers and interference signals. The analyzers boast internal single-sideband (SSB) phase noise of –132 dBc/Hz offset 10 kHz from a 1-GHz carrier. They also provide third-order-intermodulation (TOI) distortion of +22 dBm at 1 GHz as evidence of an extremely wide measurement dynamic range.

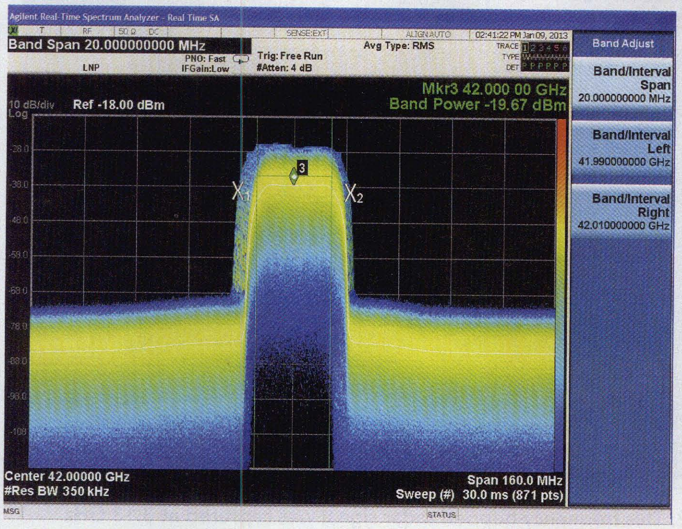

2. The real-time PXA X-Series analyzers can capture a span of signals as wide as 160 MHz at center frequencies as high as 50 GHz.

With a spurious-free dynamic range (SFDR) of 75 dB, each analyzer can detect and display extremely small signals in the presence of large signals across analysis bandwidths as wide as 160 MHz. The reference level for a real-time PXA X-Series analyzer can be set from –170 to +30 dBm in 0.01-dB steps in the log scale and from 707 pV to 7.07 V with 0.11% (0.01 dB) resolution in the linear scale.

The PXA analyzers offer excellent amplitude accuracy of ±0.19 dB for a wide range of signal levels. Furthermore, that 160-MHz analysis bandwidth (**Fig. 2**) brings with it exceptional amplitude performance and phase linearity to minimize internal errors for vector signal analysis as well as for real-time spectrum analysis. The analyzers also offer some software tools to assist with more challenging measurements, such as the noise-floor-extension (NFE) technology. The NFE functionality reduces measurement noise by as much as 10 dB. Using the NFE feature and a preamplifier, each analyzer can achieve a displayed average noise level (DANL) of –172 dBm at 1 GHz.

The NFE technology is based on the fact that 90% or more of each instrument's contributed noise power is predictable and can be measured, calibrated, and eliminated as part of a normal measurement procedure. Using the NFE technology, for example, helps achieve a wideband-code-division-multiple-access (WCDMA) adjacent-channel leakage ratio (ACLR) dynamic range of nominally –88 dBc when evaluating WCDMA cellular systems and their components.

In terms of measurement capability, these real-time PXA analyzers can make zero-span as well as swept and Fast Fourier Transform (FFT) mode measurements across their various frequency ranges. Each analyzer includes a frequency counter with marker resolution of 0.001 Hz. For zero-span measurements, sweep times can be adjusted from 1 μs to 6000 s. In addition to traditional zero-span analysis, the PXA also offers a wideband, gap-free power-versus-time display that enables users to view and measure short-duration pulses with fast rise/fall times in the time domain. For frequency spans of greater than 10 Hz, sweep times can be set from 1 ms to 4000 s. Trigger delays for zero-span measurements can be set from –150 to 500 ms. For spans greater than 10 Hz, trigger delays can be set from 0 to 500 ms, with resolution of 0.1 μs.

Measurements can be made with resolution bandwidths set from 1 Hz to 3 MHz in 10% steps, and with resolution bandwidths of 4, 5, 6, and 8 MHz. The bandwidth accuracies of these resolution-bandwidth filters is within ±1% for resolution bandwidths to 1 MHz; ±0.07% for resolution bandwidths from 1.1 to 2.0 MHz; ±0.10% for resolution bandwidths from 2.2 to 3.0 MHz; and ±0.20% for resolution bandwidths from 4 to 8 MHz.

The analyzers are available with a number of useful options for traditional signal analysis. For example, for facilities concerned with electromagnetic-compatibility (EMC) testing, the PXA X-Series analyzers can be equipped with option EMC for accurate, standards-based electromagnetic-interference (EMI) measurements. The option supports Comite International Special des Perturbations Radioelectriques (CISPR) standards for compliant EMI bandwidths of 200 Hz, 9 kHz, 120 kHz, and 1 MHz. Also supported are EMC measurements compliant to MIL-STD-461E requirements at bandwidths of 10 Hz, 100 Hz, 1 kHz, 10 kHz, 100 kHz, and 1 MHz.

The analyzers are available with video bandwidths of 1 Hz to 3 MHz in 10% steps, and 4, 5, 6, and 8 MHz with ±6% nominal accuracy in swept measurement mode and for zero-span measurements. Optional preamplifiers can be specified for 9 kHz to 3.6 GHz, 9 kHz to 8.4 GHz, 9 kHz to 13.6 GHz, 9 kHz to 26.5 GHz, 9 kHz to 43 GHz, 9 kHz to 44 GHz, and 9 kHz to 50 GHz, with 20-dB gain to 3.6 GHz, 35-dB gain from 3.6 to 26.5 GHz, and 40-dB gain from 26.5 to 50 GHz.

These high-performance signal analyzers include mechanical input attenuators to help boost the effect dynamic measurement range. The input attenuators cover a range of 0 to 70 dB in 2-dB steps for frequencies from 3 Hz to 50 GHz. As an option (EA3), the analyzes can also be outfit with an electronic attenuator with frequency range of 3 Hz to 3.6 GHz with range of 0 to 24 dB in 1-dB steps. When combined with the mechanical input attenuator, the total attenuation range is 0 to 94 dB in 1-dB steps. The real-time spectrum analyzers can handle maximum safe input levels to +30 dBm (1 W) with or without their optional preamplifier. The can work with peak pulse power levels as high as +50 dBm (100 W) for pulse widths of less than 10 μs and less than 1% duty cycle and at least 30-dB input attenuation applied.

Every PXA includes in-phase/quadrature (I/Q) analyzer functionality and Agilent PowerSuite for analysis of captured signals; in addition, captured signals can be transferred to RF/microwave signal generators for further use in testing, or to mathematics or high-frequency software simulation tools, such as the Agilent High-Frequency System Simulator (HFSS) software, for further analysis and/or reuse. Use of software tools such as the PowerSuite can speed and simplify repetitive or standards-based measurements, such as readings of third-order-intercept (TOI) point and harmonic distortion. Measurement functions that are built within each real-time PXA analyzer's code, such as frequency mask trigger (FMT), can also add to the real-time analysis capabilities of the instrument: They make it possible to capture and isolate elusive spurious signals; signals that are hidden in noisy environments; or even frequency-hopped signals (**Fig. 3**).

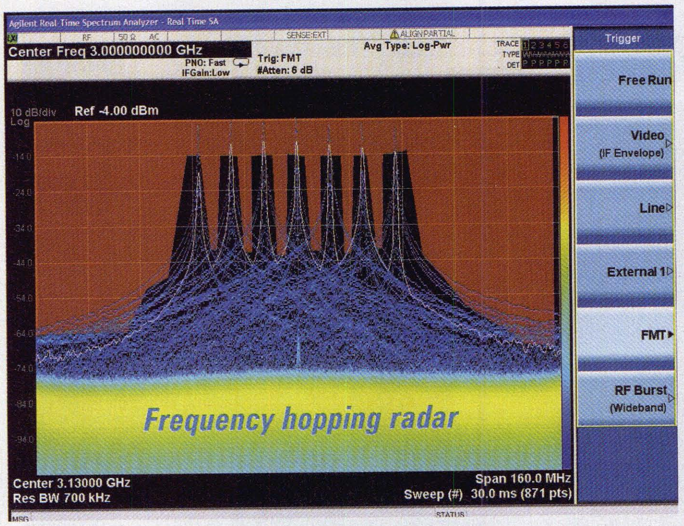

3. This frequency-hopped radar signal was captured at 3.13 GHz using a 160-MHz span and a 700-kHz resolution-bandwidth filter.

The real-time PXA analyzers also work seamlessly with Agilent's 89600 VSA software for advanced vector signal-analysis capabilities. The 89600 VSA software takes advantage of the PXA's real-time FMT which allows capture of a real-time I/Q recording or trigger other measurements. The software also provides connections to Agilent instruments such as vector signal generators and arbitrary waveform generators to play back captured signals as inputs to a device under test (DUT). The analyzers are built around an open Windows operating system which makes it possible to run software applications—such as simulators and mathematics programs—inside the analyzer. The analyzers incorporate GPIB and LXI/LAN ports for automated testing with an external computer, along with two Universal Serial Bus (USB 2.0) ports on the front panel and four on the rear panel. A wide range of measurement capabilities can be added by means of firmware-based measurement applications.

Captured signals are shown on a 21.4-cm high-resolution XGA display screen, with as many as 12 markers available to identify different segments of a signal trace. High signal quality is reinforced by sampling circuitry that relies on an embedded 16-b analog-to-digital converter (ADC). The analyzers feature soft keys to simplify operation, and allow operators to connect a digital mouse and keyboard to operate each analyzer like a personal computer (PC). Each instrument incorporates a removable central processing unit (CPU) to simplify upgrades, as well as a removable solid-state memory drive. A VGA video output port allows connection of an external display screen.

With its many measurement capabilities, each PXA X-Series analyzer can potentially replace a number of more specialized instruments, such as noise-figure analyzers and power meters. The scalable design of these analyzers also helps simplify performance enhancements and upgrades. P&A: $7224 (N9030AK-RT1 upgrade to 85-MHz real-time bandwidth), $10,320 (N9030AK-RT2 upgrade to 160-MHz real-time bandwidth), and $96,304 and up (new N9030A PXA 3.6-GHz signal analyzer with real-time option to 160 MHz bandwidth). MWRF

AGILENT TECHNOLOGIES, INC., 5301 Stevens Creek Blvd., Santa Clara, CA 95051; (877) 424-4536, (408) 345-8886, FAX: (408) 345-8475, e-mail: us@agilent.com, www.agilent.com.

JACK BROWNE | Technical Contributor

Vacuum Devices Drive High Power

Vacuum electron devices are still unmatched by solid-state devices at microwave and millimeter-wave frequencies for their output power per device.

VACUUM ELECTRON devices such as traveling-wave tubes (TWTs) may be considered "archaic technologies" by some—especially in an age of solid-state devices with ever-increasing power densities, such as gallium nitride (GaN) transistors. But vacuum devices still play vital roles in RF, microwave, and millimeter-wave applications across numerous markets, including broadcast, commercial, industrial, and military systems. When the need arises for very high power density at high frequencies, solid-state technology still doesn't come close to the capabilities of vacuum electron devices like TWTs, klystrons, and magnetrons.

1. Model MT2400 is a high-power antenna-mountable Ku-band amplifier based on a TWT active device. [Photo courtesy of MCL, Inc., a MITEQ Company (www.mcl.com).]

For commercial use, satellite-communications (satcom) systems employ a large number of high-frequency vacuum electron devices because of their needs for such high power densities to send high-power signals across great distances. But the high power densities afforded by vacuum tube devices are also essential to research applications in nuclear science; medical electronic systems; air-traffic-control (ATC) systems; and military and commercial systems. One of the largest groups of vacuum-tube-based solutions is based on TWT technology and traveling-wave-tube-amplifier (TWTA) devices.

For example, Communications & Power Industries (CPI; www.cpii.com) offers high-throughput-satellite (HTS) services for both continuous-wave (CW) and pulsed applications from UHF through Ka-band frequencies. As an example, the firm's model VKU-7891 TWTA provides 40-dB gain and 3 kW CW output power from 14.0 to 14.5 GHz while operating with 11 kV beam voltage and 1.1 A beam current. CPI recently received an order for more than $6 million for Ka-band high-power satcom amplifiers for HTS services. Late last year, the company also received orders from a US military prime contractor in excess of $5 million for both solid-state and vacuum-electron-device amplifiers, including the company's SuperLinear® high-power Ka-band satcom TWTAs. Since 1977, the company has also delivered in excess of 130 gyrotrons and produced more than 16 experimental vehicles; these range in frequency from 8 to 250 GHz, featuring output power levels from 900 kW CW and 1.3 MW pulsed output power.

Some vacuum tubes, such as magnetrons, generate rather than amplify signals by applying high-voltage energy to a series of resonant cavities. The energy fed into the resonant cavities must be carefully controlled in terms of phase and level. A heated cathode in a magnetron is the source of electrons. The electrons leave the cathode and accelerate towards the magnetron's anode due to the magnetic field resulting from the applied voltage. The frequency of the electrons is affected by the effects of their traveling through the resonant cavities.

For some radars, frequency-agile magnetrons (which are available from CPI in various forms) can help improve the system's capabilities to detect targets in environments plagued by a great deal of signal clutter, such as other sources of RF/microwave energy. Increasing the pulse-to-pulse frequency spacing can increase the detection capability of a radar system, although the magnetron must be capable of turning on and off relatively short pulses. A number of different types of frequency-agile magnetrons are available, including dither magnetrons with output frequency that varies periodically with a constant excursion and fixed center frequency.

In contrast, some magnetrons, such as beacon magnetrons developed for use in

At the heart of the next generation electronic defense systems.

The next generation air and missile defense radars demand effectiveness, reliability, power efficiency and affordability. You can count on CTT's twenty-five years of experience in microwave amplification and subsystem integration to meet these demands.

CTT offers not only form, fit, function of microwave amplifier replacements for many mature systems, but also incorporates leading-edge technology components such as GaN and GaAs.

CTT has delivered production quantities of amplifiers with power levels of 10, 20, 40, 80, and 100 Watts – and higher – for a variety of radar applications.

CTT is well positioned to offer engineering and production technology solutions – including high-rel manufacturing – to infuse new technology into legacy systems for improved reliability and life cycle costs.

- AMDR-X Radar
- Shipboard Radar
- VLO/FLO Threats
- New Land Radar

More than twenty-five years ago CTT, Inc. made a strong commitment to serve the defense electronics market with a simple goal: quality, performance, reliability, service and on-time delivery of our products.

Give us a call to find out how our commitment can support your success. **It's that simple.**

Microwave Technology Leadership

- ❖ **Power Amplifiers**
  - Radar Bands up to 400W
  - Pulse and CW
  - **NEW** Rack-Mount Configurations
  - **NEW** GaN and GaAs Models
- ❖ **Low-Noise Amplifiers**
- ❖ **Up and Downconverters**
- ❖ **Subsystems**
- ❖ **Contract Manufacturing**
- ❖ **Custom Engineered Options**

nsai

ISO 9001:2000 QUALITY

USA-based thin-film microwave production facility

CTT INC.

241 East Java Drive • Sunnyvale • California 94089 radar transponders, must be fairly small. This type of microwave vacuum electron tube produces about 5 W output power and weighs less than 8 oz. It must be frequency stable without additional electronics in a radar transponder, yet remain stable in frequency with temperature.

MCL, Inc., a MITEQ Company (www.mcl.com) has long supplied compact and reliable TWTA products for satcom applications, including the recent development of the antenna mount model MT2400 TWTA for Ku-band outdoor satcom uplink and satellite-news-gathering (SNG) applications **(Fig. 1)**. This tube amplifier is supplied in a light-weight, weather-resistant package measuring 8.9 × 8.12 × 17.3 in. (226 × 206 × 440 mm) and weighing about 32 lbs (14.5 kg) with forced-air cooling. The TWTA, which provides 208 W (+53.2 dBm) output power from 13.75 to 14.50 GHz (as much as 400 W peak output power), is available with gain levels of 60 or 70 dB, depending upon option, with worst-case gain variation of 1 dB per 80 MHz for narrowband use and 2.5 dB per 500 MHz for full-band use.

The TWTA, which is designed to meet ML-188-164A requirements, includes an Ethernet interface for computer connection and continuous attenuator adjustment in 0.1-dB steps. The amplifier features a Type-N female input connector and WR-75G Ku-band waveguide flange at the output port. It has an operating temperature range of –40 to +60°C. The compact outdoor TWTA can be customized through a variety of options, including an additional input solid-state amplifier (SSA), internal linearizer circuitry, and an input L-band block frequency upconverter.

Teledyne MEC (www.teledyne-mec.com) offers a website with excellent technical section on vacuum electron devices, including thorough descriptions of key parameters, including gain, efficiency, noise, and reliability (http://www.teledyne-mec.com/products/Technical_description.aspx). The firm also offers a number of high-performance, broadband TWTs through microwave and millimeter-wave frequencies.

Model MEC 5424 provides minimum CW output power of 250 W from 6 to 18 GHz, with 35 dB gain at 6 GHz, 46 dB gain at 12 GHz, and 35 dB gain at 18 GHz. It achieves typical saturated output power of 275 W at 6 GHz, 300 W at 12 GHz, and 275 W at 18 GHz with an operating temperature range of –40 to +85°C. For higher frequencies, the company also offers model MEC 5496, with 40-W minimum CW output power from 26.5 to 40.0 GHz. It achieves 40 W typical output power at 26.5 GHz, with 45-dB typical gain. The typical

output power is 50 W at 30 GHz, with 50-dB typical gain; 60 W typical output power at 36 GHz, with 50-dB typical gain; and 40 W typical output power at 40 GHz, with 35-dB typical gain. The TWT is designed for typical heater power of 0.7 A at –6.3 VDC, with cathode energy of –13.5 kV at 100 mA, and 6.75 kV at 10 mA for collector No. 1 and 3.38 kV at 80 mA for collector No. 2.

The TH 3977 DH series of TWTs from the Thales Group (www.thalesgroup.com) features tubes with a dual-stage collector design for high efficiency and periodic-permanent-magnet (PPM) focusing. The tubes are available with typical gain of 50 dB from 17.3 to 18.4 GHz with continuous output-power levels as high as 750 W across that frequency range. The conduction-cooled TWTs are ideal for direct-broadcast-satellite (DBS) uplinks as well as for SNG applications.

Of course, the history of high-frequency vacuum electron devices has not been restricted to this country: In Japan, Toshiba Electron Tubes & Devices Co. Ltd. (www.toshiba-tetd.co.jp) developed a high-power klystron for UHF television broadcast applications as far back as 1961. The company has developed some of the world's most powerful klystrons, including units capable of 1.2 MW continuous output power at 508 MHz and 100 MW pulsed output power at 2.8 GHz using period-permanent-magnet (PPM) focusing. At higher frequencies, the firm's model E3845 TWT delivers 12.5 kW continuous output power for satcom applications from 9.2 to 9.5 GHz. It features forced-air cooling and long-life, high-current-density cathodes for high reliability and high output power from a package measuring only 499 ×127 × 158 mm and weighing 12 kg.

A firm perhaps best known for its semiconductors, e2v (www.e2v.com), also offers a wide range of vacuum electron devices that includes klystrons, magnetrons, and helix TWTs. The company offers narrowband and wideband devices for commercial and military applications, including the model N10110 helix TWT for use from 6 to 18 GHz. It offers 45-dB gain across that range with 180-W CW minimum output power. Designed for 6200-V cathode voltage, the tube measures 329 × 50 × 62 mm.

Finally, L-3 Electron Devices Division (www.L-3Com.com), which began life as part of Litton Industries, offers a variety of vacuum electron tube devices for medical, broadcast, and military applications, including helix and coupled-cavity TWTs, klystrons, crossed-field amplifiers (CFAs), magnetrons, and thyratrons (**Fig. 2**). The company, which offers miniature TWTs for use from 2 to 46 GHz, produces devices with output levels as high as 5 kW average output power and 150 kW peak output power across 10% operating bandwidths at C-, X-, and Ku-band frequencies. It also produces microwave power modules (MPMs), which are complete microwave power amplifiers based on a TWT, a solid-state driver amplifier, and an electronic power conditioner (EPC).

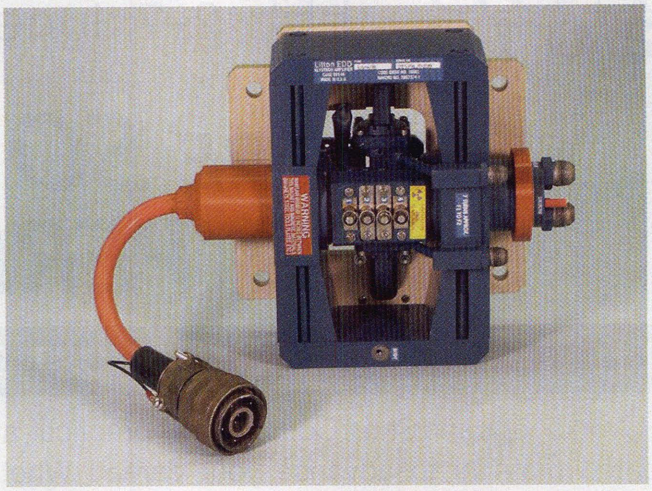

2. This high-power amplifier is based on a klystron vacuum electron device and includes power supply, active device, and supporting circuitry. [Photo courtesy of L-3 Electron Devices Division (www.L-3Com.com).]

These are a few examples of the high pulsed and CW output-power levels possible with vacuum electron devices at RF, microwave, and millimeter-wave frequencies. Although they must be powered by high-voltage supplies, these devices still deliver considerably higher power densities that possible with high-frequency solid-state devices, and likely that will continue for many years to come. MWRF

Amplifiers Aid EMC Measurements

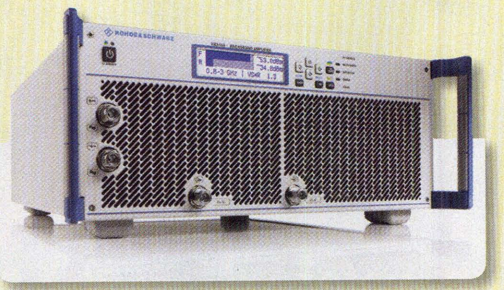

Compact amplifiers in the R&S BBA150 amplifier family support electromagnetic-compatibility (EMC) testing through 3 GHz, as well as for non-EMC applications in component production and quality assurance. The modular amplifiers can be operated manually via their front-panel displays, or else remotely via external computer and software. The first model in the series operates from 0.8 to 3.0 GHz and is available with power levels ranging from 30 to 200 W output power. The 200-W version occupies only four height units in a standard 19-in. rack.

ROHDE & SCHWARZ USA, INC., 8661A Robert Fulton Dr., Columbia, MD 21046-2265; (410) 910-7800, FAX: (410) 910-7801; e-mail: info@rsa.rohde-schwarz.com, *www.rohde-schwarz.com.*

SDLVA Captures Signals To 6 GHz

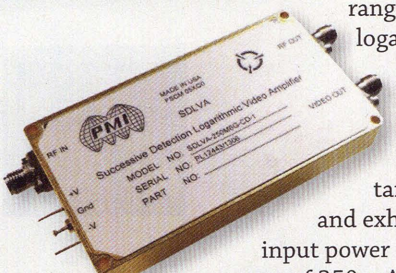

Successive-detection log-video amplifiers (SDLVAs) such as the model SDLVA-250M6G-CD-1 help process pulsed and continuous signals over a wide dynamic range. This particular unit operates from 0.25 to 6.0 GHz with a dynamic range from −70 to 0 dBm and ±2.5-dB worst-case logarithmic linearity. It features a fast rise time of 10 ns or less and recovery time of less than 60 ns. Supplied in a compact housing measuring just 3.2 × 1.8 × 0.4 in. with female SMA connectors, the SDLVA achieves typical tangential signal sensitivity (TSS) of −73 dBm and exhibits maximum VSWR of 2.0:1. It can handle input power levels as high as +17 dBm and draws nominal current of 350 mA at +15 VDC and 180 mA at −15 VDC. The amplifier, which is designed for operating temperatures from −40 to +70°C, meets the applicable requirements of MIL-STD-202F for humidty, shock, vibration, and altitude.

PLANAR MONOLITHICS INDUSTRIES, INC., 7311-F Grove Rd., Frederick, MD 21704; (301) 662-5019, FAX: (301) 662-1731, e-mail: sales@pmi-rf.com, *www.pmi-rf.com.*

Splitters Serve In-Building DAS

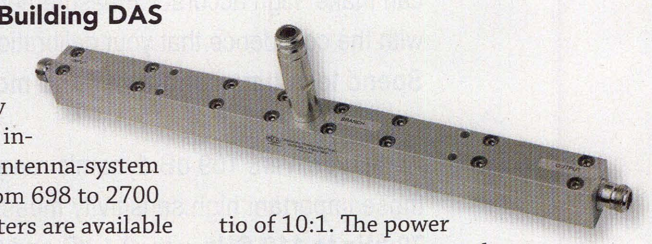

A line of unequal power splitters has been developed by MECA Electronics for in-building distributed-antenna-system (DAS) applications from 698 to 2700 MHz. The power splitters are available with split ratios of 2:1, 3:1, 4:1, 6:1, 8:1, and 10:1. They are designed to achieve minimal variations in coupling across the frequency range and are suitable for cellular communications and other wireless applications. The uneven power dividers deliver output flatness of better than ±1 dB for split ratios as high as 8:1 and worst-case output flatness of ±1.2 dB for a split ratio of 10:1. The power splitters feature outstanding passive-intermodulation (PIM) performance with a typical level of −155 dBc, and can handle power levels as high as 300 W across operating temperatures from −55 to +85°C.

MECA ELECTRONICS, 459 East Main St., Denville, NJ 07834; (973) 625-0661, (866) 444-6322, e-mail: sales@e-MECA.com, *www.e-MECA.com*

Directional Coupler Links 225 To 2500 MHz

Capable of handing high power levels in a small housing, model IPP-8042 is a dual directional coupler from Innovative Power Products with a frequency range of 225 to 2500 MHz. It is rated for 35-dB coupling and maximum input power of 100 W with less than 0.3-dB insertion loss. The directivity is better than 18 dB and the mainline VSWR is less than 1.25:1. The directional coupler, which provides separate coupled ports for both forward and reflected signals with internal terminations, achieves coupling flatness of ±1 dB across its broad frequency range. It is supplied in a miniature surface-mount package measuring only 1.00 × 1.00 in. The firm also offers 90-deg. couplers and 180-deg. baluns in miniature surface-mount packages, intended for frequency ranges meeting and exceeding that of the directional coupler.

INNOVATIVE POWER PRODUCTS, INC., 1170 Lincoln Ave., Holbrook, NY 11741; (631) 563-0088, *www.innovativepp.com.*

Amplifier Boosts Optical Signals

Model OA3MMQM is a broadband 32-Gbaud, lithium-niobate optical modulator driver amplifier. It is suitable for use in Mach Zender interferometer optical modulators and for 400-GB optical long-haul-transponder applications. It can drive 400 GB of data on an existing International Telecommunications Union (ITU) long haul wavelength-division-multiplex (WDM) fiber channel, implemented with 4 channels of 32 Giga-symbol/s data encoded as DP-16QAM modulation schemes. The driver amplifier draws 300 mA from a +5-VDC supply. It provides 20-dB gain with low 7.4-W power dissipation, flat group delay, and 11-ps rise/fall time. The driver amplifier suffers less than 0.6 ps RMS jitter.

CENTELLAX, INC., 3843 Brickway Blvd. No. 100, Santa Rosa, CA 95403; (707) 568-5900, e-mail: sales@centellax.com, *www.centellax.com.*

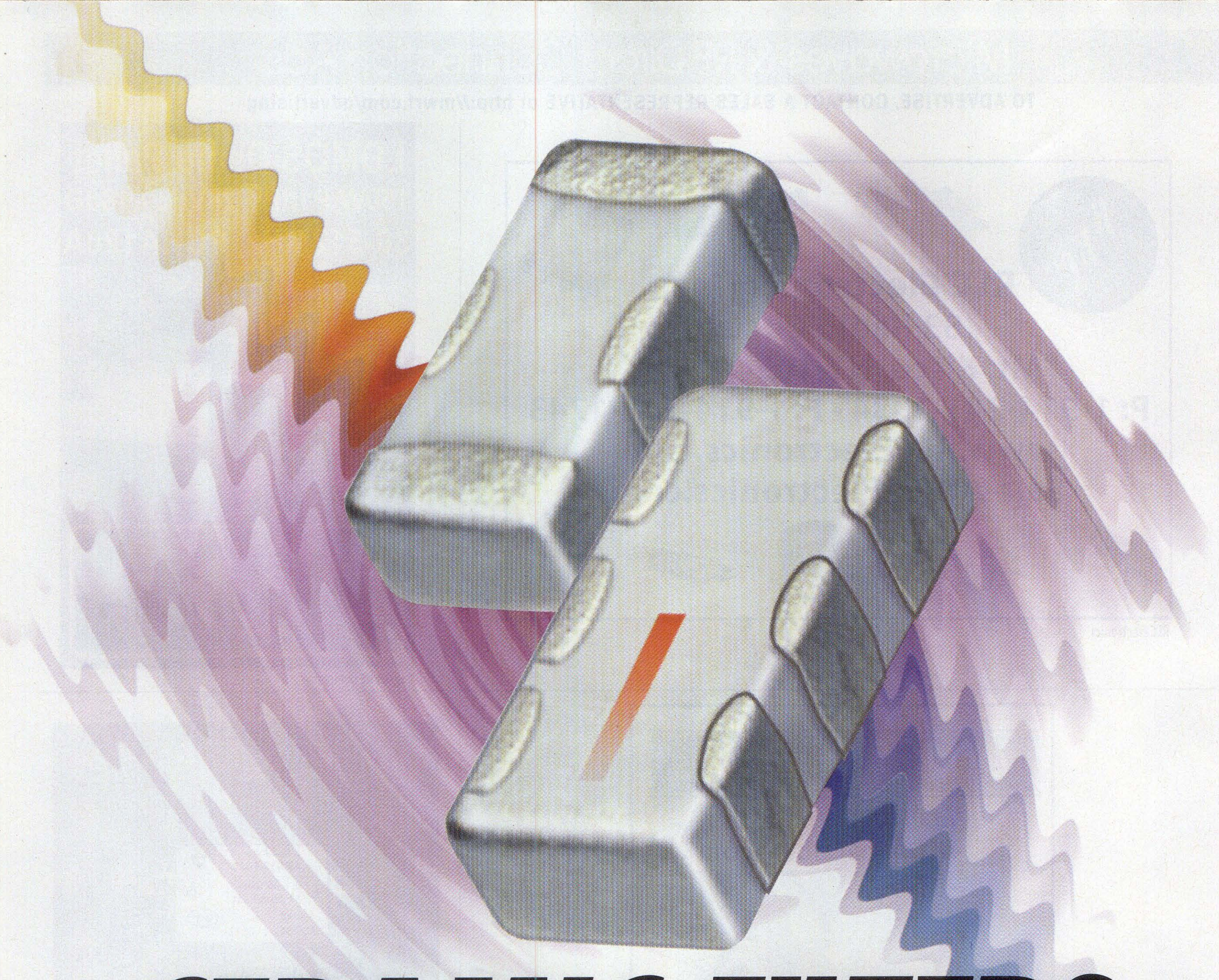

RLC Electronics

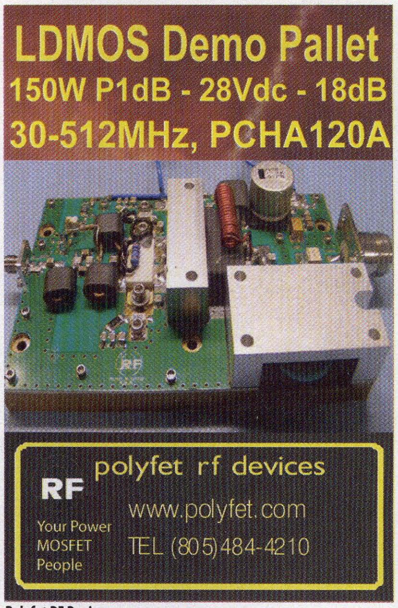

Polyfet RF Devices

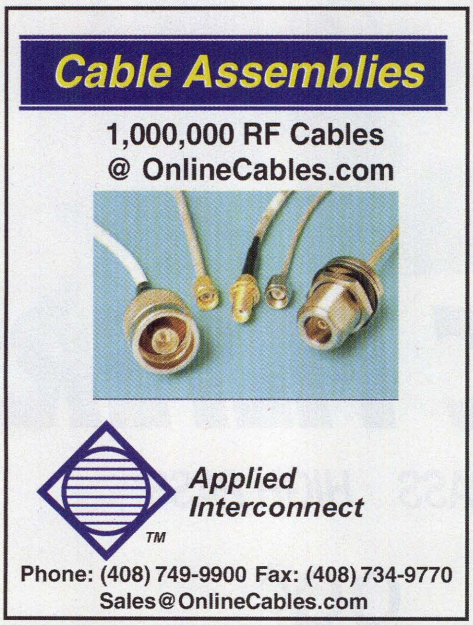

Applied Interconnect

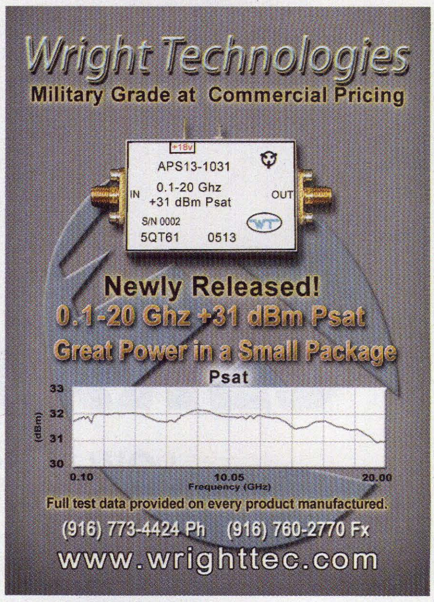

Wright Technologies

MAY 2013 ISSUE PREVIEW

Ad Close 4/15/2013 • Ad Materials due 4/25/2013

Theme: Wireless Infrastructure

Industry Insight: Thermal Management

Product Trends: Industrial, Vacuum Tubes

RF Essentials: Automotive Design Requirements

Industry Events -Wamicon, April 14-16 Orlando, FL

**Domestic Edition only **International Edition only* *This index is provided as an additional service by the publisher, who assumes no responsibility for errors or omissions.*

MARKETING & ADVERTISING STAFF

VICE PRESIDENT & MARKET LEADER
BILL BAUMANN
T: (212) 204-4365
bill.baumann@penton.com

BRAND DIRECTOR, e|DESIGN
CENTRAL U.S.
TRACY SMITH
T: (913) 967.1324 F: (913) 514.6881
E: tracy.smith@penton.com

BRAND CHAMPION
NORTHEAST
DAVID MADONIA
T: (212)-204-4331
E: dave.madonia@penton.com

SOUTH
BILL YARBOROUGH
T: (713) 636-3809 T: (713) 523-8384
E: bill.yarborough@penton.com

NORTHERN CALIFORNIA, NEVADA, NORTHWEST
JAMIE ALLEN
T: (415) 608-1959 F: (913) 514-3667
E: jamie.allen@penton.com

ONLINE SALES DEVELOPMENT DIRECTOR
STEPHANIE CAMPANA
T: (312) 840-2403-8437
stephanie.campana@penton.com

EUROPEAN SALES REP
MARK DURHAM
T: +44 (0)7958 564137
E: mark.durham@penton.com

TAIWAN, R.O.C.
CHARLES C.Y. LIU
T: (886)-2-2727-7799 F: (886)-2-2728-3686

JAPAN
HIRO MORITA
T: 81-3-3261-4591 F: 81-3-3261-6126

KOREA
JO YOUNG SANG
T: 011-82-2-739-7840
F: 011-82-732-3662

CUSTOMER SERVICE - SUBSCRIPTIONS
New/Renew/Cancel/Change Address/Missing and Back Issues
T: 866-505-7173 F: 847-763-9673
E: microwaves&rf@halldata.com

Penton
Design Engineering & Sourcing Group

Subscription Assistance and Information: Microwaves & RF (ISSN 0745-2993) is published monthly, except semi-monthly in December. **Microwaves & RF** is sent free to individuals actively engaged in high-frequency electronics engineering. In addition, paid subscriptions are available. Subscription rates for U.S. are $95 for 1 year ($120 in Canada, $150 for International). Published by Penton Media, Inc., 9800 Metcalfe Ave., Overland Park, KS 66212-2216. Periodicals Postage Paid at Shawnee Mission, KS and at additional mailing offices.

POSTMASTER: Send change of address to Microwaves & RF, Penton Media Inc., P.O. Box 2095, Skokie, IL 60076-7995. For paid subscription requests, please contact: Penton Media Inc., P.O. Box 2100, Skokie, IL 60076-7800. Canadian Post Publications Mail agreement No. 40612608. Canadian GST# R126431964. Canada return address: IMEX Global Solutions, P.O Box 25542,London, ON N6C6B2.

Portable Analyzers Scan Signals To 2.7 GHz

The PSA Series II line of microwave spectrum analyzers includes 1.3- and 2.7-GHz versions, with long rechargeable lithium-ion battery life of more than eight hours per charge to assist in-field testing. Both instruments incorporate a 4.3-in. (11-cm) backlit thin-film-transistor (TFT) color touchscreen display. The PSA Series II PSA1302 spans 1 to 1300 MHz, while the PSA Series II PSA2702 operates from 1 to 2700 MHz. Both instruments feature a noise floor of −100 dBm and 80-dB dynamic range. The resolution bandwidth can be set as fine as 15 kHz. The ruggedized casing incorporates a rubber protection buffer, a bench stand, and screen protection. For bench-top use, the instrument can be operated continuously from its AC charger. The compact handheld spectrum analyzers weigh only 20 oz. (560 g) with simple operation from the finger-operated touchscreen display.

SAELING CO., INC., 71 Perinton Pkwy., Fairport, NY 14450; (888) 7-SAELIG, (888) 772-3544, (585) 385-1750, FAX: (585) 385-1768, e-mail: info@saelig.com, ***www.saelig.com.***

Diplexer Screens CATV Systems

Model MAFL-011013 is a 75-Ω broadband diplexer filter for cable-television (CATV) applications, direct-broadcast-satellite (DBS), and cable-modem applications. It is usable over the frequency bands of 5 to 42 MHz and 54 to 1000 MHz, with typical insertion loss of only 0.5 dB in either frequency band. Signal isolation is typically 55 dB from 5 to 37 MHz; 50 dB from 54 to 100 MHz; 55 dB from 100 to 600 MHz; and 50 dB from 600 to 1000 MHz. Return loss is typically 16 dB across its full frequency range of operation. The diplexer, which is rated for maximum RF power of 250 mW and DC current of 30 mA, has an operating temperature range of −40 to +85°C. The RoHS-compliant component, which is supplied in an 11-pin surface-mount package, is available in tape-and-reel format for high-volume-production applications.

M/A-COM TECHNOLOGY SOLUTIONS, INC., 100 Chelmsford St., Lowell, MA 01851; (800) 366-2266, (978) 656-2500, ***www.macomtech.com.***

CRO Tunes From 5580 To 5685 MHz

Designed for communications applications, the model CV-CO55CXT-5580-5685 coaxial resonator oscillator (CRO) operates from 5580 to 5685 MHz with low harmonic distortion. It consists of a coaxial-based voltage-controlled oscillator (VCO) with an internal frequency doubler. The proprietary doubling circuitry controls harmonic generation to contribute to the CRO's excellent spectral purity, with low phase noise and low current consumption during normal operation. Pushing and pulling

are controlled to 1.5 MHz/V and 0.5 MHz, respectively, with typical second-harmonic suppression of −30 dBc. The model CVCO55CXT-5580-5685 CRO covers its frequency range with a tuning voltage range of +0.3 to +4.7 VDC. The coaxial VCO features a typical phase noise of −102 dBc/Hz offset 10 kHz from the carrier. It provides 0-dBm typical output power (+3 dBm maximum) into a 50-Ω load with a +5-VDC supply and maximum current consumption of 30 mA. The CRO, which is suitable for applications in digital radio equipment, fixed wireless access, and satellite communications (satcom) systems, is housed in an industry-standard 0.5 × 0.5 in. package. It has an operating temperature range of −40 to +85°C.

CRYSTEK CORP., 12730 Commonwealth Dr., Fort Myers, FL 33913; (239) 561-3311, (800) 237-3061, FAX: (239) 561-1025, ***www.crystek.com.***

GaAs Switch Controls 4.5 GHz

Model TQP4M0010 is a gallium arsenide (GaAs) field-effect-transistor (FET) absorptive switch for use from 100 to 4500 MHz. The

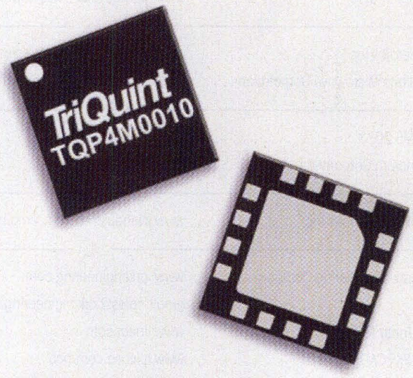

single-pole, double-throw (SPDT) switch provides 50 dB or more isolation between ports through 1 GHz and typically 40 dB or better isolation through 4.5 GHz. It minimizes insertion loss to typically 0.5 dB from 0.1 to 1.0 GHz; 0.6 dB from 1.0 to 2.5 GHz; 0.7 dB from 2.5 to 3.0 GHz; and 0.8 dB from 3.0 to 4.5 GHz. The switch, which achieves a typical input 1-dB compression point of +33 dBm at 2 GHz, can handle input signals as large as 2 W (+36 dBm). Ideal for wireless infrastructure applications and in test and measurement equipment, the GaAs switch is supplied in a 4 × 4 mm leadless surface-mount package, operates on supplies from +3 to +5 VDC, and handles operating temperatures from −40 to +85°C.

TRIQUINT SEMICONDUCTOR, INC., 2300 NE Brookwood Pkwy., Hillsboro, OR 97124; (503) 615-9000, FAX: (503) 615-8902, e-mail: info-sales@tqs.com, ***www.triquint.com.***